June 2016

Spectrally Efficient Cooperative Relay Networks using Signal Space Diversity

Muhammad Ajmal Khan
The University of Western Ontario

Supervisor
Raveendra Rao
The University of Western Ontario

Graduate Program in Electrical and Computer Engineering

A thesis submitted in partial fulfillment of the requirements for the degree in Doctor of Philosophy

Abstract

Cooperative relaying has received widespread attention in recent years from both academic and industrial communities. It offers significant benefits in enabling connectivity as well as in increasing coverage, power saving, spatial diversity and channel capacity. However, one of the main limitations of the conventional cooperative relaying system is the repetition of the received data by the relays, which reduces the spectral efficiency and the data rate. In this thesis, signal space diversity (SSD) based technique is proposed to incorporate into the conventional relaying system to enhance spectral efficiency, data rate and system performance.

Firstly, SSD is introduced into a two-way cooperative relaying system with three-phase two-way decode-and-forward (DF) protocol. In this system, four symbols are exchanged in three time slots, thereby doubling the spectral efficiency and the data rate compared to the conventional three-phase two-way DF relaying system that uses six time slots to exchange the same four symbols. Next, SSD is employed in a dual-hop relaying system using DF protocol without a direct link between the source and the destination. In this system, two symbols are transmitted in three time slots as compared to four time slots to transmit the same two symbols in the conventional dual-hop DF relaying system. These proposed systems are designed to exploit the inherent diversity in the modulation signal-space by rotating and expanding the ordinary constellation. The improvement in spectral efficiency is achieved without adding extra complexity, bandwidth or transmit power. A comprehensive analysis of these proposed systems is carried out over Rayleigh fading channels, and closed-form expressions for various performance metrics, including error probability, outage probability and channel capacity, are derived and illustrated. An asymptotic approximation for the error probability is obtained and is used to illustrate the impact of system parameters and diversity gain on the system performance. The optimization of relay location and power allocation in these systems is also examined. Extensive Monte Carlo simulations are performed to ascertain the accuracy of the analytical results presented in the thesis. Indeed, it is observed that the use of SSD in cooperative relaying can play a major role in the system design and performance improvement.

Acknowledgements

I would like to express my deep gratitude to my thesis supervisors Prof. Raveendra Rao and Prof. Xianbin Wang for their support and encouragement. I would also like to thank my supervisors to provide me the freedom to pursue my research interests in my own way, which gave me immense opportunities to explore and follow my interests in various directions and aspects.

Special thanks are due to the committee members of my thesis, Prof. Abdallah Shami, Prof. Anand Prakash, Prof. Kemal Tepe, and Prof. Vijay Parsa for their valuable feedback. I would like to thank Prof. Asrar Sheikh for his feedback to improve one of the chapter of this thesis.

I thankfully acknowledge Alexander Graham Bell Canada Graduate Scholarship (NSERC-CGSD) from the Government of Canada, Ontario Graduate Scholarship (OGS) from the Government of Ontario, and Western Graduate Research Scholarship from the University of Western Ontario. I also acknowledge Innovation Centre for Information Engineering, the University of Western Ontario, and Electrical and Computer Engineering department for providing me excellent working conditions.

I would like to thank all my friends and colleagues in the research groups of Prof. Rao and Prof. Wang, who created the friendly research environment. I would also like to thank all my friends in the University as well as in the city of London who made my stay enjoyable and fun.

Last, but not least, special thanks to my late parents for all their unconditional love and care, particularly great thanks to my late mother, who encouraged me to pursue doctoral studies and passed away during the mid of my doctoral studies. My sincere appreciation to my wife and my children for their patience, cooperation, support and love.

Table of Contents

List of Figures

List of Abbreviations

2W-SSC	Two-Way Signal Space Cooperative System
2W-SSC-1R	Two-Way Signal Space Cooperative System with Single Relay
4-QAM	4-ary Quadrature Amplitude Modulation
5G	Fifth Generation Mobile Networks
AF	Amplify-and-Forward
ARQ	Automatic Repeat reQuest
AWGN	Additive White Gaussian Noise
BEP	Bit Error Probability
CDF	Cumulative Density Function
CF	Compress-and-Forward
CRC	Cyclic Redundancy Check
DF	Decode-and-Forward
DH-SSC	Dual-Hop Signal Space Relaying System
DH-SSC-1R	Dual-Hop Signal Space Relaying System with Single Relay
et al.	and others
EPA	Equal Power Allocation
HARQ	Hybrid Automatic Repeat reQuest
MABC	Multiple-Access Broadcast Channel
ML	Maximum Likelihood Detection
M-PSK	M-ary Phase-Shift Keying
M-QAM	M-ary Quadrature Amplitude Modulation
OPA	Optimal Power Allocation
ORP	Optimal Relay Position
OSA	Optimal Source Power Allocation
PA	Power Allocation
PDF	Probability Density Function
QPSK	Quadrature Phase-Shift Keying
SEP	Symbol Error Probability

SNR	Signal-to-Noise Ratio
SSC	Signal Space Cooperative System
SSD	Signal Space Diversity
TDBC	Time-Division Broadcast Channel
TDMA	Time-Division Multiple Access
TS	Time-Slot

List of Symbols

a_i	Channel Coefficient of $\mathsf{R}_i - \mathsf{T}_1$ or $\mathsf{R}_i^{(2)} - \mathsf{D}$ Link
B	Bandwidth of the Channel
b_i	Channel Coefficient of $\mathsf{R}_i - \mathsf{T}_2$ or $\mathsf{R}_i^{(3)} - \mathsf{D}$ Link
$\mathcal{C}$	Set of Relays that decoded the received symbols correctly
$\lvert\mathcal{C}\rvert$	Size of $\mathcal{C}$
$\overline{C}$	Average Channel Capacity
$\overline{C}_{ik}$	Average Channel Capacity of $i \to k$ Link
D	Destination
d_{ik}	Distance between Node i and Node k
$\mathbb{E}\{\cdot\}$	Expectation Operator
$E_1(\cdot)$	Exponential Integral
E_b/N_0	Average SNR
E_R	Symbol Energy at the Relay
E_S	Symbol Energy at the Source
E_{tot}	Total Transmit Power of the System
E_{T_i}	Symbol Energy at ith Source Terminal
$f_\gamma(\gamma)$	PDF of the SNR γ
h_i	Channel Coefficient of $\mathsf{T}_i - \mathsf{T}_k$ or $\mathsf{S} - \mathsf{R}_i$ Link
I	In-Phase Component
$I_{\text{i}}^{\text{coop}}$	Average Mutual Information of the Cooperative Link
$\Im\{\cdot\}$	Quadrature (Q) Component
j	$\sqrt{-1}$
K	Number of Cooperative Relays in the System
ln	Natural Logarithm
$\log_A$	Logarithm to the base A

m	Number of Information Bits per Symbol
M	Modulation Level
N_0	Variance of AWGN
$\mathcal{P}_{\text{out}}$	Outage Probability
$\mathcal{P}_{\text{out}}^{\text{coop}}$	Outage Probability of the Cooperative Link
$\mathcal{P}_{\text{out}}^{i}$	Outage Probability for a Signal transmitted by Node i
$\mathcal{P}_{\text{out}}^{ik}$	Outage Probability for a Signal transmitted from Node i to Node k
$\mathcal{P}_{\text{out}}^{\text{off}}$	Outage Probability when a relay link to Source has failed
$\mathcal{P}_{\text{off}}$	Probability that the Relay fails to detect Source signals correctly
$\mathcal{P}_{\text{sym}}^{\text{coop}}(e)$	Error Probability of the Cooperative Link
$\mathcal{P}_{\text{sym}}^{e2e}(e)$	End-to-End Average SEP
$\mathcal{P}_{\text{sym}}^{\text{i}}(e)$	Average SEP of Signal transmitted by Node i
$\mathcal{P}_{\text{sym}}^{ik}(e)$	Error Probability of a Signal transmitted from Node i to Node k
$\mathcal{P}_{\text{sym}}^{ik}(e\|\gamma_k)$	Conditional SEP of the $i \to k$ link for a given γ_k
Q	Quadrature Component
$Q(\cdot)$	Gaussian Q-function
$(r_{i,1}, r_{i,2})$	Received Signals after de-Interleaver transmitted by Node i
R	Cooperative Relay
R_i	ith Cooperative Relay
R_t	Best Cooperative Relay
$\mathsf{R} \to \mathsf{T}_i$	Cooperative Relay to ith Source Terminal Link
$\mathsf{R}_i \to \mathsf{T}_k$	ith Cooperative Relay to kth Source Terminal Link
$\mathsf{R}_i^{(2)} - \mathsf{D}$	ith Relay to Destination Link in 2nd Phase
$\mathsf{R}_i^{(3)} - \mathsf{D}$	ith Relay to Destination Link in 3rd Phase
$\Re\{\cdot\}$	In-Phase (I) Component
S	Source
$(s_{i,1}, s_{i,2})$	Original Symbols of Source i
T_i	ith Source Terminal
$\mathsf{T}_i \to \mathsf{R}$	ith Source Terminal to Cooperative Relay link
$\mathsf{T}_i \to \mathsf{R}_k$	ith Source Terminal to kth Cooperative Relay link
$\mathsf{T}_i \to \mathsf{T}_k$	ith Source Terminal to kth Source Terminal link

$w_{i,k}$	Zero-mean AWGN at Node k
$(x_{i,1}, x_{i,2})$	Rotated Symbols of Source i
$\hat{x}$	Estimated (Detected) Rotated Symbols
w	Additive White Gaussian Noise (AWGN)
y_{ik}	Received Signal at Node k Transmitted by Node i
$(z_{i,1}, z_{i,2})$	Expanded (SSD) Symbols of Source i
α_x, β_x	Parameters for Ordinary Constellation
α_z, β_z	Parameters for Expanded Constellation
$\in$	Belongs to
γ_{a_i}	Instantaneous SNR of $\mathsf{R}_i \rightarrow \mathsf{T}_1$ or $\mathsf{R}_i^{(2)} - \mathsf{D}$ Link
$\overline{\gamma}_{a_i}$	Average SNR of $\mathsf{R}_i \rightarrow \mathsf{T}_1$ or $\mathsf{R}_i^{(2)} - \mathsf{D}$ Link
γ_{b_i}	Instantaneous SNR of $\mathsf{R}_i \rightarrow \mathsf{T}_2$ or $\mathsf{R}_i^{(3)} - \mathsf{D}$ Link
$\overline{\gamma}_{b_i}$	Average SNR of $\mathsf{R}_i \rightarrow \mathsf{T}_2$ or $\mathsf{R}_i^{(3)} - \mathsf{D}$ Link
γ_{h_i}	Instantaneous SNR of $\mathsf{T}_i \rightarrow \mathsf{T}_k$ or $\mathsf{S} - \mathsf{R}_i$ Link
$\overline{\gamma}_{h_i}$	Average SNR of $\mathsf{T}_i \rightarrow \mathsf{T}_k$ or $\mathsf{S} - \mathsf{R}_i$ Link
γ_{sa_i}	Instantaneous SNR of $\mathsf{T}_1 \rightarrow \mathsf{R}_i$ Link
$\overline{\gamma}_{sa}$	Average SNR of $\mathsf{T}_1 \rightarrow \mathsf{R}_i$ Link
γ_{sb_i}	Instantaneous SNR of $\mathsf{T}_2 \rightarrow \mathsf{R}_i$ Link
$\overline{\gamma}_{sb}$	Average SNR of $\mathsf{T}_2 \rightarrow \mathsf{R}_i$ Link
$\Gamma(\cdot)$	Gamma Function
λ_{ik}	Geometric Gain between Node i and Node k
ν	Path Loss Exponent
Φ	Ordinary Constellation
Φ_r	Rotated Constellation
σ_a^2	Variance of Channel Coefficients of $\mathsf{R} - \mathsf{T}_1$ or $\mathsf{R}_i^{(2)} - \mathsf{D}$ links
σ_b^2	Variance of Channel Coefficients of $\mathsf{R} - \mathsf{T}_2$ or $\mathsf{R}_i^{(3)} - \mathsf{D}$ links
σ_h^2	Variance of Channel Coefficients of $\mathsf{T}_1 - \mathsf{T}_2$ or $\mathsf{S} - \mathsf{R}_i$ links
θ	Rotation Angle for Rotated Constellation Φ_r
Υ	Expanded Constellation
$\lvert\Upsilon\rvert$	Size of Expanded Constellation
$*$	Complex Conjugation

Chapter 1
Introduction

In the last few decades, wireless and mobile communication systems have tremendously contributed to the development of our beautiful world in several ways, especially in terms of economy and social networking [1]. Today, these systems have become an integral part of our daily lives and almost everyone has some kind of a wireless device such as smartphone, tablet or laptop. The use of mobile devices has grown enormously and it is projected that there will be over 10 billion mobile-ready devices by 2020 [2]. Due to the growing use of wireless devices and bandwidth-hungry applications, the mobile traffic has been projected to increase by nearly a thousand times in less than a decade, compared to the traffic of present day [3]. In this context, several challenges are required to be addressed in the design and development of future mobile networks to meet the demands of high throughput and guaranteed connectivity, particularly, in a limited radio spectrum that suffers from a variety of interference, distortion, fading etc. The demand for a variety of services in mobile networks is also growing at a fast pace requiring reliable and extremely high-speed data transmission over radio channels.

The radio signals while propagating through wireless channels undergo rapid signal fluctuations in amplitude and phase, known as channel fading resulting from continuously changing physical environment consisting of reflectors, scatterers and diffractors [4]. The nature of wireless environment thus results in multiple signal components with random signal strengths and phases. Moreover, due to the movement

of terminals, signal path characteristic can become time-variant causing random and rapid changes in the received signals. Thus, the multipath signals at the receiver can combine destructively and result in serious degradation in the system performance. The disruptive characteristics of wireless channels make it difficult to accomplish the objectives of wireless and mobile communications, posing research challenges in the design and implementation of communication systems and networks.

A natural means to overcome the problems due to channel fading is to provide several replicas of the transmitted signal at the receiver. It is highly unlikely that all replicas will be in deep fade simultaneously, which can be used at the receiver to detect and decode the received signals correctly. Such a kind of mechanism is known as diversity [5,6], and can be accomplished by creating independently faded replicas of transmitted signal in time, frequency, or spatial domains. There are various diversity techniques used to overcome the effects of channel fading, such as time diversity, frequency diversity, and space diversity. When the same signal is transmitted over a wireless channel using more than one time slot, the technique is called time diversity. In frequency diversity, signal copies are transmitted using different carrier frequencies, and in space diversity or antenna diversity, multiple transmit and/or receive antennas are used.

However, due to the size and cost limitations of wireless devices, installing multiple antennas is not always a feasible solution to achieve diversity. Thus, cooperative diversity, an alternative way of providing spatial diversity, has emerged as a key technique to overcome the limitations in wireless devices [7]. Cooperative diversity is beneficial in scenarios, where time, frequency and antenna diversity are not feasible. In cooperative diversity, several nodes establish a network to assist each other with their transmission and reception. In general, a source node broadcasts its information message to intermediate nodes, known as relays, and these relays process the received

message and then forward it to the intended destination node. In this way, the destination receives the information message from the source directly and via intermediate relays, which can be combined to increase diversity without adding multiple antennas and/or increasing transmit power.

Depending on the role relays play in processing the received information, cooperative diversity techniques [8] can use the following protocols: (i) amplify-and-forward (AF) [9], (ii) decode-and-forward (DF) [9], (iii) coded cooperation [10], (iv) compress-and-forward (CF) [11], and (v) filter-and-forward [12]. The most extensively studied protocols in cooperative diversity techniques are AF and DF. In AF, the relay amplifies the received information message from the source node before forwarding it to the destination. In DF, the relay decodes the received information from the source node before forwarding it to the destination.

1.1 Related Work and Problem Motivation

The concept of relay channel was first introduced by van der Meulen [13, 14]. Later, Cover *et al.* [15, 16] worked on relay channels and proposed a general one-hop relay system and examined it in additive white Gaussian noise (AWGN) channels. The idea of cooperation among the neighbouring nodes to provide diversity was first introduced by Sendonaris *et al.* [7,17,18], who examined the channel capacity and system's robustness of the cooperative diversity over fading channels. They showed that an improvement in the outage performance can be achieved using cooperative diversity. Later, Laneman *et al.* [9] provided the mathematical framework for cooperative diversity using AF and DF protocols. Hunter and Nosratinia [10, 19] introduced coded cooperation technique by combining channel coding and cooperative diversity with

additional parities through relay channel to achieve enhanced decoding performance at the destination.

Signal superposition approach in cooperative relay networks was introduced by Larsson *et al.* [20], in which each user superposed their information message with other users' message received in the previous time slots for transmission. Due to different power allocation in each users' message, this signal superposition based cooperative relaying approach is very sensitive to the power allocation. Zheng *et al.* [21] combined this signal superposition approach with coded cooperation, where each user transmits a combination of its own and other user's incremental parity bits during the relay phase. This resulted in a larger constellation to achieve better spectral efficiency during the relay phase. Similarly, the concept of constellation rearrangement, adopted from Hybrid Automatic Repeat-reQuest (HARQ) [22], was introduced in cooperative relay networks [23], where the signal points of the ordinary constellation is rearranged at the relay to benefit from the combination of source and the relay signals at the destination. However, in this approach the complexity increases with the increase in the constellation size to find the optimal symbol mapping at the relay.

The idea of signal space diversity (SSD) was pioneered by Boull and Belfiore [24] and later expanded by Boutros and Viterbo [25]. SSD exploits the inherent diversity in the modulation signal space by rotating and expanding the ordinary constellation [25]. In SSD, the original symbol points in signal space are rotated by a certain angle [26, 27] so that each signal point of the rotated symbols carries enough information in its in-phase (I) and quadrature (Q) components in order to uniquely represent the original symbols. An I/Q interleaver is employed to guarantee that each component is affected by independent channel fading. In this way, the ordinary constellation is rearranged to the expanded constellation, which contains all possible combinations of different components of signal points in the ordinary constellation.

Thus, SSD extracts the inherent diversity from the modulation signal space without adding any extra bandwidth or transmit power [28, 29].

Signal space diversity has been combined with space-time codes, known as coordinate interleaved space-time codes, where both I and Q components of signal points are interleaved and then passed through space-time encoder to achieve spatial diversity [30, 31]. Coordinate interleaved approach has also been extended with multiple antenna relay networks [32]. SSD has also been utilized with coded cooperation to increase the diversity order of the system [33].

A variety of cooperative systems have been investigated in the literature to meet various communication requirements, including dual-hop cooperative system [34, 35], multi-hop cooperative system [36], and two-way cooperative system [37]. In a dual-hop cooperative system, the source broadcasts information signal to the relay in the first time slot, and then relay broadcasts it to the destination in the second time slot [35].

Two-way cooperative relaying establishes bidirectional connection between two source terminals to exchange independent messages with the help of relays. Operating in the half-duplex mode with DF strategy, two-way cooperative relaying can employ three protocols based on requirements and channel conditions [37–39]; (i) the naive four-phase, which uses four time slots for an information exchange and is spectrally inefficient [37], (ii) three-phase (also known as time-division broadcast channel, TDBC) protocol [40, 41], which requires three time slots and is commonly used in two-way relaying [37], and (iii) two-phase (multiple-access broadcast channel, MABC) protocol [42], which uses two time slots and requires network coding [43–45].

In conventional cooperative relaying system operating in the half-duplex mode, source broadcasts the data to the relay and the destination in the first time slot, and then relay repeats it to the destination using its own subchannel in the subsequent

time slot [46]. This repetition-based relaying approach reduces the overall system spectral efficiency and limits the achievable data rate [47–50]. In the thesis, thus signal space diversity [25] is proposed to incorporate into the conventional cooperative relaying system with the aim of improving the spectral efficiency and the system performance.

Recently, SSD was considered with DF protocol to improve the system performance [51, 52]. In DF relaying systems with SSD, the source rotates and interleaves the original symbols before transmission to the relay. The relay decodes and transmits a symbol different from the one transmitted by the source. In contrast to the conventional cooperative relaying system, the relay no longer repeats the same symbol received from the source, which enhances the spectral efficiency of the system [51, 52]. In [51], SSD is used with a single-relay DF cooperative system with a direct link between the source and the destination, where the source and the relay cooperate to transmit different symbols to the destination. The performance of this SSD-based cooperative system is shown to offer superiority over other cooperative systems, such as the distributed turbo coded cooperative systems [53, 54] and the trans-modulation system [23]. A similar cooperative system with single-relay is analyzed in [52], and a tight closed-form upper bound on the end-to-end bit error probability is derived.

The aforementioned works [51, 52] have considered SSD for one-way DF relaying with a direct link between the source and the destination. However, the complete absence of a direct link between the source and the destination results in the destination to entirely depend on the relay transmission, thereby reducing the overall system performance and efficiency. Moreover, two-way relaying is of primary importance due to the bi-directional communication link between two users with the help of relays. To the best of our knowledge, SSD for two-way cooperative relaying and dual-hop relaying systems have not been addressed in the literature. Thus, this thesis proposes

novel schemes to enhance the spectral efficiency, data rate and system performance of the conventional two-way cooperative relaying and conventional dual-hop relaying systems by incorporating SSD in them.

1.2 Problems Addressed and Contributions

The problems addressed in this thesis are given in the following four subsections.

Two-Way Signal Space Cooperative System using Single Relay

Signal space diversity in a two-way cooperative relaying system is addressed, where two source terminals exchange information directly and via a single intermediate relay using the three-phase two-way decode-and-forward (DF) protocol. The proposed two-way signal space cooperative system exchanges four symbols in three time slots and thus, doubles the spectral efficiency as compared to the conventional three-phase two-way DF relaying system, in which six time slots are used to exchange the same four symbols. This improvement in spectral efficiency is achieved without additional complexity, bandwidth or transmit power. This system will be referred to as 2W-SSC-1R, and the main contributions are summarized as follows:

- Two-way signal space cooperative system with a single DF relay is analyzed over Rayleigh fading channel.
- A closed-form expression for the error probability performance of the system is derived.
- An asymptotic approximation for the error probability is obtained and parameters that affect the system performance are identified.

- The performance of the 2W-SSC-1R system is compared with the conventional two-way cooperative relaying system.
- Monte Carlo simulations of the system are carried out, and the results are compared with the analytical results to confirm the accuracy of the latter.

Two-Way Signal Space Cooperative System using Multiple Relays

An enhanced 2W-SSC-1R system that employs multiple intermediate relays is proposed and investigated. This system will be referred to as 2W-SSC. As more than one relay is available for cooperation in the 2W-SSC system, the problem of relay selection is addressed to select the best relay for forwarding the data to the destination terminals. In this system, the problem of optimum power allocation at both source terminals is addressed. Next, the problem of optimization of relay location and power allocation is addressed and investigated. The main contributions of this work are summarized below:

- Two-way signal space cooperative system with K intermediate DF relays is addressed and its performance analysis over Rayleigh fading channels is analyzed.
- A closed-form expression for the end-to-end error probability is derived, and the error performance of the system for different number of relays is illustrated and discussed.
- An asymptotic approximation for the error probability is obtained, that can be used to examine the impact of system parameters on the system performance. In addition, this asymptotic expression is used to confirm the diversity order of the system.

- The optimization of the system performance for power allocation (PA) and relay position is addressed. The investigation for system optimization include optimizing relay position under fixed power allocation, optimizing power allocated to the source terminals and the relay under fixed relay location, and optimizing source power allocation under fixed relay power and position.
- Closed-form expressions for exact and asymptotic outage probabilities of the system are derived.
- Closed-form expressions for average channel capacity and an upper bound on channel capacity are derived.
- Extensive Monte Carlo simulations are carried out and the results are compared with the analytical results.

Dual-Hop Signal Space Cooperative System using Single Relay

Signal space diversity is proposed in a dual-hop cooperative system using a decode-and-forward (DF) relay. This dual-hop signal space cooperative system transmits two symbols in three phases to improve the spectral efficiency of the system, without using additional complexity, bandwidth or transmit power. This proposed system will be referred to as DH-SSC-1R. The main contributions of this work are summarized below:

- Dual-hop signal space cooperative system with single DF relay is proposed and investigated over Rayleigh fading channels.
- A closed-form expression for the error probability of the system is derived and the error performance of the system is illustrated.

- An asymptotic approximation for the error probability is obtained and used to examine the impact of system parameters on the system performance.
- The performance of the system is compared with the conventional dual-hop DF relaying, direct transmission, and suggested two-phase SSD-based dual-hop DF relaying systems.
- Analytical results are compared with Monte Carlo simulation results to confirm the accuracy of the former.

Dual-Hop Signal Space Cooperative System using Multiple Relays

An enhanced DH-SSC-1R system that uses multiple intermediate relays is proposed and will be referred to as DH-SSC. In this system, the relay position from the source and the destination is considered to investigate the optimum relay position and optimum power allocation. Also, a relay selection criteria is used to determine the best relay in the system. The main contributions of this work are summarized below:

- Dual-hop signal space cooperative system with K intermediate DF relays is proposed and its performance analysis is carried out in Rayleigh fading channels.
- A closed-form expression for the error probability of the system is derived, and the error performance of the system for different number of cooperative relays is discussed.
- An asymptotic approximation for the error probability of the system is obtained and used to examine the influence of system parameters on the performance. The asymptotic expression also verifies the diversity gain of the system.

- The optimization of the system is investigated to improve the system performance, that include the optimization of power allocation (PA) under fixed relay position, the optimization of relay position under fixed PA, and the joint optimization of PA and relay position.

- Closed-form expressions for exact and asymptotic outage probabilities are derived and illustrated as a function of information rate and signal-to-noise ratio for different number of relays.

- Closed-form expressions for average channel capacity and an upper bound on channel capacity are derived and illustrated as a function of signal-to-noise ratio for different number of relays.

- Monte Carlo simulations of the system performance are presented and compared with the analytical results.

1.3 Dissertation Organization

The thesis is organized as follows: Chapter 2 describes the fundamental concepts of cooperative relay networks, cooperative relay protocols, two-way cooperative relaying, and signal space diversity. Chapter 3 presents the proposed two-way signal space cooperative system with single decode-and-forward relay. The enhanced system with multiple intermediate relays and its analysis is performed in Chapter 4. Chapter 5 describes the proposed dual-hop signal space cooperative system with a single DF relay and its enhanced system with multiple relays is considered in Chapter 6. In Chapters 3–6, system model, mathematical analysis, results and discussion, and conclusion are presented. Finally, the conclusions of the thesis and future work are sketched in Chapter 7.

Chapter 2

Background

This chapter presents an overview of cooperative relay networks, cooperative relay protocols, and signal space diversity (SSD). The benefits and limitations of the cooperative relaying are also discussed. The signal constellation and detection of signals in SSD are discussed and simulation results are presented. It is shown that SSD provides significant performance improvement in fading channels compared to the conventional systems.

2.1 Cooperative Relay Networks

Cooperative relaying has attracted a lot of interest from both academic and industrial communities due to its application prospects in range-rate improvements of wireless communication systems [55–57]. Cooperative relaying has been included in several standards such as 3GPP LTE-Advanced, IEEE 802.11j and IEEE 802.11m, where fixed-relays can be deployed in the mobile networks to extend the coverage [58–60]. User-terminal based cooperative relaying techniques are highly expected to be employed in 5G standards [61].

Cooperative relaying refers to the sharing of resources and exploits the broadcast nature of the wireless transmission. In cooperative relaying, a source (S) transmits information signal to the destination (D) directly and/or via intermediate relays (R).

Figure 2.1 illustrates a cooperative relay network, where a source (S) broadcasts its data to the destination (D) and to the relay (R) over the channel with channel coefficients h and a. The relay (R) then repeats the data received from the source (S) to the destination (D) over fading channel with channel coefficient b using the same frequency resources in the consecutive transmission slot. Thus, the destination (D) receives two copies of the same data, one from S and the other from R, in two transmission slots. These copies can be processed at the destination to improve the reliability and capacity of the system, significantly.

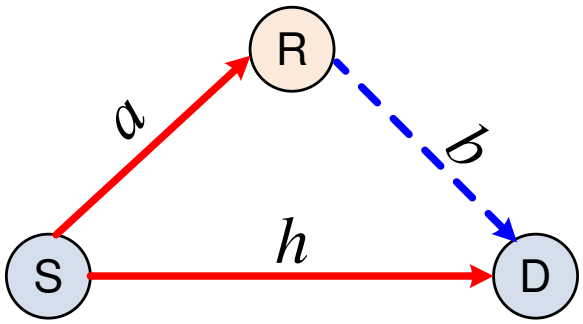

Figure 2.1: Cooperative relay network.

2.2 Benefits of Cooperative Relaying

Cooperative relaying offers significant performance benefits in enabling connectivity as well as in increasing coverage, power saving, spatial diversity and channel capacity [7, 62]. In the following, two major benefits of cooperative relaying systems are discussed.

2.2.1 Increased Coverage

If a source is unable to reach the destination or no direct link exists between the source and the destination, an intermediate node can act as a relay to transmit and

receive the source information to and from the destination. Figure 2.2 illustrates a user, who is out of range to the base station, can be connected to the base station via an intermediate relay. This cooperation enables connectivity for the out of range user as well as extends the coverage area without increasing the transmit power of the base station. For example, if a mobile user at the edge of the cellular coverage area frequently changes its location between two cells, the devices will spend significant amount of time and resources for handover between two cells. The use of cooperative relay can overcome such a situation and can keep the mobile user connected to the same base station.

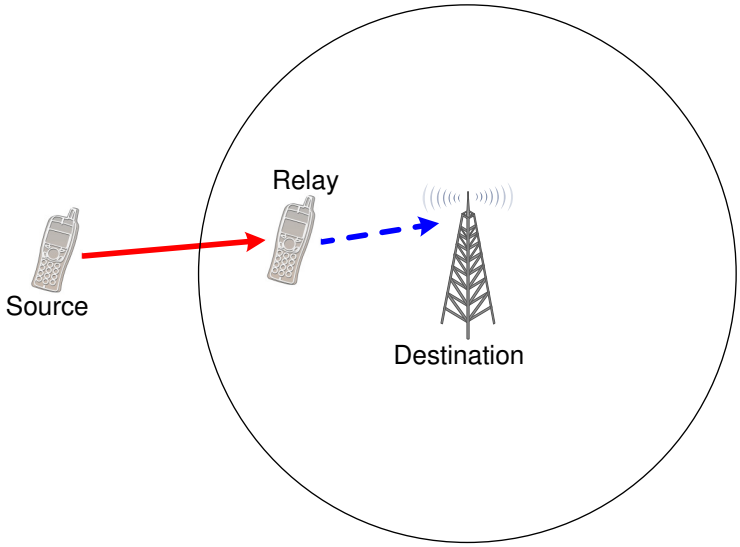

Figure 2.2: Increasing coverage using cooperative relaying.

2.2.2 Enhanced Spatial Diversity

Multiple antennas is one of the key technique to provide spatial diversity. However, due to the size and the associated cost, installing multiple antennas on mobile devices is not a feasible solution. On the other hand, cooperative relaying provides multiple copies of the transmitted data at the destination with the help of intermediate relays,

as shown in Figure 2.3. For example, if the source to destination link is affected by deep fade, the destination can use the copy of the data received from the relay. Thus, cooperative relaying can be used to improve the probability of successful transmission in the event direct transmission from source to destination fails. In addition, cooperative relaying systems increase the diversity order without the use of multiple antennas on the mobile device.

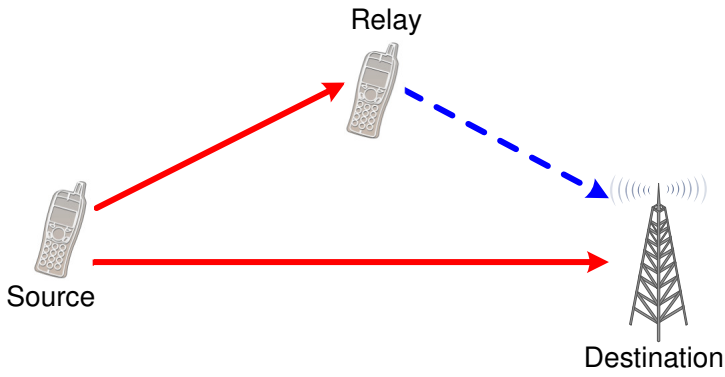

Figure 2.3: Enhancing spatial diversity using cooperative relaying.

2.3 Limitations of Cooperative Relaying

Although cooperative relaying has several performance benefits, it also has limitations and hence, requires a careful design of the system to exploit all the advantages.

The main benefit of cooperative relaying is to increase spatial diversity and this comes at the cost of spectral efficiency. Since, the relay repeats the information signal received from the source using its own subchannel in the next transmission slot, extra transmission slot is required. Thus, this repetition-based relaying approach reduces the overall spectral efficiency and limits the achievable data rate.

The additional relay traffic in cooperative relaying causes extra interference, which needs to be dealt with careful design of the system that minimizes the de-

terioration of system performance. Moreover, the reception and decoding of the information signal by the relay introduce extra latency in the transmission.

2.4 Cooperative Relay Protocols

A number of cooperative relaying protocols such as amplify-and-forward (AF) [9], decode-and-forward (DF) [9], coded cooperation [10], compress-and-forward (CF) [11] and filter-and-forward [12], are used to meet different communication requirements [8, 63]. In the following, the two most widely used cooperative relay protocols, AF and DF, are discussed.

2.4.1 Amplify-and-Forward (AF)

In AF protocol, relay amplifies the information received from the source before forwarding it to the destination [9]. AF protocol is simple in operation, as it requires only amplification of the received signal by the relay before forwarding it further. However, the noise component of the received signal is also retransmitted from the relays after amplification. Moreover, the information signal is forwarded without checking for errors in the received signal.

2.4.2 Decode-and-Forward (DF)

In DF protocol, relay decodes the information received from the source before forwarding it to the destination [9]. The advantage is that the relay removes the noise as well as it checks for errors before forwarding it to the destination.

2.4.3 Best Relay Selection Scheme

The cooperative relay network may consist of more than one relay to achieve cooperation between the source and the destination nodes. In a simple cooperative relay system with K intermediate relays, all the relays forward the received signal to the destination. Also, to maintain the same total power of the system, the power is equally distributed to all relays. The transmissions from all the relays result in increased interference, processing complexity and overheads at the destination node. Therefore, one relay out of K intermediate relays is selected for transmission, which is know as the best relay. Various relay selection criterion based on different conditions, relay types and relay networks have been presented in the literature [64]. Once, the best relay is chosen, it is used to forward the information signal to the destination. The performance of the system with the best relay is equivalent to the performance of the system that uses all K relays, with the same overall transmit power.

2.5 Dual-Hop Cooperative Relay Network

The dual-hop cooperative relaying plays an important role when the direct link between the source and the destination is not practical due to deep fade and/or power constraints. In such a case, an intermediate node can be used to relay the information signal between the source and the destination nodes [34, 65]. This dual-hop cooperative relaying system can be used to enable connectivity and to increase the coverage without increasing the transmit power. In this system, the source broadcasts information signal to the relay which in turn broadcasts it to the destination and hence, this system uses two time slots to transmit one symbol, as shown in Figure 2.4.

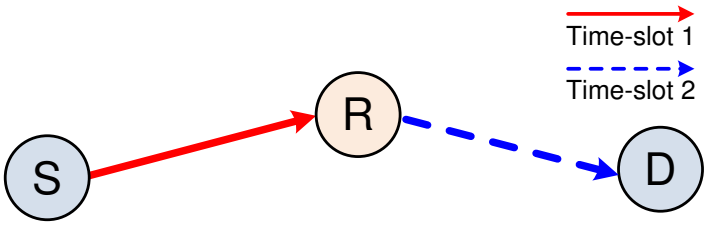

Figure 2.4: Dual-hop cooperative relay network.

2.6 Two-Way Cooperative Relay Network

Two-way cooperative relaying establishes bidirectional connection between two source terminals to exchange independent messages with the help of relays. Operating in the half-duplex mode with DF relays, a two-way cooperative relaying system has three protocols based on communication requirements and channel conditions [37–39], as described below.

2.6.1 The Naive Four-Phase Two-Way Relaying

In the Naive four-phase two-way relaying, the source terminal (T_1) broadcasts its information signal to the other source terminal (T_2) and to the relay (R), in the first time slot. In the second time slot, the relay forwards the information signal received from T_1 to terminal T_2. In the third time slot, the terminal T_2 broadcasts its information signal to the terminal T_1 and to the relay (R). In the fourth time slot, the relay (R) forwards the information signal received from T_2 to the terminal T_1. Thus, the Naive four-phase two-way relaying system uses four time slots for an information exchange between two source terminals, as shown in Figure 2.5. The use of four time slots makes the Naive four-phase two-way relaying system spectrally inefficient [37].

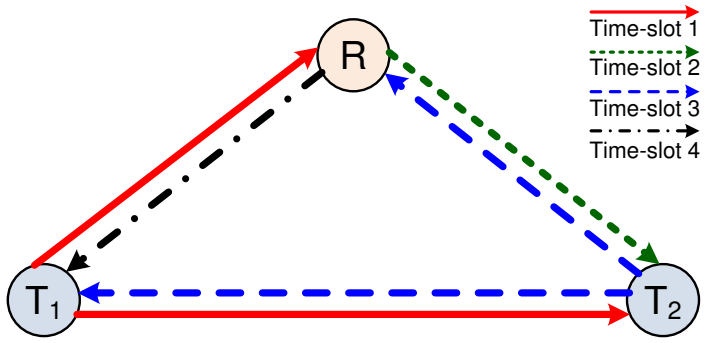

Figure 2.5: The Naive four-phase two-way cooperative relay network.

2.6.2 Three-Phase Two-Way Relaying

The three-phase two-way relaying is also known as time-division broadcast channel (TDBC) protocol [40, 41]. In this approach, the first source terminal (T_1) broadcasts its information signal to the second source terminal (T_2) and to the relay (R) in the first time slot. In the second time slot, the terminal T_2 broadcasts its information signal to the terminal T_1 and to the relay (R). Then, the relay decodes the information signals received from both source terminals (T_1 and T_2) and broadcasts the combination of both signals to both terminals in the third time slot. Since each source terminal perfectly knows its transmitted signal, it can cancel the self-interference term. Thus, in the conventional three-phase two-way DF relaying system, the exchange of two information messages takes place in three time slots, as shown in Figure 2.6. Three-phase two-way relaying exploits the direct link between the source terminals and is commonly used in two-way relaying [37].

2.6.3 Two-Phase Two-Way Relaying

The two-phase two-way relaying, also known as multiple-access broadcast channel (MABC) protocol [42], uses two time slots and requires network coding [43–45]. Figure 2.7 illustrates a two-phase two-way relaying system. In the first time slot, both

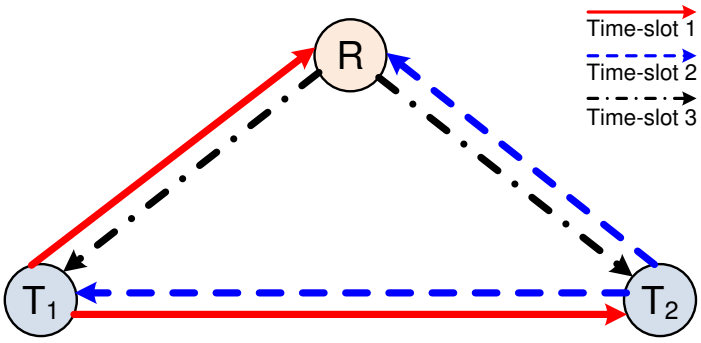

Figure 2.6: Three-phase two-way cooperative relay network.

terminals T_1 and T_2 simultaneously broadcast their information signals to the relay R. In the second time slot, the relay forwards the received signals to both terminals in the second time slot.

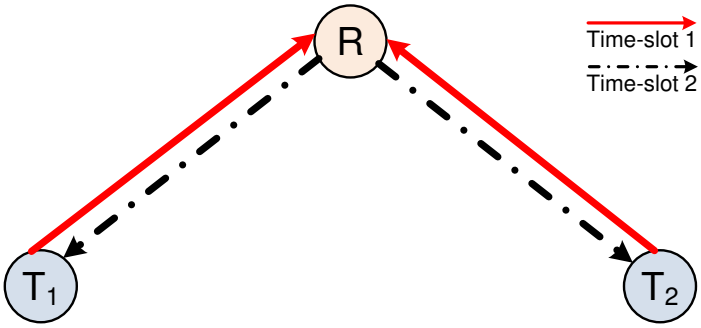

Figure 2.7: Three-phase two-way cooperative relay network.

2.7 Signal Space Diversity (SSD)

Signal space diversity is a kind of diversity, inherent in the modulation signal space and can be achieved using novel constellation rearrangement [25]. In SSD, a certain rotation angle is applied to the original symbols in the ordinary constellation Φ such as M-ary quadrature amplitude modulation (M-QAM) or M-ary phase-shift keying (M-PSK). The optimum rotation angle [26, 27] guarantees that each signal

point possesses sufficient information in its in-phase (I) and quadrature (Q) components to individually represent the original symbols. Each component of the signal point is transmitted over an independent fading channel, and an I/Q interleaver is employed for this purpose. After rotation and interleaving, the ordinary constellation is transformed to the expanded constellation Υ, which covers all possible combinations of different components of signal points. Therefore, SSD can effectively improve error performance, diversity gain, spectral efficiency and data rate without additional complexity, bandwidth or transmit power.

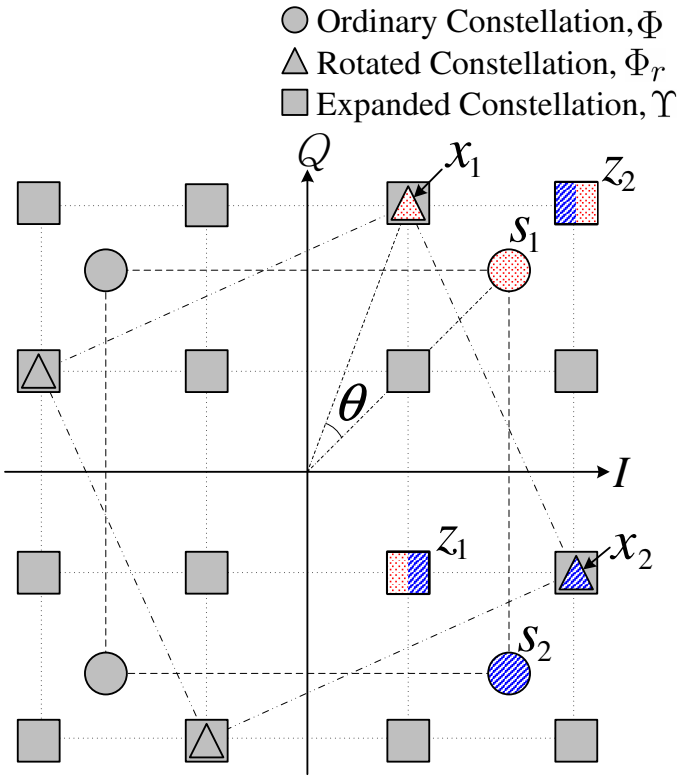

Figure 2.8: Constellation rotation and expansion in SSD.

Figure 2.8 shows the constellation rotation and expansion in SSD. First, each $m = \log_2(M)$ information bits at each source terminal are grouped and mapped to ordinary constellation using a digital modulation scheme such as M-ary quadrature

amplitude modulation (M-QAM). Let $\mathbf{s} = (s_1, s_2)$ be the two original signal points from the ordinary constellation Φ (e.g. 4-QAM), i.e. $(s_1, s_2) \in \Phi$. The symbols are complex and can be denoted as $s_1 = \Re\{s_1\} + j\Im\{s_1\}$ and $s_2 = \Re\{s_2\} + j\Im\{s_2\}$, where $j = \sqrt{-1}$, and $\Re\{\cdot\}$ and $\Im\{\cdot\}$ are I and Q components of the symbols, respectively. Then, s_1 and s_2 are rotated by the angle θ, i.e. $x_1 = s_1\, e^{j\theta}$ and $x_2 = s_2\, e^{j\theta}$. The rotated symbols, $\mathbf{x} = (x_1, x_2)$, correspond to a rotated constellation Φ_r, which is generated by applying a transformation Θ to the ordinary constellation as

$$\Theta = \begin{bmatrix} \cos\theta & -\sin\theta \\ \sin\theta & \cos\theta \end{bmatrix}. \tag{2.1}$$

The rotation angle θ is chosen carefully to ensure that each signal point in the rotated constellation carries enough information in one component, either I or Q, and uniquely represents the original signal point [25,51]. A list of θ for various modulation schemes can be found in [26, 27], such as the rotation angles θ of 26.6°, 14.0° and 7.1° are chosen for 4-, 16- and 64-QAM constellations, respectively. The new SSD symbols, $\mathbf{z} = (z_1, z_2)$, for transmission are formed by interleaving the Q components of the rotated symbols, x_1 and x_2, and are given by

$$z_1 = \Re\{x_1\} + j\Im\{x_2\}, \tag{2.2}$$

$$z_2 = \Re\{x_2\} + j\Im\{x_1\}. \tag{2.3}$$

The SSD symbols, z_1 and z_2, for transmission belong to an expanded constellation Υ, i.e $\Upsilon = \Re\{\Phi_r\} \times \Im\{\Phi_r\}$, where $\times$ is the Cartesian product of two sets. It is important to mention that each member of Υ consists of two components, i.e. a real component from a member of Φ_r and an imaginary component from another member of Φ_r. Moreover, each component identifies a specific membership of Φ_r.

Thus, the decoding of a member of Υ leads to decoding two different members of Φ_r (i.e. x_1 and x_2). It is highlighted that the expanded constellation, resulting from component interleaving and ordinary constellation rotation, does not convert a low order constellation to a higher one. In addition, the expanded constellation maintains the same number of bits per signal point as in the ordinary constellation.

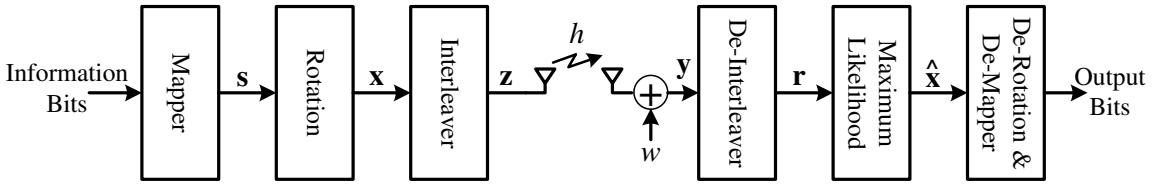

Figure 2.9: System model of SSD-based Communication System.

Consider a wireless communication system having one transmitter and one receiver with the fading channel coefficient h, as shown in Figure 2.9. The SSD symbols, z_1 and z_2, are transmitted over the wireless channel to the receiver, hence the received signals at the receiver can be represented as

$$y_1 = \sqrt{E}\, h_1\, z_1 + w_1 \tag{2.4}$$

$$y_2 = \sqrt{E}\, h_2\, z_2 + w_2, \tag{2.5}$$

where E denotes the symbol energy at the transmitter, and w_1 and w_2 denote zero-mean AWGN at the receiver.

Let $\mathbf{r} = (r_1, r_2)$ be the signal after component de-interleaver at the receiver, which can be written as

$$r_1 = \Re\{h_1^*\, y_1\} + j\Im\{h_2^*\, y_2\}, \tag{2.6}$$

$$r_2 = \Re\{h_2^*\, y_2\} + j\Im\{h_1^*\, y_1\}. \tag{2.7}$$

Similar to the detection of ordinary digital modulation schemes, the maximum likelihood detection is applied to detect the transmitted signal in SSD, using

$$\hat{x}_1 = \arg \min_{x \in \Phi_r} \left[\left| \Re\{r_1\} - \sqrt{E}|h_1|^2 \Re\{x_1\} \right|^2 + \left| \Im\{r_1\} - \sqrt{E}|h_2|^2 \Im\{x_1\} \right|^2 \right], \quad (2.8)$$

$$\hat{x}_2 = \arg \min_{x \in \Phi_r} \left[\left| \Re\{r_2\} - \sqrt{E}|h_2|^2 \Re\{x_2\} \right|^2 + \left| \Im\{r_2\} - \sqrt{E}|h_1|^2 \Im\{x_2\} \right|^2 \right]. \quad (2.9)$$

The original signal points, s_1 and s_2, can be obtained after de-rotating of x_1 and x_2.

To study the benefits of using SSD, the average bit error probability (BEP) of 4-QAM with SSD is obtained using rotation angle $\theta = 26.6^\circ$ over Rayleigh fading channel, and compared with the conventional 4-QAM in Figure 2.10. In this figure, the average BEP of 4-QAM with SSD is represented by solid line with $\circ$ markers, while the bit error probabilities of the conventional 4-QAM with diversity order of 1 and 2 are shown by $\times$ and $\square$ markers, respectively. It is clearly evident that the SSD greatly improves the error performance of 4-QAM. For example, BEP= 10^{-3} can be achieved at $E_b/N_0 = 16.3$ dB with the SSD-based 4-QAM or at $E_b/N_0 = 24$ dB with the conventional 4-QAM. Thus, compared to the conventional 4-QAM, an E_b/N_0 gain of about 7.7 dB is obtained with the SSD-based 4-QAM. It is observed that the average BEP of SSD-based 4-QAM is just short of less than 2 dB than that of the conventional 4-QAM with diversity order of 2. This improvement indicates that the SSD-based M-QAM or M-PSK modulation schemes increases the diversity order to 2 without adding extra transmit/receive antenna, bandwidth or transmit power.

The effect of rotation angle θ on the error performance of the SSD-based 4-QAM is shown in Figure 2.11. The average BEP of the SSD-based 4-QAM as a function of rotation angle θ is obtained at $E_b/N_0 = 15$ dB. It is clearly evident from the figure that the average BEP of the SSD-based 4-QAM varies with the rotation

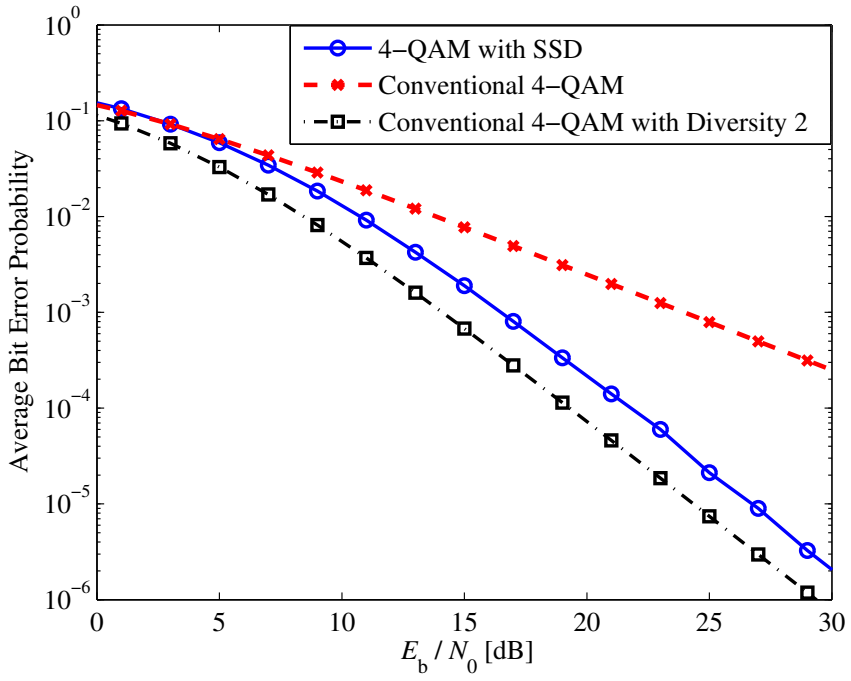

Figure 2.10: Improvement in error performance of 4-QAM with SSD.

angle θ. Error probability of the SSD-based 4-QAM is high when the rotation angle is around 0°, 45° or 90°, and low when the rotation angle is around 26.6° or 63.4°. The error probability of SSD-based 4-QAM improves when the rotation angle increases from 0° to 26.6°, and reduces when the rotation angle decreases from 26.6° to 45°. Thus, nearly 10 times improvement in the error probability is observed with optimum rotation angle.

The average BEP of the SSD-based 4-QAM for different rotation angle θ is shown in Figure 2.12. It is observed from the figure that the error probability of the SSD-based 4-QAM becomes equivalent to the conventional 4-QAM when $\theta = 0°$ and 90°, which is obvious because SSD-based 4-QAM turns to conventional 4-QAM if the constellation is rotated at $\theta = 0°$ or 90°. This figure also verifies that the error probability of the SSD-based 4-QAM is optimal with optimum rotation angle of $\theta = 26.6°$. For example, BEP= 10^{-3} can be achieved using SSD-based 4-QAM

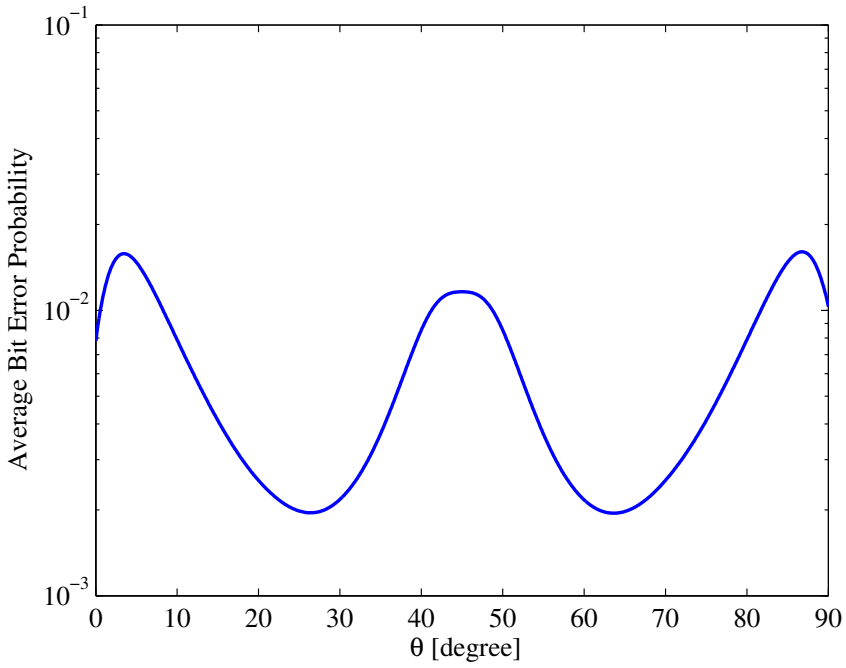

Figure 2.11: Effect of rotation angle θ on the error probability of SSD-based 4-QAM, when $E_b/N_0 = 15$ dB.

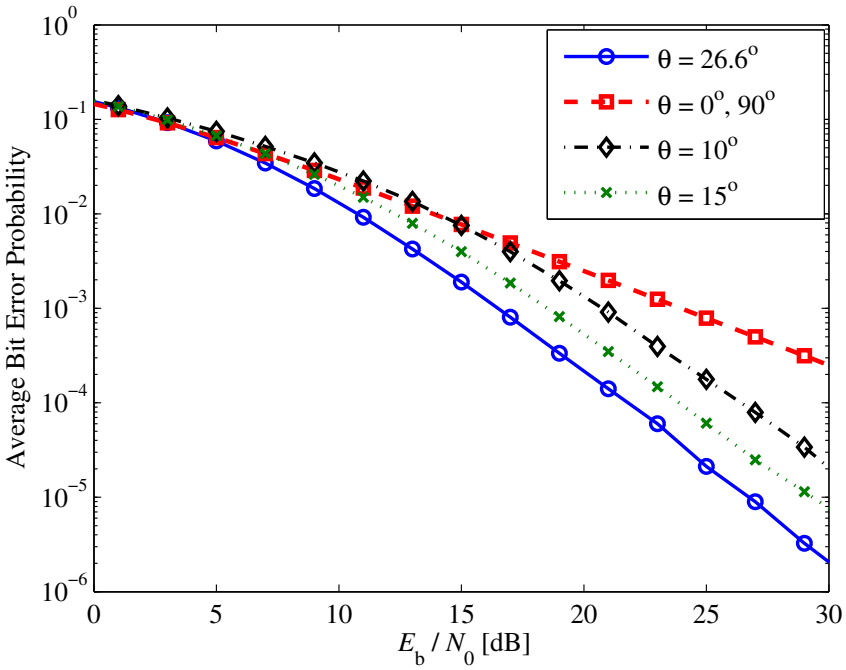

Figure 2.12: Error probability of SSD-based 4-QAM, when $\theta = 0°, 10°, 15°, 26.6°$, and $90°$.

at $E_b/N_0 = 24$ dB with $\theta = 0^\circ$ or 90°, or at $E_b/N_0 = 20.7$ dB with $\theta = 10^\circ$, or at $E_b/N_0 = 18.4$ dB with $\theta = 15^\circ$, or at $E_b/N_0 = 16.3$ dB with $\theta = 26.6^\circ$. Thus, compared to the rotation angle of $\theta = 0^\circ$ and 90°, an E_b/N_0 gain of about 3.3 dB, 5.6 dB and 7.7 dB is achieved with $\theta = 10^\circ$, 15° and 26.6°, respectively.

In order to show the introduction of SSD into higher order modulation schemes, the error performances of SSD-based 16-QAM and 8-PSK are studied. The effect of rotation angle θ on the error probability of SSD-based 16-QAM is shown in Figure 2.13, where the average BEP of SSD-based 16-QAM is illustrated as a function of θ at $E_b/N_0 = 20$ dB. It is observed that the average BEP of SSD-based 16-QAM is changed with the variation of θ and optimum θ is found to be 14° from the figure. The average BEP of the SSD-based 16-QAM for different rotation angles θ is shown in Figure 2.14. The average BEP of conventional 16-QAM is also plotted for comparison. It is evident from the figure that SSD-based 16-QAM has better performance than conventional 16-QAM. For example, BEP$= 10^{-4}$ can be obtained using SSD-based 16-QAM at $E_b/N_0 = 37$ dB with $\theta = 0^\circ$, or at $E_b/N_0 = 29.5$ dB with $\theta = 10^\circ$, or at $E_b/N_0 = 27.5$ dB with $\theta = 14^\circ$. Thus, compared to the conventional 16-QAM, an E_b/N_0 gain of about 7.5 dB and 9.5 dB is achieved using SSD-based 16-QAM with $\theta = 10^\circ$ and 14°, respectively.

Similarly, the average BEP of SSD-based 8-PSK for different θ is obtained and shown in Figure 2.15. It is observed that compared to the conventional 8-PSK, an E_b/N_0 gain of about 7.5 dB and 9 dB is achieved using SSD-based 8-PSK with $\theta = 5^\circ$ and 13.8°, respectively.

This concept of introducing SSD can be extended to any two-dimensional digital modulation scheme. The optimum rotation angles for various modulation schemes are available in [26, 27].

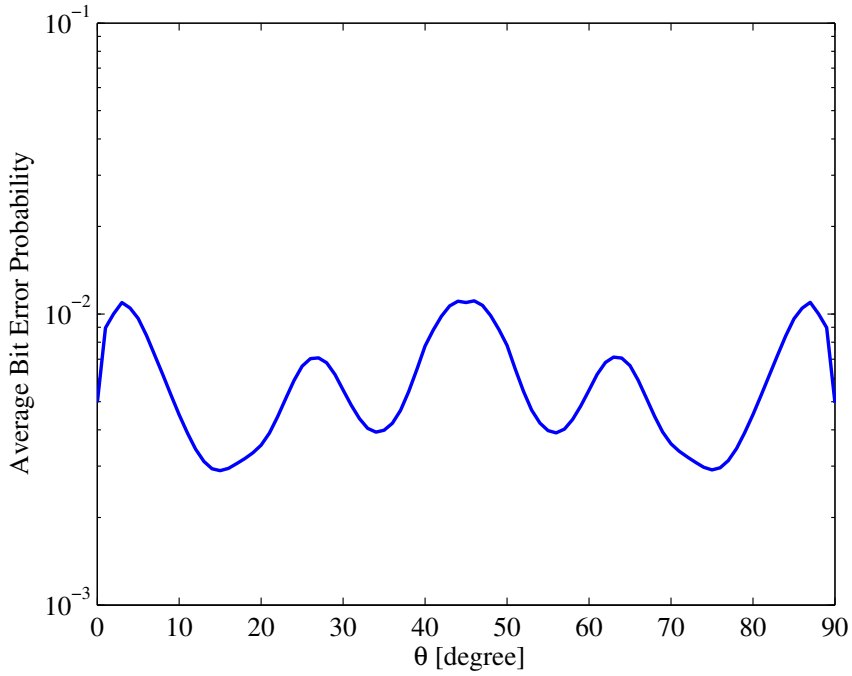

Figure 2.13: Effect of rotation angle θ on the performance of SSD-based 16-QAM, when $E_b/N_0 = 20$ dB.

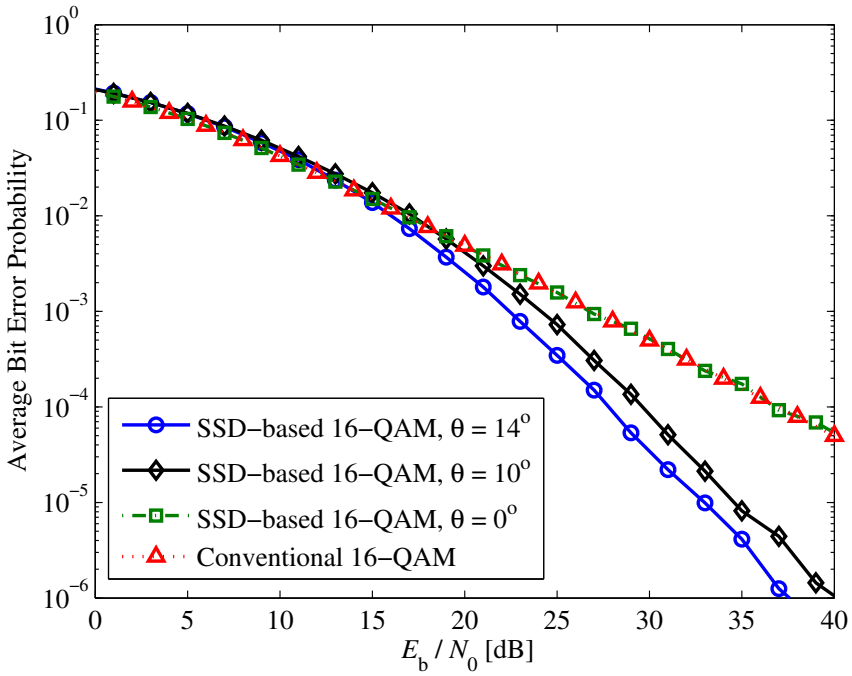

Figure 2.14: Error performance of conventional and SSD-based 16-QAM with $\theta = 0°, 10°, 14°$.

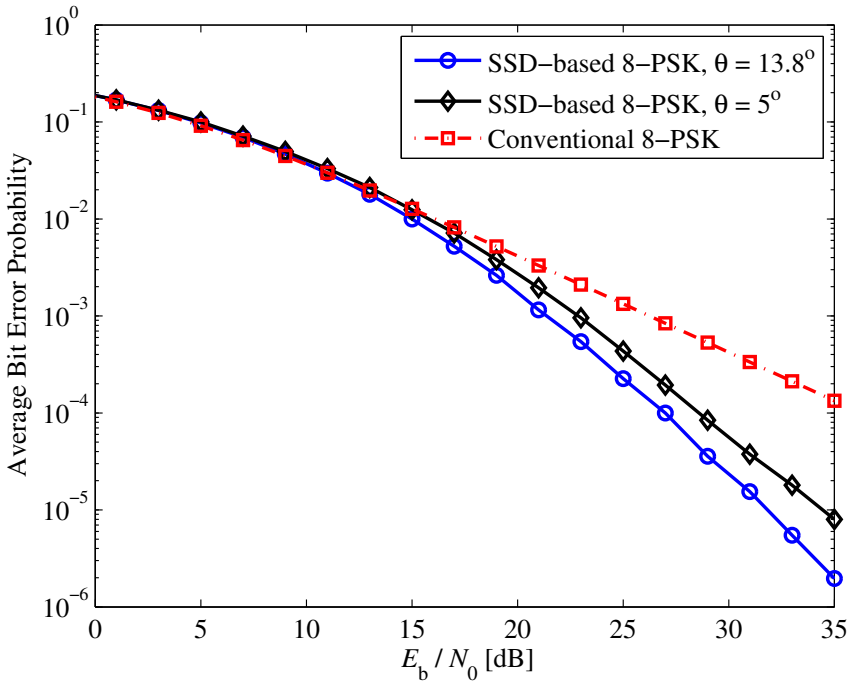

Figure 2.15: Error performance of conventional and SSD-based 8-PSK with $\theta = 5°, 13.8°$.

2.8 Summary

In this chapter, cooperative relay networks, cooperative relay protocols and signal space diversity (SSD) were briefly reviewed. The signal constellation, rotation, and expansion in SSD were discussed. Mathematical model of the signal transmission in SSD was explained. Maximum likelihood detection was applied in SSD to detect the received signal. The simulation results of the bit error probability with and without SSD were obtained and discussed. It was shown that SSD improves the performance and the diversity order of the system. The significance of rotation angle in SSD was discussed and it was shown that the careful selection of rotation angle can reap the benefits of SSD. In summary, the topics discussed in this chapter would serve as background for understanding the problems addressed in the thesis.

Chapter 3

Two-Way Signal Space Cooperative System using Single Relay

In this chapter, a novel scheme is proposed to enhance the spectral efficiency of a two-way cooperative relaying system, where two source terminals exchange information directly and via an intermediate relay using the three-phase two-way decode-and-forward (DF) protocol. Signal space diversity is used in the system that rotates and expands the modulation signal space of an ordinary constellation. Hereafter, the proposed two-way signal space cooperative system using a single DF relay will be referred to as 2W-SSC-1R.

In the conventional two-way cooperative system using the three-phase relaying decode-and-forward (DF) protocol, a direct link between two source terminals and an indirect link via intermediate relay are used to achieve diversity. In the first time slot, one source terminal broadcasts its one symbol to the relay and to the second source terminal. In the second time slot, the second terminal broadcasts its one symbol to the relay and to the first terminal. Then, the relay decodes the symbols received from both terminals and broadcasts the combination of both received symbols to both terminals in the third time slot. Since each terminal perfectly knows its transmitted signal, it can use this knowledge to recover the symbol transmitted by the other terminal. Thus, the conventional two-way cooperative system exchanges two symbols in three

time slots [37]. This repetition-based relaying approach is inefficient and therefore, signal space diversity (SSD) [25] is proposed to employ in the conventional two-way cooperative system to enhance the spectral efficiency and the system performance.

In the proposed 2W-SSC-1R system, first source terminal broadcasts its first symbol from the expanded constellation to the other source terminal and to the relay in the first time slot. Then, the first symbol of the first terminal is decoded and the second symbol of the first terminal is recovered at the relay due to SSD. In the second time slot, the second source terminal broadcasts its first symbol from the expanded constellation to the other terminal and to the relay. Similarly, the first symbol of the second terminal is decoded and its second symbol is recovered at the relay due to SSD. Assuming the relay correctly decodes the received symbols, then it forwards a combination of second symbols of both terminals to the terminals in the third time slot. Thus, the 2W-SSC-1R system exchanges four symbols in three time slots and enhances the spectral efficiency by 100% compared to the conventional two-way cooperative system, without adding extra complexity, bandwidth or transmit power.

In this chapter, the system model of the proposed system is described in Section 3.1. The closed-form expressions for the average symbol error probability (SEP) and asymptotic SEP are derived in Section 3.2. The error performance of the 2W-SSC-1R system is compared with the conventional two-way cooperative system in Section 3.3. Finally, the performance results using analytical expressions and Monte Carlo simulations are presented in Section 3.3. The chapter is summarized in Section 3.4.

3.1 System Model

The system model of the proposed two-way signal space cooperative system (2W-SSC-1R) consisting of two source terminals (T_1 and T_2) and a single relay (R) is shown

in Figure 3.1. Each node in this system is equipped with one antenna and operates in half-duplex mode. In this system, both terminals T_1 and T_2 communicate with each other directly and through the relay over slow Rayleigh fading channels. The channel information is available at all the receiving nodes as well as at the relay. The channel coefficients of $\mathsf{T}_1 \rightarrow \mathsf{T}_2$, $\mathsf{R} \rightarrow \mathsf{T}_1$ and $\mathsf{R} \rightarrow \mathsf{T}_2$ links are denoted as h, a and b with variances σ_h^2, σ_a^2 and σ_b^2, respectively. The channel coefficients are assumed to be reciprocal and to remain constant during each transmission phase as well as all channels are mutually independent and have no interference with each other.

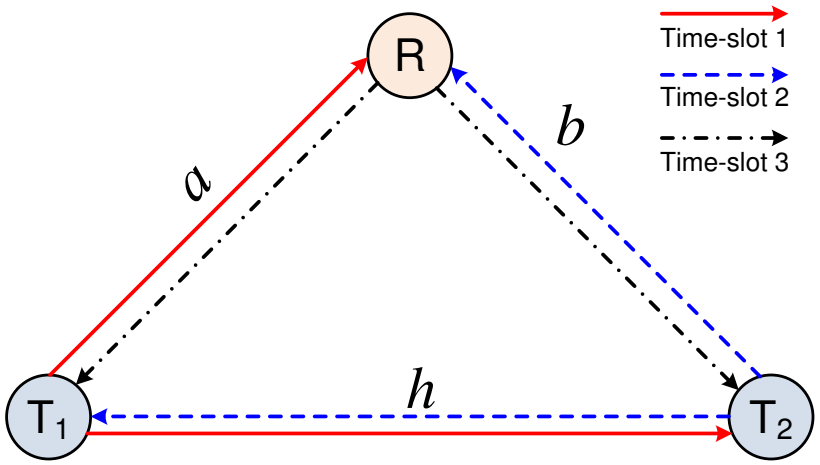

Figure 3.1: System model of two-way signal space cooperative system with a single DF relay (2W-SSC-1R).

The total transmit power constraint E_{tot} is imposed on the exchange of every four symbols in three time slots at two source terminals and the relay. For a fair analysis, the total transmit power E_{tot} is always equal to the total energy of four symbols. The symbol energies at the terminals (T_1 and T_2) and at the relay (R) are denoted as E_T and E_R, respectively. Zero-mean additive white Gaussian noise (AWGN) with variance N_0 is assumed over all channels. The distances of $\mathsf{T}_1 - \mathsf{T}_2$, $\mathsf{T}_1 - \mathsf{R}_i$ and $\mathsf{T}_2 - \mathsf{R}$ links are denoted as $d_{T_1T_2}$, d_{T_1R} and d_{T_2R}, respectively, and their geometric gains

are represented as $\lambda_{T_1R} = (d_{T_1T_2}/d_{T_1R})^{\nu}$ and $\lambda_{T_2R} = (d_{T_1T_2}/d_{T_2R})^{\nu}$, respectively, where ν is the path loss exponent. The instantaneous signal-to-noise ratios (SNRs) of $\mathsf{T}_1 \to \mathsf{R}$, $\mathsf{T}_2 \to \mathsf{R}$, $\mathsf{R} \to \mathsf{T}_1$ and $\mathsf{R} \to \mathsf{T}_2$ links are denoted as $\gamma_{sa} = |a|^2 \lambda_{T_1R} E_T/N_0$, $\gamma_{sb} = |b|^2 \lambda_{T_2R} E_T/N_0$, $\gamma_a = |a|^2 \lambda_{T_1R} E_R/N_0$ and $\gamma_b = |b|^2 \lambda_{T_2R} E_R/N_0$, and corresponding average SNRs are $\overline{\gamma}_{sa} = \sigma_a^2 \lambda_{T_1R} E_T/N_0$, $\overline{\gamma}_{sb} = \sigma_b^2 \lambda_{T_2R} E_T/N_0$, $\overline{\gamma}_a = \sigma_a^2 \lambda_{T_1R} E_R/N_0$ and $\overline{\gamma}_b = \sigma_b^2 \lambda_{T_2R} E_R/N_0$, respectively. As both terminals (T_1 and T_2) have the same transmit power E_T, the instantaneous SNR between T_1 and T_2 link is $\gamma_h = |h|^2 E_T/N_0$ and the average SNR is $\overline{\gamma}_h = \sigma_h^2 E_T/N_0$.

In this system, SSD is applied at the terminals and the relay. First, each $m = \log_2(M)$ information bits at each source terminal are grouped and mapped to some ordinary constellation using a digital modulation scheme such as M-ary quadrature amplitude modulation (M-QAM) or M-ary phase-shift keying (M-PSK).

Let $\mathbf{s}_{T_1} = (s_{T_1,1}, s_{T_1,2})$ be the two original signal points at T_1 from the ordinary constellation Φ (e.g. 4-QAM, or QPSK), i.e. $s_{T_1,1}, s_{T_1,2} \in \Phi$. The original complex symbols can be denoted as $s_{T_1,1} = \Re\{s_{T_1,1}\} + j\Im\{s_{T_1,1}\}$ and $s_{T_1,2} = \Re\{s_{T_1,2}\} + j\Im\{s_{T_1,2}\}$, where $j = \sqrt{-1}$, and $\Re\{\cdot\}$ and $\Im\{\cdot\}$ are I and Q components of the symbols, respectively. Then, $s_{T_1,1}$ and $s_{T_1,2}$ are rotated by the angle θ, i.e. $x_{T_1,1} = s_{T_1,1}\, e^{j\theta}$ and $x_{T_1,2} = s_{T_1,2}\, e^{j\theta}$. The rotated symbols, $\mathbf{x}_{T_1} = (x_{T_1,1}, x_{T_1,2})$, correspond the points in the rotated constellation Φ_r. The new SSD symbols, $\mathbf{z}_{T_1} = (z_{T_1,1}, z_{T_1,2})$, for transmission are formed by interleaving the Q components of the rotated symbols, $x_{T_1,1}$ and $x_{T_1,2}$, and are given by

$$z_{T_1,1} = \Re\{x_{T_1,1}\} + j\Im\{x_{T_1,2}\}, \tag{3.1}$$

$$z_{T_1,2} = \Re\{x_{T_1,2}\} + j\Im\{x_{T_1,1}\}. \tag{3.2}$$

The SSD symbols, $z_{T_1,1}$ and $z_{T_1,2}$, for transmission from T_1, belong to an

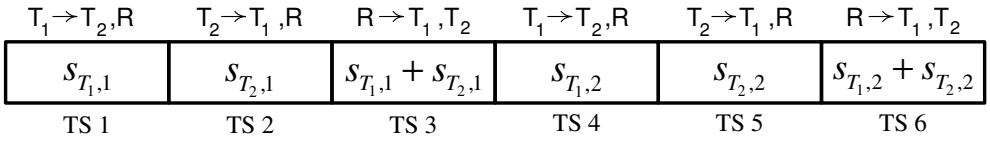

(a)

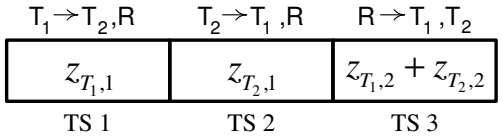

(b)

Figure 3.2: Time slots (TS) allocation to: (a) the conventional two-way cooperative system, and (b) the 2W-SSC-1R system.

expanded constellation Υ. In the first time slot, T_1 broadcasts only one of the two SSD symbols (i.e. $z_{T_1,1}$), as shown in Figure 3.2. The received signal at T_2 and the relay can be written as

$$y_{T_1T_2} = \sqrt{E_T}\, h\, z_{T_1,1} + w_{T_2}, \tag{3.3}$$

$$y_{T_1R} = \sqrt{E_T \lambda_{T_1R}}\, a\, z_{T_1,1} + w_{T_1,R}, \tag{3.4}$$

where w_{T_2} and $w_{T_1,R}$ denote zero-mean AWGN with a variance of N_0 at T_2 and the relay, respectively. The two rotated symbols, $x_{T_1,1}$ and $x_{T_1,2}$, are detected using the transmitted SSD symbol, $z_{T_1,1} = \Re\{x_{T_1,1}\} + j\Im\{x_{T_1,2}\}$, at the relay as

$$\hat{x}_{T_1,1} = \arg\min_{x\in\Phi_r} \left| \Re\{a^*\, y_{T_1R}\} - \sqrt{E_T \lambda_{T_1R}}\, |a|^2\, \Re\{x_{T_1,1}\} \right|^2, \tag{3.5}$$

$$\hat{x}_{T_1,2} = \arg\min_{x\in\Phi_r} \left| \Im\{a^*\, y_{T_1R}\} - \sqrt{E_T \lambda_{T_1R}}\, |a|^2\, \Im\{x_{T_1,2}\} \right|^2, \tag{3.6}$$

where $*$ denotes complex conjugation.

Next, T_2 prepares two SSD symbols, $z_{T_2,1}$ and $z_{T_2,2}$, by component interleaving

of its two rotated symbols, $x_{T_2,1}$ and $x_{T_2,2}$, as

$$z_{T_2,1} = \Re\{x_{T_2,1}\} + j\Im\{x_{T_2,2}\}, \tag{3.7}$$

$$z_{T_2,2} = \Re\{x_{T_2,2}\} + j\Im\{x_{T_2,1}\}. \tag{3.8}$$

Similarly, in the second time slot, T_2 broadcasts only one of the two SSD symbols (i.e. $z_{T_2,1}$), which is received at T_1 and the relay, as

$$y_{T_2T_1} = \sqrt{E_T}\, h\, z_{T_2,1} + w_{T_1}, \tag{3.9}$$

$$y_{T_2R} = \sqrt{E_T \lambda_{T_2R}}\, b\, z_{T_2,1} + w_{T_2,R}, \tag{3.10}$$

where w_{T_1} and $w_{T_2,R}$ denote zero-mean AWGN with a variance of N_0 at T_1 and the relay, respectively. Then, the two rotated symbols, $x_{T_2,1}$ and $x_{T_2,2}$, are detected using the transmitted SSD symbol, $z_{T_2,1}$, at the relay as

$$\hat{x}_{T_2,1} = \arg\min_{x\in\Phi_r} \left| \Re\{b^*\, y_{T_2R}\} - \sqrt{E_T \lambda_{T_2R}}\, |b|^2\, \Re\{x_{T_2,1}\} \right|^2, \tag{3.11}$$

$$\hat{x}_{T_2,2} = \arg\min_{x\in\Phi_r} \left| \Im\{b^*\, y_{T_2R}\} - \sqrt{E_T \lambda_{T_2R}}\, |b|^2\, \Im\{x_{T_2,2}\} \right|^2. \tag{3.12}$$

The SSD symbol received from a terminal at the relay consists of two components that represents two different original symbols. If the relay successfully decodes an SSD symbol, $z_{T_1,1}$, from T_1, it can recover both symbols, $x_{T_1,1}$ and $x_{T_1,2}$, correctly due to the SSD technique. Similarly, the relay can recover $x_{T_2,1}$ and $x_{T_2,2}$ correctly upon successful decoding of $z_{T_2,1}$ from T_2. A failure in decoding is conveyed through a reliable feedback channel to the terminals. These assumptions are based on ARQ and CRC protection features which are part of the advanced wireless standards such as IEEE 802.16 [66]. The relay (R) forwards the combined signal of $z_{T_1,2}$ and $z_{T_2,2}$

to the terminals in the third time slot, as shown in Figure 3.2. Thus, the received signals at the terminals can be written as

$$y_{RT_1} = \sqrt{E_R \lambda_{T_1 R}}\, a\, z_{T_1,2} + \sqrt{E_R \lambda_{T_1 R}}\, a\, z_{T_2,2} + w_{1,2}, \tag{3.13}$$

$$y_{RT_2} = \sqrt{E_R \lambda_{T_2 R}}\, b\, z_{T_1,2} + \sqrt{E_R \lambda_{T_2 R}}\, b\, z_{T_2,2} + w_{2,2}, \tag{3.14}$$

where $w_{1,2}$ and $w_{2,2}$ denote zero-mean AWGN with a variance of N_0 at T_1 and T_2, respectively. Since each terminal perfectly knows its transmitted signal, it can cancel the self-interference term and decode the received symbol. The resulting signals at T_1 and T_2 can be written as

$$y_{RT_1} = \sqrt{E_R \lambda_{T_1 R}}\, a\, z_{T_2,2} + w_{1,2}, \tag{3.15}$$

$$y_{RT_2} = \sqrt{E_R \lambda_{T_2 R}}\, b\, z_{T_1,2} + w_{2,2}. \tag{3.16}$$

Let $\mathbf{r}_{T_1} = (r_{T_1,1}, r_{T_1,2})$ be the signal after component de-interleaver at T_2, transmitted by T_1, which can be expressed as

$$r_{T_1,1} = \Re\{h^*\, y_{T_1 T_2}\} + j\Im\{b^*\, y_{RT_2}\}, \tag{3.17}$$

$$r_{T_1,2} = \Re\{b^*\, y_{RT_2}\} + j\Im\{h^*\, y_{T_1 T_2}\}. \tag{3.18}$$

The maximum likelihood detection is applied at T_2 to detect the message transmitted by T_1 using

$$\hat{x}_{T_1,1} = \arg \min_{x \in \Phi_r} \left[\left| \Re\{r_{T_1,1}\} - \sqrt{E_T}|h|^2 \Re\{x_{T_1,1}\} \right|^2 + \left| \Im\{r_{T_1,1}\} - \sqrt{E_R \lambda_{T_2 R}}|b|^2 \Im\{x_{T_1,1}\} \right|^2 \right], \tag{3.19}$$

$$\hat{x}_{T_1,2} = \arg\min_{x\in\Phi_r} \left[\left| \Re\{r_{T_1,2}\} - \sqrt{E_R \lambda_{T_2R}}|b|^2 \Re\{x_{T_1,2}\} \right|^2 + \left| \Im\{r_{T_1,2}\} - \sqrt{E_T}|h|^2 \Im\{x_{T_1,2}\} \right|^2 \right]. \tag{3.20}$$

Similarly, the signal at T_1, $\mathbf{r}_{T_2} = (r_{T_2,1}, r_{T_2,2})$, after component de-interleaver can be expressed as

$$r_{T_2,1} = \Re\{h^* y_{T_2T_1}\} + j\Im\{a^* y_{RT_1}\}, \tag{3.21}$$

$$r_{T_2,2} = \Re\{a^* y_{RT_1}\} + j\Im\{h^* y_{T_2T_1}\}. \tag{3.22}$$

The message at T_1, transmitted by T_2, is detected using

$$\hat{x}_{T_2,1} = \arg\min_{x\in\Phi_r} \left[\left| \Re\{r_{T_2,1}\} - \sqrt{E_T}|h|^2 \Re\{x_{T_2,1}\} \right|^2 + \left| \Im\{r_{T_2,1}\} - \sqrt{E_R \lambda_{T_1R}}|a|^2 \Im\{x_{T_2,1}\} \right|^2 \right], \tag{3.23}$$

$$\hat{x}_{T_2,2} = \arg\min_{x\in\Phi_r} \left[\left| \Re\{r_{T_2,2}\} - \sqrt{E_R \lambda_{T_1R}}|a|^2 \Re\{x_{T_2,2}\} \right|^2 + \left| \Im\{r_{T_2,2}\} - \sqrt{E_T}|h|^2 \Im\{x_{T_2,2}\} \right|^2 \right]. \tag{3.24}$$

It is important to note that the 2W-SSC-1R system exchanges four symbols in three time slots. On the other hand, the conventional two-way cooperative system [37] requires three time slots to exchange two symbols, thus, requiring six time slots for four symbols. In addition, if one of the two transmitted SSD symbols is not received correctly at the other terminal in the 2W-SSC-1R system, it will still be able to recover both symbols from one SSD symbol due to the SSD technique. Therefore, the 2W-SSC-1R system increases the data rate, spectral efficiency and diversity when compared with the conventional two-way cooperative system without any additional bandwidth or transmit power.

3.2 Error Probability Analysis

In this section, a closed-form expression for the end-to-end error probability of the 2W-SSC-1R system over Rayleigh fading channel is derived. An asymptotic approximation of this error probability is also presented and examined to reveal the behaviour of the system as a function of its parameters.

3.2.1 Average Error Probability

The average symbol error probability (SEP) of the system depends on the probability that the relay detects the signal received from both source terminals with or without an error, and the probability of erroneous detection of signal received from one source terminal to the other. In addition, when the relay has correctly detected the received signals from the terminals, the average SEP of the system depends on the cooperative link between the relay and the terminals. Due to two-way communication, the analysis is first focused at T_2 for the signal received from T_1.

Let $\mathcal{P}_{\text{off}}$ denote the probability that the relay fails to detect both source signals correctly and remains silent during the third time slot. Also, let $\mathcal{P}_{\text{sym}}^{T_1,\text{coop}}(e)$ be the conditional error probability of the cooperative link between $\mathsf{T}_1 \rightarrow \mathsf{T}_2$ and $\mathsf{R} \rightarrow \mathsf{T}_2$ when the relay detects both source signals correctly. Furthermore, $\mathcal{P}_{\text{sym}}^{T_1T_2}(e)$, $\mathcal{P}_{\text{sym}}^{T_2T_1}(e)$, $\mathcal{P}_{\text{sym}}^{T_1R}(e)$ and $\mathcal{P}_{\text{sym}}^{T_2R}(e)$ be the error probabilities of a signal transmitted from T_1 to T_2 and T_2 to T_1, T_1 to R, and T_2 to R, respectively. Thus, the average SEP of the signal transmitted by T_1 can be written as

$$\mathcal{P}_{\text{sym}}^{\text{T}_1}(e) = \mathcal{P}_{\text{off}}\, \mathcal{P}_{\text{sym}}^{T_1T_2}(e) + [1 - \mathcal{P}_{\text{off}}]\, \mathcal{P}_{\text{sym}}^{T_1,\text{coop}}(e), \tag{3.25}$$

where

$$\mathcal{P}_{\text{off}} = 1 - \left[1 - \mathcal{P}_{\text{sym}}^{T_1R}(e)\right]\left[1 - \mathcal{P}_{\text{sym}}^{T_2R}(e)\right]. \tag{3.26}$$

The conditional SEP of a two-dimensional modulation for a given γ_{sa} of the $\mathsf{T}_1 \to \mathsf{R}$ link, $\mathcal{P}_{\text{sym}}^{T_1R}(e|\gamma_{sa})$, can be tightly upper bounded as

$$\mathcal{P}_{\text{sym}}^{T_1R}(e|\gamma_{sa}) \leq \alpha_z Q\left(\sqrt{\beta_z \gamma_{sa}}\right), \tag{3.27}$$

where $Q(u) = \frac{1}{\sqrt{2\pi}} \int_u^\infty e^{-t^2/2} dt$ is the Gaussian Q-function [67, 26.2.3], α_z and β_z are determined by the type of the expanded constellation and its size $|\Upsilon|$. For example, for M-QAM, $\alpha_z = 4$ and $\beta_z = 3/(|\Upsilon|-1)$; and for M-PSK, $\alpha_z = 2$ and $\beta_z = 2\sin^2(\pi/|\Upsilon|)$ [5]. Therefore, $\mathcal{P}_{\text{sym}}^{T_1R}(e)$ over Rayleigh fading channel can be written as

$$\mathcal{P}_{\text{sym}}^{T_1R}(e) \leq \int_0^\infty \alpha_z Q\left(\sqrt{\beta_z \gamma_{sa}}\right) f_{\gamma_{sa}}(\gamma_{sa})\, d\gamma_{sa}, \tag{3.28}$$

where $f_{\gamma_{sa}}(\gamma_{sa}) = \frac{1}{\overline{\gamma}_{sa}} e^{-\gamma_{sa}/\overline{\gamma}_{sa}}$ is the PDF of the SNR γ_{sa} [68]. Solving the integration in (3.28) using (A.12), $\mathcal{P}_{\text{sym}}^{T_1R}(e)$ can be written as

$$\mathcal{P}_{\text{sym}}^{T_1R}(e) \leq \frac{1}{2}\,\alpha_z \left(1 - \sqrt{\frac{\beta_z \overline{\gamma}_{sa}}{\beta_z \overline{\gamma}_{sa} + 2}}\right). \tag{3.29}$$

Similarly, the SEP at the relay for a signal received from by T_2 over Rayleigh fading channel is given by

$$\mathcal{P}_{\text{sym}}^{T_2R}(e) \leq \frac{1}{2}\,\alpha_z \left(1 - \sqrt{\frac{\beta_z \overline{\gamma}_{sb}}{\beta_z \overline{\gamma}_{sb} + 2}}\right), \tag{3.30}$$

and the SEP at T_2 for a signal received from by T_1 over Rayleigh fading channel is

given by

$$\mathcal{P}_{\text{sym}}^{T_1T_2}(e) \leq \frac{1}{2}\,\alpha_z \left(1 - \sqrt{\frac{\beta_z \overline{\gamma}_h}{\beta_z \overline{\gamma}_h + 2}}\right). \tag{3.31}$$

The SEP of the cooperative link between $\mathsf{T}_1 \rightarrow \mathsf{T}_2$ and $\mathsf{R} \rightarrow \mathsf{T}_2$ depends on the total SNR of the cooperative link, $\gamma_{e_1} = \gamma_h + \gamma_b$. Thus, the SEP of the cooperative link for given SNRs γ_a, γ_b and γ_h can be represented as

$$\mathcal{P}_{\text{sym}}^{T_1,\text{coop}}(e|\gamma_h, \gamma_a, \gamma_b) = \alpha_x Q\left(\sqrt{\beta_x \gamma_{e_1}}\right), \tag{3.32}$$

where $\alpha_x = 2(|\Phi_r| - 1)/|\Phi_r|$, $\beta_x = 3/(|\Phi_r|^2 - 1)$ [5]. Thus, $\mathcal{P}_{\text{sym}}^{T_1,\text{coop}}(e)$ over the fading channel can be written as

$$\mathcal{P}_{\text{sym}}^{T_1,\text{coop}}(e) = \int_0^\infty \alpha_x Q\left(\sqrt{\beta_x \gamma_{e_1}}\right) f_{\gamma_{e_1}}\left(\gamma_{e_1}\right) d\gamma_{e_1}, \tag{3.33}$$

where $f_{\gamma_{e_1}}(\gamma_{e_1})$ is the PDF of the SNR γ_{e_1}, which is evaluated by convolving $f_{\gamma_h}(\gamma) = \frac{1}{\overline{\gamma}_h} e^{-\gamma/\overline{\gamma}_h}$ and $f_{\gamma_b}(\gamma) = \frac{1}{\overline{\gamma}_b} e^{-\gamma_b/\overline{\gamma}_b}$, thus using (C.6) $f_{\gamma_{e_1}}(\gamma)$ can be expressed as

$$f_{\gamma_{e_1}}(\gamma) = \frac{1}{\overline{\gamma}_h - \overline{\gamma}_b}\left(e^{-\gamma/\overline{\gamma}_h} - e^{-\gamma/\overline{\gamma}_b}\right). \tag{3.34}$$

Substituting (3.34) in (3.33) and solving the integration using (A.12), $\mathcal{P}_{\text{sym}}^{T_1,\text{coop}}(e)$ can be expressed as

$$\mathcal{P}_{\text{sym}}^{T_1,\text{coop}}(e) = \frac{\alpha_x}{2}\,\frac{1}{\overline{\gamma}_h - \overline{\gamma}_b}\left\{\overline{\gamma}_h\left(1 - \sqrt{\frac{\beta_x \overline{\gamma}_h}{\beta_x \overline{\gamma}_h + 2}}\right) - \overline{\gamma}_b\left(1 - \sqrt{\frac{\beta_x \overline{\gamma}_b}{\beta_x \overline{\gamma}_b + 2}}\right)\right\} \tag{3.35}$$

Finally, substituting (3.29), (3.30), (3.31) and (3.35) into (3.25), a closed-form expression for the average SEP at terminal T_2 for the signal transmitted by T_1 can be easily obtained. It is noted that a similar expression can be obtained for the average

SEP at terminal T_1 for the signal transmitted by T_2, $\mathcal{P}_{\text{sym}}^{T_2}(e)$, by following the same procedure or simply interchanging $\overline{\gamma}_b$ and $\overline{\gamma}_a$ in the expression for $\mathcal{P}_{\text{sym}}^{T_1}(e)$. Thus, the end-to-end average SEP of the 2W-SSC-1R system can be obtained using the following expression

$$\mathcal{P}_{\text{sym}}^{e2e}(e) = \frac{\mathcal{P}_{\text{sym}}^{T_1}(e) + \mathcal{P}_{\text{sym}}^{T_2}(e)}{2}. \tag{3.36}$$

3.2.2 Asymptotic Error Probability

Although the derived average SEP expression of the system is very useful in evaluating the error performance of the system, it is not straightforward to use this expression to quantify the diversity gain and the effect of system parameters. Consequently, simple asymptotic SEP expression is derived, which is of special interest in moderate to high SNR region. The asymptotic SEP at terminal T_2 for the signal transmitted by T_1 can be expressed as

$$\mathcal{P}_{\text{sym}}^{T_1}(e) \simeq \mathcal{P}_{\text{off}}\, \mathcal{P}_{\text{sym}}^{T_1 T_2}(e) + \mathcal{P}_{\text{sym}}^{T_1,\text{coop}}(e). \tag{3.37}$$

For high SNR, $\mathcal{P}_{\text{off}}$ from (3.26) can be approximated as

$$\mathcal{P}_{\text{off}} \approx \mathcal{P}_{\text{sym}}^{T_1 R}(e) + \mathcal{P}_{\text{sym}}^{T_2 R}(e). \tag{3.38}$$

Utilizing the Taylor series expansion of the exponential function and neglecting the higher order terms, the PDF of γ_{sa} can be approximated as

$$f_{\gamma_{sa}}(\gamma) \simeq \frac{1}{\overline{\gamma}_{sa}}. \tag{3.39}$$

Thus, the approximate symbol error probabilities can be written as

$$\mathcal{P}_{\text{sym}}^{T_1R}(e) \simeq \frac{\alpha_z}{2\beta_z}\frac{1}{\overline{\gamma}_{sa}}, \tag{3.40}$$

$$\mathcal{P}_{\text{sym}}^{T_2R}(e) \simeq \frac{\alpha_z}{2\beta_z}\frac{1}{\overline{\gamma}_{sb}}, \tag{3.41}$$

and

$$\mathcal{P}_{\text{sym}}^{T_1T_2}(e) \simeq \frac{\alpha_z}{2\beta_z}\frac{1}{\overline{\gamma}_{h}}. \tag{3.42}$$

The PDF of γ_{e_1} from (3.34) using the Taylor series expansion can be approximated as

$$f_{\gamma_{e_1}}(\gamma) \simeq \frac{1}{\overline{\gamma}_h\overline{\gamma}_b}. \tag{3.43}$$

Thus,

$$\mathcal{P}_{\text{sym}}^{T_1,\text{coop}}(e) \simeq \frac{\alpha_x}{2\beta_x}\frac{1}{\overline{\gamma}_h\overline{\gamma}_b}, \tag{3.44}$$

From (3.37), (3.40), (3.41), (3.42) and (3.44), the asymptotic SEP at terminal T_2 for the signal transmitted by T_1 can be written as

$$\mathcal{P}_{\text{sym}}^{T_1}(e) \simeq \left(\frac{\alpha_z}{2\beta_z}\right)^2 \frac{1}{\overline{\gamma}_h}\left(\frac{1}{\overline{\gamma}_{sa}}+\frac{1}{\overline{\gamma}_{sb}}\right) + \frac{\alpha_x}{2\beta_x}\frac{1}{\overline{\gamma}_h\overline{\gamma}_b} \tag{3.45}$$

Similarly, the asymptotic SEP at terminal T_1 for the signal transmitted by T_2, $\mathcal{P}_{\text{sym}}^{T_2}(e)$, can be obtained by interchanging $\overline{\gamma}_b$ and $\overline{\gamma}_a$ in (3.45). Thus, the end-to-end asymptotic SEP of the 2W-SSC-1R system can be written as

$$\mathcal{P}_{\text{sym}}^{e2e}(e) \simeq \left(\frac{\alpha_z}{2\beta_z}\right)^2 \frac{1}{\overline{\gamma}_h}\left(\frac{1}{\overline{\gamma}_{sa}}+\frac{1}{\overline{\gamma}_{sb}}\right) + \frac{\alpha_x}{4\beta_x}\left(\frac{1}{\overline{\gamma}_h\overline{\gamma}_a}+\frac{1}{\overline{\gamma}_h\overline{\gamma}_b}\right) \tag{3.46}$$

3.3 Results and Discussion

In this section, the numerical results are presented to illustrate the error performance of the 2W-SSC-1R system using the derived analytical expressions and numerical simulations over a slow Rayleigh fading channel. The analytical results are validated using Monte Carlo simulations, which were performed with 10^9 trials for each simulation point for accuracy and correctness. The variances of channel coefficients are set to $\sigma_h^2 = \sigma_a^2 = \sigma_b^2 = 1$ and the path loss exponent to $\nu = 3$. The 2W-SSC-1R system is assumed to have a single relay located at the middle of the terminals. For the fair analysis, the total power budget to exchange four symbols in the 2W-SSC-1R system is equivalent to that of the direct transmission system, thus $E_T = 1$ for first and second time slots and $E_R = 2$ for the third time slot, making the total power budget equals to 4 units.

Figure 3.3 compares the error performance of the 2W-SSC-1R system with the conventional two-way cooperative and direct transmission systems using 4-QAM. The SSD scheme is using 4-QAM modulation with rotation angle of 26.6°. In this figure, the average bit error probabilities (BEP) of 2W-SSC-1R, conventional two-way and direct transmission systems are represented by solid line, ○ and □ markers, respectively. It is evident from the figure that the 2W-SSC-1R system has nearly the same performance as the conventional two-way cooperative system. It is observed that both two-way cooperative systems have improved performance than the direct transmission system, which is obviously due to the diversity gain by using relay. For example, BEP=10^{-3} can be obtained at $E_b/N_0 = 16$ dB with the 2W-SSC-1R system, or at $E_b/N_0 = 24$ dB with the direct transmission system, thus achieving an E_b/N_0 gain of about 8 dB.

Figure 3.4 shows the average BEP of the 2W-SSC-1R system using 4-QAM as a

function of the average SNR (E_b/N_0). The simulation result in this plot is represented by $\diamond$ markers while analytical and asymptotic results are shown by solid and dashed lines, respectively. It is clear from this figure that analytical results for the error probability, given in (3.36), are in perfect agreement with the simulation results, thus validating the derived mathematical expressions. Also, the asymptotic results, given by (3.46), are tight and have a good match with the analytical and simulation results at medium and high SNRs. It is observed that beyond $E_b/N_0 = 13$ dB asymptotic error probability follows the exact error probability.

In order to show the robustness of the 2W-SSC-1R system with higher order modulation scheme, the average BEP of the 2W-SSC-1R system using 16-QAM with $\theta = 13.8^\circ$ is illustrated in Figure 3.5. The average BEP of the conventional direct transmission using 16-QAM is also shown for comparison. It is observed from figure that the 2W-SSC-1R system provides an E_b/N_0 gain of 11 dB to achieve an average BEP of 10^{-4} compared to the direct transmission system.

3.4 Summary

In this chapter, a two-way cooperative system with signal space diversity using a single DF relay is presented and its performance was analyzed. The error probability expression of the 2W-SSC-1R system was derived over the Rayleigh fading channel. The closed-form expression for the asymptotic error probability was obtained. The error performance of the 2W-SSC-1R system was found nearly same as the performance of the conventional two-way cooperative system. Thus, it was shown that the 2W-SSC-1R system enhances the performance and doubles the spectral efficiency compared to the conventional two-way cooperative system system without degrading the system performance. This 2W-SSC-1R system can be further enhanced with the

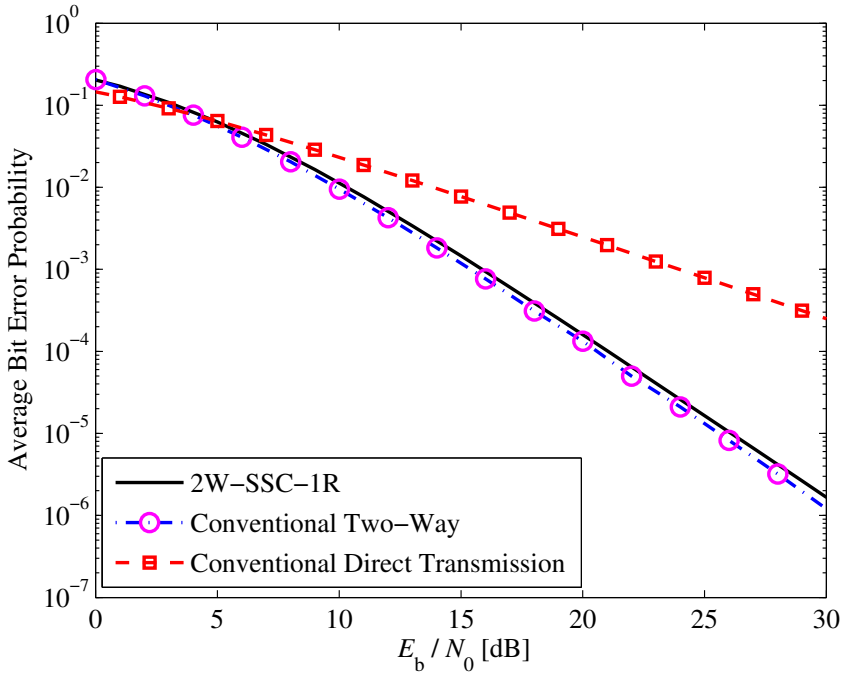

Figure 3.3: Error performance comparison of the 2W-SSC-1R system with the conventional two-way and direct transmission systems using 4-QAM.

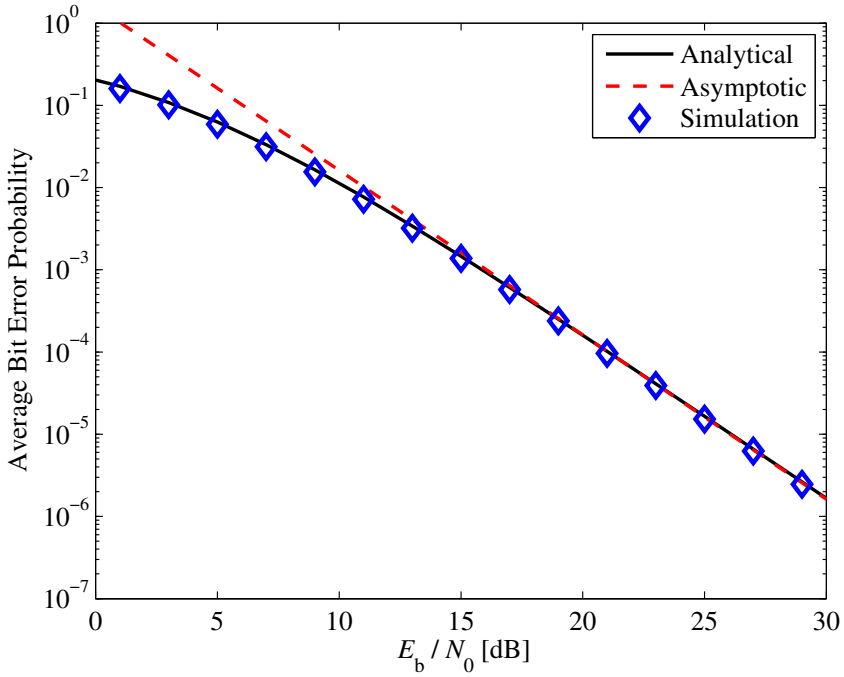

Figure 3.4: Error probability of the 2W-SSC-1R system using 4-QAM.

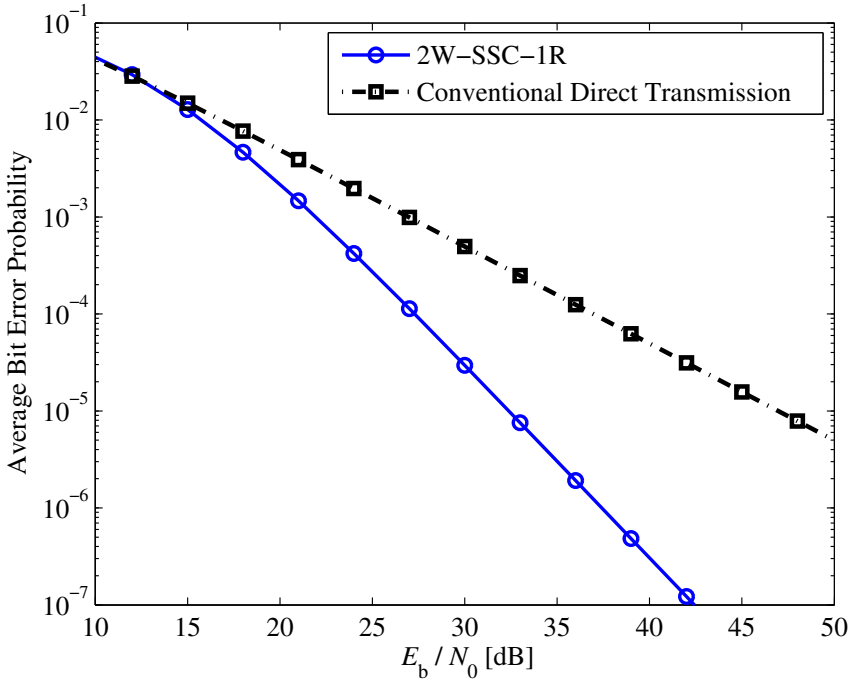

Figure 3.5: Error probability of 2W-SSC-1R and direct transmission systems using 16-QAM.

use of multiple relays to improve the diversity order and the system performance, which is presented in the next chapter.

Chapter 4

Two-Way Signal Space Cooperative System using Multiple Relays

In the previous chapter, the two-way signal space cooperative system (2W-SSC-1R) that uses a single DF relay is considered and its performance analysis along with numerical results are presented. This chapter extends the use of multiple intermediate relays into the two-way signal space cooperative system. Hereafter, this proposed system will be referred to as 2W-SSC. This chapter presents the comprehensive analysis of the 2W-SSC system for various performance metrics including error probability, outage probability and channel capacity. In addition, this chapter addresses the optimality relay location, power allocation and the best relay selection.

In the 2W-SSC system, each source terminal broadcasts its first symbol from the expanded constellation to the other terminal and the relays in two different time slots, i.e. the first and the second time slots. Then, these first symbols received from both terminals are decoded and their second symbols are recovered at the relays. Based on the channel conditions between the relays and the terminals, the best relay is selected from the group of relays that have correctly decoded the symbols. This best relay then forwards both second symbols to the terminals in the third time slot. Thus, there are four symbols exchanged in three time slots which implies doubling of spectral efficiency and data transmission, without adding extra complexity, bandwidth or

transmit power. This is in contrast to the exchange of two symbols over three time slots in the conventional two-way cooperative system.

This chapter is organized as follows: Section 4.1 describes the system and channel models of the 2W-SSC system. Section 4.2 deals with the derivations of closed-form expressions for the average symbol error probability (SEP), asymptotic SEP and the diversity order of the system. Section 4.3 examines the optimization of relay position and power allocations to source terminals and relays. Section 4.4 presents the analysis for exact and asymptotic outage probability of the system. Section 4.5 demonstrates the derivations for average channel capacity and an upper bound on channel capacity. Section 4.6 compares and analyzes analytical and simulation results, and Section 4.7 summarizes the chapter.

4.1 System Model

Figure 4.1 shows the proposed two-way signal space cooperative system, which consists of two source terminals (T_1 and T_2) and K number of relays (R_i, $i = 1, 2, ..., K$), each equipped with one antenna and operates in half-duplex mode. In this system, both T_1 and T_2 communicate with each other directly and through K relays over slow Rayleigh fading channel. The channel information is available at all the receiving nodes as well as at the K relays. The channel coefficients of $\mathsf{T}_1 \rightarrow \mathsf{T}_2$, $\mathsf{R}_i \rightarrow \mathsf{T}_1$ and $\mathsf{R}_i \rightarrow \mathsf{T}_2$ links are denoted as h, a_i and b_i with variances σ_h^2, σ_a^2 and σ_b^2, respectively. The channel coefficients are assumed to be reciprocal and to remain constant during each transmission phase. The channels are assumed to be mutually independent and have no interference with each other.

The total transmit power constraint E_{tot} is imposed on the exchange of every four symbols in three time slots at both terminals and the best relay. For a fair analy-

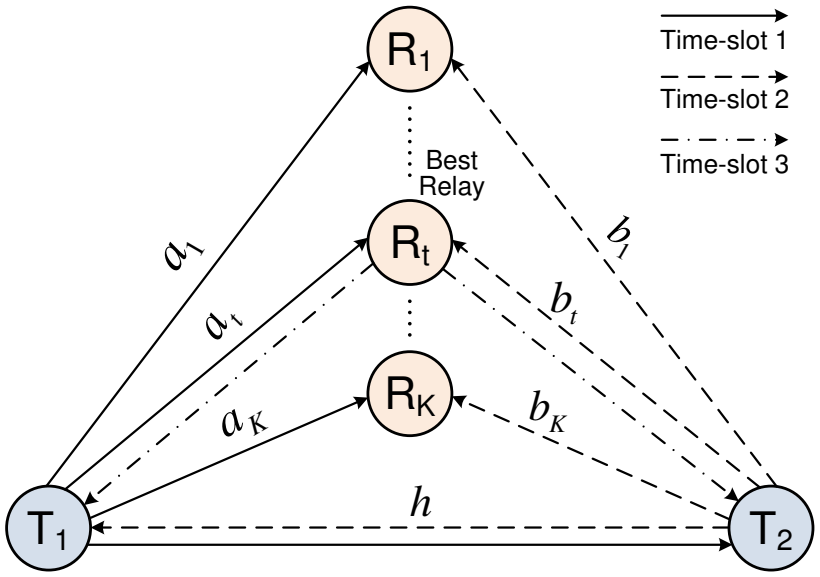

Figure 4.1: System model of the two-way signal space cooperative system (2W-SSC) with K DF relays.

sis, the total transmit power E_{tot} is always equal to the total energy of four symbols. The symbol energies at both terminals (T_1 and T_2) and at the relays (R_i) are denoted as E_{T_1}, E_{T_2} and E_R, respectively. Zero-mean additive white Gaussian noise (AWGN) with variance N_0 is assumed over all channels. The distances of $\mathsf{T}_1 - \mathsf{T}_2$, $\mathsf{T}_1 - \mathsf{R}_i$ and $\mathsf{T}_2 - \mathsf{R}_i$ links are denoted as $d_{T_1T_2}$, d_{T_1R} and d_{T_2R}, respectively, and their geometric gains are represented as $\lambda_{T_1R} = (d_{T_1T_2}/d_{T_1R})^{\nu}$ and $\lambda_{T_2R} = (d_{T_1T_2}/d_{T_2R})^{\nu}$, respectively, where ν is the path loss exponent. The instantaneous signal-to-noise ratios (SNRs) of $\mathsf{T}_1 \to \mathsf{T}_2$, $\mathsf{T}_2 \to \mathsf{T}_1$, $\mathsf{T}_1 \to \mathsf{R}_i$, $\mathsf{T}_2 \to \mathsf{R}_i$, $\mathsf{R}_i \to \mathsf{T}_1$ and $\mathsf{R}_i \to \mathsf{T}_2$ links are denoted as $\gamma_{h_1} = |h|^2 E_{T_1}/N_0$, $\gamma_{h_2} = |h|^2 E_{T_2}/N_0$, $\gamma_{sa_i} = |a_i|^2 \lambda_{T_1R} E_{T_1}/N_0$, $\gamma_{sb_i} = |b_i|^2 \lambda_{T_2R} E_{T_2}/N_0$, $\gamma_{a_i} = |a_i|^2 \lambda_{T_1R} E_R/N_0$ and $\gamma_{b_i} = |b_i|^2 \lambda_{T_2R} E_R/N_0$, while average SNRs are $\overline{\gamma}_{h_1} = \sigma_h^2 E_{T_1}/N_0$, $\overline{\gamma}_{h_2} = \sigma_h^2 E_{T_2}/N_0$, $\overline{\gamma}_{sa} = \sigma_a^2 \lambda_{T_1R} E_{T_1}/N_0$, $\overline{\gamma}_{sb} = \sigma_b^2 \lambda_{T_2R} E_{T_2}/N_0$, $\overline{\gamma}_a = \sigma_a^2 \lambda_{T_1R} E_R/N_0$ and $\overline{\gamma}_b = \sigma_b^2 \lambda_{T_2R} E_R/N_0$, respectively.

In the 2W-SSC system, SSD is used at the terminals and the relays. First, each $m = \log_2(M)$ information bits at each source terminal are grouped and mapped to

a point in the ordinary constellation either M-ary quadrature amplitude modulation (M-QAM) or M-ary phase-shift keying (M-PSK) modulation.

Let $\mathbf{s}_{T_1} = (s_{T_1,1}, s_{T_1,2})$ be the two original signal points of source terminal T_1 from the ordinary constellation Φ (e.g. 4-QAM, or QPSK), i.e. $s_1, s_2 \in \Phi$. The original complex symbols can be denoted as $s_{T_1,1} = \Re\{s_{T_1,1}\} + j\Im\{s_{T_1,1}\}$ and $s_{T_1,2} = \Re\{s_{T_1,2}\} + j\Im\{s_{T_1,2}\}$, where $j = \sqrt{-1}$, and $\Re\{\cdot\}$ and $\Im\{\cdot\}$ are I and Q components of the symbols, respectively. Then, $s_{T_1,1}$ and $s_{T_1,2}$ are rotated by the angle θ, i.e. $x_{T_1,1} = s_{T_1,1}\, e^{j\theta}$ and $x_{T_1,2} = s_{T_1,2}\, e^{j\theta}$. The rotated symbols, $\mathbf{x}_{T_1} = (x_{T_1,1}, x_{T_1,2})$, correspond to a rotated constellation Φ_r. The new SSD symbols, $\mathbf{z}_{T_1} = (z_{T_1,1}, z_{T_1,2})$, for transmission are formed by interleaving the Q components of the rotated symbols, $x_{T_1,1}$ and $x_{T_1,2}$, and are given by

$$z_{T_1,1} = \Re\{x_{T_1,1}\} + j\Im\{x_{T_1,2}\}, \tag{4.1}$$

$$z_{T_1,2} = \Re\{x_{T_1,2}\} + j\Im\{x_{T_1,1}\}. \tag{4.2}$$

The SSD symbols, $z_{T_1,1}$ and $z_{T_1,2}$, for transmission from T_1 belong to an expanded constellation Υ. In the first time slot, T_1 broadcasts only one of the two SSD symbols (i.e. $z_{T_1,1}$). Thus, the received signal at T_2 and the ith relay can be written as

$$y_{T_1T_2} = \sqrt{E_{T_1}}\, h\, z_{T_1,1} + w_{T_2,1}, \tag{4.3}$$

$$y_{T_1R_i} = \sqrt{E_{T_1}\lambda_{T_1R}}\, a_i\, z_{T_1,1} + w_{T_1,R_i}, \tag{4.4}$$

where $w_{T_2,1}$ and w_{T_1,R_i} denote zero-mean AWGN with a variance of N_0 at T_2 and the ith relay, respectively. The two rotated symbols, $x_{T_1,1}$ and $x_{T_1,2}$, are detected

using the transmitted SSD symbol, $z_{T_1,1} = \Re\{x_{T_1,1}\} + j\Im\{x_{T_1,2}\}$, at the ith relay as

$$\hat{x}_{T_1,1} = \arg\min_{x\in\Phi_r} \left| \Re\{a_i^* \, y_{T_1R_i}\} - \sqrt{E_{T_1}\lambda_{T_1R}}\,|a_i|^2\,\Re\{x_{T_1,1}\} \right|^2, \tag{4.5}$$

$$\hat{x}_{T_1,2} = \arg\min_{x\in\Phi_r} \left| \Im\{a_i^* \, y_{T_1R_i}\} - \sqrt{E_{T_1}\lambda_{T_1R}}\,|a_i|^2\,\Im\{x_{T_1,2}\} \right|^2, \tag{4.6}$$

where $*$ denotes complex conjugation.

Secondly, T_2 prepares two SSD symbols, $z_{T_2,1}$ and $z_{T_2,2}$, by component interleaving of its two rotated symbols, $x_{T_2,1}$ and $x_{T_2,2}$, as

$$z_{T_2,1} = \Re\{x_{T_2,1}\} + j\Im\{x_{T_2,2}\}, \tag{4.7}$$

$$z_{T_2,2} = \Re\{x_{T_2,2}\} + j\Im\{x_{T_2,1}\}. \tag{4.8}$$

Similarly, in the second time slot, T_2 broadcasts only one of the two SSD symbols (i.e. $z_{T_2,1}$), which is received at T_1 and the ith relay as

$$y_{T_2T_1} = \sqrt{E_{T_2}}\,h\,z_{T_2,1} + w_{T_1,1}, \tag{4.9}$$

$$y_{T_2R_i} = \sqrt{E_{T_2}\lambda_{T_2R}}\,b_i\,z_{T_2,1} + w_{T_2,R_i}, \tag{4.10}$$

where $w_{T_1,1}$ and w_{T_2,R_i} denote zero-mean AWGN with a variance of N_0 at T_1 and the ith relay, respectively. Then, the two rotated symbols, $x_{T_2,1}$ and $x_{T_2,2}$, are detected using the transmitted SSD symbol, $z_{T_2,1}$, at the ith relay as

$$\hat{x}_{T_2,1} = \arg\min_{x\in\Phi_r} \left| \Re\{b_i^* \, y_{T_2R_i}\} - \sqrt{E_{T_2}\lambda_{T_2R}}\,|b_i|^2\,\Re\{x_{T_2,1}\} \right|^2, \tag{4.11}$$

$$\hat{x}_{T_2,2} = \arg\min_{x\in\Phi_r} \left| \Im\{b_i^* \, y_{T_2R_i}\} - \sqrt{E_{T_2}\lambda_{T_2R}}\,|b_i|^2\,\Im\{x_{T_2,2}\} \right|^2. \tag{4.12}$$

Due to the SSD technique, an SSD symbol received from a terminal at the relays

consists of two components to represent two different original symbols. If the relay successfully decodes an SSD symbol, $z_{T_1,1}$, from T_1, it can recover both symbols, $x_{T_1,1}$ and $x_{T_1,2}$, correctly due to the SSD technique. Similarly, the relay can recover $x_{T_2,1}$ and $x_{T_2,2}$ correctly upon successful decoding of $z_{T_2,1}$ from T_2. Otherwise, the failure in decoding is conveyed through a reliable feedback channel to the terminals.

Let $\mathcal{C}$ be the set of relays that have correctly decoded the messages in the first and second time slots, and $|\mathcal{C}|$ its cardinality. Let R_t be the best relay among the relays that correctly decode both source messages and have good channel conditions to both terminals. Thus, the relay selection criteria, based on γ_{a_i} and γ_{b_i}, can be expressed as

$$\mathsf{R}_t = \arg\max_{i \in \mathcal{C}} \left\{ \min\left(\gamma_{a_i}, \gamma_{b_i}\right) \right\}. \tag{4.13}$$

The best relay (R_t) then forwards the combined signal of $z_{T_1,2}$ and $z_{T_2,2}$ to both terminals in the third time slot. Thus, the received signals at both terminals can be written as

$$y_{R_tT_1} = \sqrt{E_R \lambda_{T_1R}}\, a_t\, z_{T_1,2} + \sqrt{E_R \lambda_{T_1R}}\, a_t\, z_{T_2,2} + w_{1,2}, \tag{4.14}$$

$$y_{R_tT_2} = \sqrt{E_R \lambda_{T_2R}}\, b_t\, z_{T_1,2} + \sqrt{E_R \lambda_{T_2R}}\, b_t\, z_{T_2,2} + w_{2,2}, \tag{4.15}$$

where $w_{1,2}$ and $w_{2,2}$ denote zero-mean AWGN with a variance of N_0 at T_1 and T_2, respectively. Since each terminal perfectly knows its transmitted signal, it can cancel the self-interference term. Thus, the resulting signals at T_1 and T_2 can be written as

$$y_{R_tT_1} = \sqrt{E_R \lambda_{T_1R}}\, a_t\, z_{T_2,2} + w_{1,2}, \tag{4.16}$$

$$y_{R_tT_2} = \sqrt{E_R \lambda_{T_2R}}\, b_t\, z_{T_1,2} + w_{2,2}. \tag{4.17}$$

Let $\mathbf{r}_{T_1} = (r_{T_1,1}, r_{T_1,2})$ be the signal after component de-interleaver at T_2, received from T_1, which can be expressed as

$$r_{T_1,1} = \Re\{h^*\, y_{T_1T_2}\} + j\Im\{b_t^*\, y_{R_tT_2}\}, \tag{4.18}$$

$$r_{T_1,2} = \Re\{b_t^*\, y_{R_tT_2}\} + j\Im\{h^*\, y_{T_1T_2}\}. \tag{4.19}$$

The maximum likelihood detection is applied at T_2 to detect the message received from T_1 using

$$\begin{aligned}\hat{x}_{T_1,1} = \arg\min_{x\in\Phi_r} \Bigg[&\left|\Re\{r_{T_1,1}\} - \sqrt{E_{T_1}}|h|^2\Re\{x_{T_1,1}\}\right|^2 \\ &+ \left|\Im\{r_{T_1,1}\} - \sqrt{E_R\lambda_{T_2R}}|b_t|^2\Im\{x_{T_1,1}\}\right|^2\Bigg], \end{aligned}\tag{4.20}$$

$$\begin{aligned}\hat{x}_{T_1,2} = \arg\min_{x\in\Phi_r} \Bigg[&\left|\Re\{r_{T_1,2}\} - \sqrt{E_R\lambda_{T_2R}}|b_t|^2\Re\{x_{T_1,2}\}\right|^2 \\ &+ \left|\Im\{r_{T_1,2}\} - \sqrt{E_{T_1}}|h|^2\Im\{x_{T_1,2}\}\right|^2\Bigg]. \end{aligned}\tag{4.21}$$

Similarly, the signal at T_1, $\mathbf{r}_{T_2} = (r_{T_2,1}, r_{T_2,2})$, after component de-interleaver can be expressed as

$$r_{T_2,1} = \Re\{h^*\, y_{T_2T_1}\} + j\Im\{a_t^*\, y_{R_tT_1}\}, \tag{4.22}$$

$$r_{T_2,2} = \Re\{a_t^*\, y_{R_tT_1}\} + j\Im\{h^*\, y_{T_2T_1}\}. \tag{4.23}$$

The message at T_1, received from T_2, is detected as

$$\begin{aligned}\hat{x}_{T_2,1} = \arg\min_{x\in\Phi_r} \Bigg[&\left|\Re\{r_{T_2,1}\} - \sqrt{E_{T_2}}|h|^2\Re\{x_{T_2,1}\}\right|^2 \\ &+ \left|\Im\{r_{T_2,1}\} - \sqrt{E_R\lambda_{T_1R}}|a_t|^2\Im\{x_{T_2,1}\}\right|^2\Bigg], \end{aligned}\tag{4.24}$$

$$\hat{x}_{T_2,2} = \arg \min_{x \in \Phi_r} \left[\left| \Re\{r_{T_2,2}\} - \sqrt{E_R \lambda_{T_1 R}} |a_t|^2 \Re\{x_{T_2,2}\} \right|^2 + \left| \Im\{r_{T_2,2}\} - \sqrt{E_{T_2}} |h|^2 \Im\{x_{T_2,2}\} \right|^2 \right]. \quad (4.25)$$

It is important to note that in the 2W-SSC system, there are four symbols exchanged in three time slots. In contrast, in the conventional two-way cooperative system [37], three time slots are required to exchange two symbols, thus, requiring six time slots for four symbols. In addition, if one of the two transmitted SSD symbols are not received correctly at the other terminal in the 2W-SSC system, it will still be able to recover both symbols from one SSD symbol due to the SSD technique. The 2W-SSC system therefore increases the data rate, spectral efficiency and diversity as compared to the conventional two-way cooperative system, without additional bandwidth or transmit power.

4.2 Error Probability Analysis

In this section, a closed-form expression for the end-to-end error probability of the 2W-SSC system is derived over Rayleigh fading channel. Moreover, an asymptotic approximation of the error probability and diversity gain of the system are given.

4.2.1 Average Error Probability

The average symbol error probability (SEP) of the system depends on the probability that the relays detect the signal received from both terminals with or without an error, and the probability of erroneous detection of signal received from one terminal to the other. In addition, when a set of relays is available that have correctly detected the received signals from both terminals, the average SEP of the system depends

on the cooperative links between the best relay and the terminals. Due to two-way communication, the analysis is first focused at T_2 for the signal received from T_1. $\Pr\{|\mathcal{C}| = 0\}$ denotes the probability that no relay is able to correctly detect the signals received from both terminals, and $\Pr\{|\mathcal{C}| = k\}$ the probability that k relays detect signals from source terminals correctly. Let $\mathcal{P}_{\text{sym}}^{T_1,\text{coop}}(e|k)$ be the conditional error probability of the cooperative link between $\mathsf{T}_1 \rightarrow \mathsf{T}_2$ and $\mathsf{R}_t \rightarrow \mathsf{T}_2$ when k relays detect both signals from the terminals correctly. Furthermore, $\mathcal{P}_{\text{sym}}^{T_1T_2}(e)$ and $\mathcal{P}_{\text{sym}}^{T_2T_1}(e)$ are the error probabilities of a signal transmitted from T_1 to T_2 and T_2 to T_1, respectively. Thus, the average SEP of the signal received from T_1 can be written as

$$\mathcal{P}_{\text{sym}}^{\mathrm{T}_1}(e) = \Pr\{|\mathcal{C}| = 0\}\mathcal{P}_{\text{sym}}^{T_1T_2}(e) + \sum_{k=1}^{K} \Pr\{|\mathcal{C}| = k\}\mathcal{P}_{\text{sym}}^{T_1,\text{coop}}(e|k), \tag{4.26}$$

where

$$\Pr\{|\mathcal{C}| = 0\} = [\mathcal{P}_{\text{off}}]^K, \tag{4.27}$$

$$\Pr\{|\mathcal{C}| = k\} = \binom{K}{k} [\mathcal{P}_{\text{off}}]^{K-k} [1 - \mathcal{P}_{\text{off}}]^k, \tag{4.28}$$

where $\mathcal{P}_{\text{off}}$ denotes the probability that a relay fails to detect both source signals correctly and remains silent during the third time slot. If $\mathcal{P}_{\text{sym}}^{T_1R_i}(e)$ and $\mathcal{P}_{\text{sym}}^{T_2R_i}(e)$ denote the error probabilities at the ith relay for signal received from T_1 and T_2, respectively. Then, $\mathcal{P}_{\text{off}}$ can be written as

$$\mathcal{P}_{\text{off}} = 1 - \left[1 - \mathcal{P}_{\text{sym}}^{T_1R_i}(e)\right] \left[1 - \mathcal{P}_{\text{sym}}^{T_2R_i}(e)\right]. \tag{4.29}$$

The average SEP of T_1 can then be expressed as

$$\mathcal{P}_{\text{sym}}^{T_1}(e) = [\mathcal{P}_{\text{off}}]^K \, \mathcal{P}_{\text{sym}}^{T_1 T_2}(e) + \sum_{k=1}^{K} \binom{K}{k} [\mathcal{P}_{\text{off}}]^{K-k} [1 - \mathcal{P}_{\text{off}}]^k \, \mathcal{P}_{\text{sym}}^{T_1,\text{coop}}(e|k). \quad (4.30)$$

In what follows, the expressions for each of these probabilities are derived.

The conditional SEP for a given γ_{sa_i} of the $\mathsf{T}_1 \rightarrow \mathsf{R}_i$ link, $\mathcal{P}_{\text{sym}}^{T_1 R_i}(e|\gamma_{sa_i})$, can be tightly upper bounded as

$$\mathcal{P}_{\text{sym}}^{T_1 R_i}(e|\gamma_{sa_i}) \leq \alpha_z Q\left(\sqrt{\beta_z \gamma_{sa_i}}\right), \quad (4.31)$$

where $Q(u) = \frac{1}{\sqrt{2\pi}} \int_u^\infty e^{-t^2/2} dt$ is the Gaussian Q-function [67, 26.2.3], α_z and β_z are determined by the type of the expanded constellation and its size $|\Upsilon|$. For example, for M-QAM, $\alpha_z = 4$ and $\beta_z = 3/(|\Upsilon|-1)$; and for M-PSK, $\alpha_z = 2$ and $\beta_z = 2\sin^2(\pi/|\Upsilon|)$ [5]. Therefore, $\mathcal{P}_{\text{sym}}^{T_1 R_i}(e)$ over Rayleigh fading channel can be written as

$$\mathcal{P}_{\text{sym}}^{T_1 R_i}(e) \leq \int_0^\infty \alpha_z Q\left(\sqrt{\beta_z \gamma_{sa_i}}\right) f_{\gamma_{sa_i}}\left(\gamma_{sa_i}\right) d\gamma_{sa_i}, \quad (4.32)$$

where $f_{\gamma_{sa_i}}(\gamma_{sa_i}) = \frac{1}{\overline{\gamma}_{sa}} e^{-\gamma_{sa_i}/\overline{\gamma}_{sa}}$ is the PDF of the SNR γ_{sa_i} [68]. Solving the integration in (4.32) using (A.12), $\mathcal{P}_{\text{sym}}^{T_1 R_i}(e)$ can be written as

$$\mathcal{P}_{\text{sym}}^{T_1 R_i}(e) \leq \frac{1}{2} \alpha_z \left(1 - \sqrt{\frac{\beta_z \overline{\gamma}_{sa}}{\beta_z \overline{\gamma}_{sa} + 2}}\right). \quad (4.33)$$

Similarly, the SEP at the ith relay for a signal received from T_2 can be expressed as

$$\mathcal{P}_{\text{sym}}^{T_2 R_i}(e) \leq \frac{1}{2} \alpha_z \left(1 - \sqrt{\frac{\beta_z \overline{\gamma}_{sb}}{\beta_z \overline{\gamma}_{sb} + 2}}\right), \quad (4.34)$$

and the SEP at T_2 for a signal received from T_1 can be written as

$$\mathcal{P}_{\text{sym}}^{T_1T_2}(e) \leq \frac{1}{2}\,\alpha_z \left(1 - \sqrt{\frac{\beta_z \overline{\gamma}_{h_1}}{\beta_z \overline{\gamma}_{h_1} + 2}}\right). \tag{4.35}$$

The SEP of the cooperative link between $\mathsf{T}_1 \rightarrow \mathsf{T}_2$ and $\mathsf{R}_t \rightarrow \mathsf{T}_2$ depends on the total SNR of the cooperative link, $\gamma_{e_1} = \gamma_{h_1} + \gamma_{b_t}$, where γ_{b_t} is the SNR of the best relay chosen under the relay selection criterion, given by (4.13). Thus, the SEP of the cooperative link for given SNRs γ_{a_i}, γ_{b_i}, γ_{h_1} and k active relays can be represented as

$$\mathcal{P}_{\text{sym}}^{T_1,\text{coop}}(e|k, \gamma_{h_1}, \gamma_{a_i}, \gamma_{b_i}) = \alpha_x Q\left(\sqrt{\beta_x \gamma_{e_1}}\right), \tag{4.36}$$

where $\alpha_x = 2(|\Phi_r| - 1)/|\Phi_r|$, $\beta_x = 3/(|\Phi_r|^2 - 1)$ [5]. Then, $\mathcal{P}_{\text{sym}}^{T_1,\text{coop}}(e|k)$ over the fading channel can be written as

$$\mathcal{P}_{\text{sym}}^{T_1,\text{coop}}(e|k) = \int_0^\infty \alpha_x Q\left(\sqrt{\beta_x \gamma_{e_1}}\right) f_{\gamma_{e_1}}\left(\gamma_{e_1}\right) d\gamma_{e_1}, \tag{4.37}$$

where $f_{\gamma_{e_1}}(\gamma_{e_1})$ is the PDF of the SNR γ_{e_1}. To evaluate $f_{\gamma_{e_1}}(\gamma_{e_1})$, PDF of γ_{b_t} is derived first with the help of the PDFs of γ_{a_i} and γ_{b_i}, that are $f_{\gamma_{a_i}}(\gamma_{a_i}) = \frac{1}{\overline{\gamma}_a} e^{-\gamma_{a_i}/\overline{\gamma}_a}$ and $f_{\gamma_{b_i}}(\gamma_{b_i}) = \frac{1}{\overline{\gamma}_b} e^{-\gamma_{b_i}/\overline{\gamma}_b}$, respectively. Thus, using (B.21), $f_{\gamma_{b_t}}(\gamma)$ can be expressed as

$$\begin{aligned} f_{\gamma_{b_t}}(\gamma) = &\sum_{k=1}^{|\mathcal{C}|} \binom{|\mathcal{C}|}{k} \frac{(-1)^{k-1}}{\overline{\gamma}_a} \frac{k\overline{\gamma}_m}{k\overline{\gamma}_b - \overline{\gamma}_m} \left(e^{-\gamma/\overline{\gamma}_b} - e^{-k\gamma/\overline{\gamma}_m}\right) \\ &+ \sum_{k=1}^{|\mathcal{C}|} \binom{|\mathcal{C}|}{k} \frac{(-1)^{k-1}}{\overline{\gamma}_b}\, k\, e^{-k\gamma/\overline{\gamma}_m}, \end{aligned} \tag{4.38}$$

where $\overline{\gamma}_m = \overline{\gamma}_a \overline{\gamma}_b / (\overline{\gamma}_a + \overline{\gamma}_b)$. $f_{\gamma_{e_1}}(\gamma)$ can be evaluated by convolving $f_{\gamma_{h_1}}(\gamma) =$

$\frac{1}{\overline{\gamma}_{h_1}} e^{-\gamma/\overline{\gamma}_{h_1}}$ and $f_{\gamma_{b_t}}(\gamma)$ from (4.38), thus $f_{\gamma_{e_1}}(\gamma)$ can be expressed as

$$
\begin{aligned}
f_{\gamma_{e_1}}(\gamma) = & \sum_{k=1}^{|\mathcal{C}|} \binom{|\mathcal{C}|}{k} \frac{(-1)^{k-1}}{\overline{\gamma}_a} \frac{k\overline{\gamma}_m}{k\overline{\gamma}_b - \overline{\gamma}_m} \left[\frac{\overline{\gamma}_b}{\overline{\gamma}_{h_1} - \overline{\gamma}_b} \left(e^{-\gamma/\overline{\gamma}_{h_1}} - e^{-\gamma/\overline{\gamma}_b} \right) \right. \\
& \left. - \frac{\overline{\gamma}_m}{k\overline{\gamma}_{h_1} - \overline{\gamma}_m} \left(e^{-\gamma/\overline{\gamma}_{h_1}} - e^{-k\gamma/\overline{\gamma}_m} \right) \right] \\
& + \sum_{k=1}^{|\mathcal{C}|} \binom{|\mathcal{C}|}{k} \frac{(-1)^{k-1}}{\overline{\gamma}_b} \frac{k\overline{\gamma}_m}{k\overline{\gamma}_{h_1} - \overline{\gamma}_m} \left(e^{-\gamma/\overline{\gamma}_{h_1}} - e^{-k\gamma/\overline{\gamma}_m} \right). \qquad (4.39)
\end{aligned}
$$

Substituting (4.39) into (4.37) and solving the integration using (A.12), $\mathcal{P}_{\text{sym}}^{T_1,\text{coop}}(e|k)$ can be expressed as

$$
\begin{aligned}
& \mathcal{P}_{\text{sym}}^{T_1,\text{coop}}(e|k) = \frac{1}{2}\,\alpha_x \sum_{i=1}^{k} \binom{k}{i} \frac{(-1)^{i-1}}{\overline{\gamma}_a} \frac{i\overline{\gamma}_m}{i\overline{\gamma}_b - \overline{\gamma}_m} \times \\
& \left[\frac{\overline{\gamma}_b}{\overline{\gamma}_{h_1} - \overline{\gamma}_b} \left\{ \overline{\gamma}_{h_1} \left(1 - \sqrt{\frac{\beta_x \overline{\gamma}_{h_1}}{\beta_x \overline{\gamma}_{h_1} + 2}} \right) - \overline{\gamma}_b \left(1 - \sqrt{\frac{\beta_x \overline{\gamma}_b}{\beta_x \overline{\gamma}_b + 2}} \right) \right\} \right. \\
& \left. - \frac{\overline{\gamma}_m}{i\overline{\gamma}_{h_1} - \overline{\gamma}_m} \left\{ \overline{\gamma}_{h_1} \left(1 - \sqrt{\frac{\beta_x \overline{\gamma}_{h_1}}{\beta_x \overline{\gamma}_{h_1} + 2}} \right) - \frac{\overline{\gamma}_m}{i} \left(1 - \sqrt{\frac{\beta_x \overline{\gamma}_m}{\beta_x \overline{\gamma}_m + 2\,i}} \right) \right\} \right] \\
& + \frac{1}{2}\,\alpha_x \sum_{i=1}^{k} \binom{k}{i} \frac{(-1)^{i-1}}{\overline{\gamma}_b} \frac{i\overline{\gamma}_m}{i\overline{\gamma}_{h_1} - \overline{\gamma}_m} \left[\overline{\gamma}_{h_1} \left(1 - \sqrt{\frac{\beta_x \overline{\gamma}_{h_1}}{\beta_x \overline{\gamma}_{h_1} + 2}} \right) \right. \\
& \left. - \frac{\overline{\gamma}_m}{i} \left(1 - \sqrt{\frac{\beta_x \overline{\gamma}_m}{\beta_x \overline{\gamma}_m + 2\,i}} \right) \right]. \qquad (4.40)
\end{aligned}
$$

Finally, substituting (4.33), (4.34), (4.35) and (4.40) into (4.30), a closed-form expression for the average SEP at T_2 for the signal received from T_1 can be easily obtained. It is noted that a similar expression can be obtained for the average SEP at T_1 for the signal received from T_2, $\mathcal{P}_{\text{sym}}^{T_2}(e)$, by following the same procedure or simply replacing $\overline{\gamma}_{h_1}$ with $\overline{\gamma}_{h_2}$, and by interchanging $\overline{\gamma}_b$ and $\overline{\gamma}_a$ in the expression for $\mathcal{P}_{\text{sym}}^{T_1}(e)$. Thus, the end-to-end average SEP of the 2W-SSC system can be obtained

using the expression given below:

$$\mathcal{P}_{\text{sym}}^{e2e}(e) = \frac{\mathcal{P}_{\text{sym}}^{T_1}(e) + \mathcal{P}_{\text{sym}}^{T_2}(e)}{2}. \tag{4.41}$$

4.2.2 Asymptotic Error Probability

Although the derived expression for the average SEP expression of the system can be used to evaluate the error performance of the system, it does not clearly quantify the diversity gain and the effects of system parameters on the performance. Thus, a simple asymptotic expression for SEP is derived in the region of moderate to high SNR. The asymptotic SEP at T_2 for the signal received from T_1 can be expressed as

$$\mathcal{P}_{\text{sym}}^{T_1}(e) \simeq [\mathcal{P}_{\text{off}}]^K \, \mathcal{P}_{\text{sym}}^{T_1T_2}(e) + \sum_{k=1}^{K} \binom{K}{k} [\mathcal{P}_{\text{off}}]^{K-k} \, \mathcal{P}_{\text{sym}}^{T_1,\text{coop}}(e|k). \tag{4.42}$$

For high SNR, $\mathcal{P}_{\text{off}}$ from (4.29) can be approximated as

$$\mathcal{P}_{\text{off}} \approx \mathcal{P}_{\text{sym}}^{T_1R_i}(e) + \mathcal{P}_{\text{sym}}^{T_2R_i}(e). \tag{4.43}$$

Utilizing the Taylor series expansion of the exponential function and neglecting the higher order terms, the PDF of γ_{sa_i} can be approximated as

$$f_{\gamma_{sa_i}}(\gamma) \simeq \frac{1}{\overline{\gamma}_{sa}}. \tag{4.44}$$

Thus,

$$\mathcal{P}_{\text{sym}}^{T_1R_i}(e) \simeq \frac{\alpha_z}{2\beta_z} \frac{1}{\overline{\gamma}_{sa}}. \tag{4.45}$$

Similarly,

$$\mathcal{P}_{\text{sym}}^{T_2R_i}(e) \simeq \frac{\alpha_z}{2\beta_z}\frac{1}{\overline{\gamma}_{sb}}, \tag{4.46}$$

and

$$\mathcal{P}_{\text{sym}}^{T_1T_2}(e) \simeq \frac{\alpha_z}{2\beta_z}\frac{1}{\overline{\gamma}_{h_1}}. \tag{4.47}$$

The PDF of γ_{h_1} using the Taylor series expansion can be approximated as

$$f_{\gamma_{h_1}}(\gamma) \simeq \frac{1}{\overline{\gamma}_{h_1}}. \tag{4.48}$$

and $f_{\gamma_{b_t}}(\gamma)$ can be approximated as

$$f_{\gamma_{b_t}}(\gamma) \simeq k\gamma^{k-1}\frac{1}{\overline{\gamma}_b}\left(\frac{1}{\overline{\gamma}_m}\right)^{k-1}. \tag{4.49}$$

From (4.48) and (4.49), the approximate PDF of γ_{e_1} is obtained as

$$f_{\gamma_{e_1}}(\gamma) \simeq \frac{1}{\overline{\gamma}_{h_1}\overline{\gamma}_b}\left(\frac{1}{\overline{\gamma}_m}\right)^{k-1}\gamma^k. \tag{4.50}$$

Thus, substituting (4.50) into (4.37) and solving the integration using [69, 3.351.2]

$$\mathcal{P}_{\text{sym}}^{T_1,\text{coop}}(e|k) \simeq \frac{1}{\overline{\gamma}_{h_1}\overline{\gamma}_b}\left(\frac{1}{\overline{\gamma}_m}\right)^{k-1}\frac{\alpha_x 2^k\Gamma(k+\frac{3}{2})}{(k+1)\beta_x^{k+1}\sqrt{\pi}}, \tag{4.51}$$

where $\Gamma(\cdot)$ is the gamma function, given by $\Gamma(u) = \int_0^\infty e^{-t}t^{u-1}dt$ [67, 6.1.1]. From (4.42), (4.45), (4.46), (4.47) and (4.51), the asymptotic SEP at T_2 for the signal

received from T_1 can be written as

$$\mathcal{P}_{\text{sym}}^{T_1}(e) \simeq \left(\frac{\alpha_z}{2\beta_z}\right)^{K+1} \frac{1}{\overline{\gamma}_{h_1}} \left(\frac{1}{\overline{\gamma}_{sa}} + \frac{1}{\overline{\gamma}_{sb}}\right)^{K} + \sum_{k=1}^{K} \binom{K}{k} \times \Psi_k \left[\frac{\alpha_z}{2\beta_z}\left(\frac{1}{\overline{\gamma}_{sa}} + \frac{1}{\overline{\gamma}_{sb}}\right)\right]^{K-k} \frac{1}{\overline{\gamma}_{h_1}\overline{\gamma}_b} \left(\frac{1}{\overline{\gamma}_m}\right)^{k-1}, \tag{4.52}$$

where Ψ_k is defined as

$$\Psi_k = \frac{\alpha_x 2^k \Gamma(k+\frac{3}{2})}{(k+1)\beta_x^{k+1}\sqrt{\pi}}. \tag{4.53}$$

Similarly, the asymptotic SEP at T_1 for the signal received from T_2, $\mathcal{P}_{\text{sym}}^{T_2}(e)$, can be obtained by replacing $\overline{\gamma}_{h_1}$ with $\overline{\gamma}_{h_2}$, and by interchanging $\overline{\gamma}_b$ and $\overline{\gamma}_a$ in (4.52). Thus, the end-to-end asymptotic SEP of the 2W-SSC system can be written as

$$\mathcal{P}_{\text{sym}}^{e2e}(e) \simeq \frac{1}{2}\left(\frac{\alpha_z}{2\beta_z}\right)^{K+1} \left(\frac{1}{\overline{\gamma}_{h_1}} + \frac{1}{\overline{\gamma}_{h_2}}\right) \left(\frac{1}{\overline{\gamma}_{sa}} + \frac{1}{\overline{\gamma}_{sb}}\right)^{K} + \frac{1}{2}\sum_{k=1}^{K} \binom{K}{k} \Psi_k \left[\frac{\alpha_z}{2\beta_z}\left(\frac{1}{\overline{\gamma}_{sa}} + \frac{1}{\overline{\gamma}_{sb}}\right)\right]^{K-k} \left(\frac{1}{\overline{\gamma}_{h_1}\overline{\gamma}_b} + \frac{1}{\overline{\gamma}_{h_2}\overline{\gamma}_a}\right) \left(\frac{1}{\overline{\gamma}_m}\right)^{k-1} \tag{4.54}$$

4.2.3 Diversity Gain Analysis

To obtain the diversity gain of the 2W-SSC system, the end-to-end asymptotic SEP, given by (4.54), is examined. For the purpose, equal power is allocated to both terminals, i.e. $E_{T_1} = E_{T_2} = E_R = E_e$, and therefore, (4.54) can be written as

$$\mathcal{P}_{\text{sym}}^{e2e}(e) = \left(\frac{N_0}{E_e}\right)^{K+1} \frac{1}{\sigma_h^2} \left(\frac{1}{\sigma_a^2\lambda_{T_1R}} + \frac{1}{\sigma_b^2\lambda_{T_2R}}\right)^{K} \times \left[\left(\frac{\alpha_z}{2\beta_z}\right)^{K+1} + \sum_{k=1}^{K} \binom{K}{k} \frac{\Psi_k}{2} \left(\frac{\alpha_z}{2\beta_z}\right)^{K-k}\right]. \tag{4.55}$$

It is observed from this expression that the 2W-SSC system achieves a diversity gain of $K+1$, which is one higher than the number of relays in the system.

4.3 System Optimization

4.3.1 Optimizing Relay Position under Fixed Power Allocation

In order to determine optimum relay position, normalized distance between both terminals (i.e. $d_{T_1T_2} = 1$) is used. The placement of relays in the system is on the straight-line, joining both terminals (i.e. $d_{T_1R} = d$ and $d_{T_2R} = 1 - d$), in order to reduce the impact of path loss on the system performance. In addition, it is assumed that at least one of K relays correctly decodes signals received from both terminals, for the optimization to be meaningful. Under the condition of fixed power allocated to both terminals (E_{T_1} and E_{T_2}) and the relays (E_R), the relay location optimization problem can be formulated as

$$\begin{aligned} \min_{d} \quad & \mathcal{P}_{\text{sym}}^{e2e}(e) \\ \text{subject to} \quad & 0 \leq d \leq 1 \end{aligned} \tag{4.56}$$

In order to carry out tractable mathematical analysis of all optimization cases, binomial expansion [69] is applied on (4.54) and the following expression of the end-

to-end asymptotic SEP is obtained, which is used in all optimization analysis,

$$\mathcal{P}_{\text{sym}}^{e2e}(e) \simeq \frac{1}{2}\left(\frac{\alpha_z}{2\beta_z}\right)^{K+1}\left(\frac{1}{\overline{\gamma}_{h_1}}+\frac{1}{\overline{\gamma}_{h_2}}\right)\left(\frac{1}{\overline{\gamma}_{sa}}+\frac{1}{\overline{\gamma}_{sb}}\right)^{K} + \frac{\Psi_K}{2}\left(\frac{1}{\overline{\gamma}_{h_1}\overline{\gamma}_b}+\frac{1}{\overline{\gamma}_{h_2}\overline{\gamma}_a}\right)\left(\frac{1}{\overline{\gamma}_m}\right)^{K-1}, \tag{4.57}$$

where

$$\Psi_K = \frac{\alpha_x 2^K \Gamma(K+\frac{3}{2})}{(K+1)\beta_x^{K+1}\sqrt{\pi}}. \tag{4.58}$$

The expression in (4.57) can be written as

$$\mathcal{P}_{\text{sym}}^{e2e}(e) = \mathcal{A}\left[\mathcal{C}d^{\nu}+\mathcal{H}\left(1-d\right)^{\nu}\right]^{K} + \left[\mathcal{J}d^{\nu}+\mathcal{U}\left(1-d\right)^{\nu}\right]\left[\mathcal{W}d^{\nu}+\mathcal{Z}\left(1-d\right)^{\nu}\right]^{K-1} \tag{4.59}$$

where the notations in the previous expression are defined as

$$\mathcal{A} = \frac{1}{2}\left(\frac{\alpha_z}{2\beta_z}\right)^{K+1}\left(\frac{N_0}{\sigma_h^2 E_{T_1}}+\frac{N_0}{\sigma_h^2 E_{T_2}}\right), \tag{4.60}$$

$$\mathcal{C} = \frac{N_0}{\sigma_a^2 E_{T_1}}, \tag{4.61}$$

$$\mathcal{H} = \frac{N_0}{\sigma_b^2 E_{T_2}}, \tag{4.62}$$

$$\mathcal{J} = \frac{\Psi_K}{2}\frac{N_0}{\sigma_h^2 E_{T_2}}\frac{N_0}{\sigma_a^2 E_R}, \tag{4.63}$$

$$\mathcal{U} = \frac{\Psi_K}{2}\frac{N_0}{\sigma_h^2 E_{T_1}}\frac{N_0}{\sigma_b^2 E_R}, \tag{4.64}$$

$$\mathcal{W} = \frac{N_0}{\sigma_a^2 E_R}, \tag{4.65}$$

$$\mathcal{Z} = \frac{N_0}{\sigma_b^2 E_R}. \tag{4.66}$$

In order to check the convexity of $\mathcal{P}_{\text{sym}}^{e2e}(e)$, given by (4.59), the second derivative

of (4.59) is evaluated with respect to d and it is easily found that $\partial^2 \mathcal{P}_{\text{sym}}^{e2e}(e)/\partial d^2$ is positive in the interval $[0, 1]$. This shows that the objective function is strictly a convex function of d in the interval $[0, 1]$. Thus, taking the first derivative of $\mathcal{P}_{\text{sym}}^{e2e}(e)$ with respect to d and equating it to zero, the following expression is obtained

$$\begin{aligned}
&\mathcal{A}K\left[\mathcal{C}d^{\nu} + \mathcal{H}\left(1-d\right)^{\nu}\right]^{K-1}\left[\mathcal{C}\nu d^{\nu-1} - \mathcal{H}\nu\left(1-d\right)^{\nu-1}\right] \\
&+ \left[\mathcal{J}\nu d^{\nu-1} - \mathcal{U}\nu\left(1-d\right)^{\nu-1}\right]\left[\mathcal{W}d^{\nu} + \mathcal{Z}\left(1-d\right)^{\nu}\right]^{K-1} \\
&+ \left(K-1\right)\left[\mathcal{J}d^{\nu} + \mathcal{U}\left(1-d\right)^{\nu}\right]\left[\mathcal{W}d^{\nu} + \mathcal{Z}\left(1-d\right)^{\nu}\right]^{K-2} \times \\
&\left[\mathcal{W}\nu d^{\nu-1} - \mathcal{Z}\nu\left(1-d\right)^{\nu-1}\right] = 0. \qquad (4.67)
\end{aligned}$$

This expression is very complex and it is very hard to find the closed-form expression for the optimal relay position (d^*) from (4.67). However, iterative techniques such as bisection method can be used to find the optimum position of the relay, d^*.

4.3.2 Optimizing Power Allocation under Fixed Relay Position

In this section, the problem of optimal power allocation (OPA) at both terminals and the relay is investigated. The problem is further simplified by assuming equal power allocation to both terminals (i.e. $E_T = E_{T_1} = E_{T_2}$). Under the condition of fixed relay location (d_{T_1R}, d_{T_2R}), the power optimization problem can be expressed as

$$\begin{aligned}
\min_{E_T, E_R} \quad & \mathcal{P}_{\text{sym}}^{e2e}(e) \\
\text{subject to} \quad & E_{T_1} + E_{T_2} + E_R = 2E_T + E_R \leq E_{\text{tot}}, \\
& E_T, E_R > 0,
\end{aligned} \qquad (4.68)$$

where E_{tot} is the total power budget of the system. δ is defined such that $0 < \delta < 1$, so that the optimum values of the power allocated to both terminals and the relay can be expressed as $E_T = \delta E_{\text{tot}}/2$ and $E_R = (1-\delta)E_{\text{tot}}$. By substituting these values into (4.57), the following expression is obtained

$$\mathcal{P}_{\text{sym}}^{e2e}(e) = \mathcal{I}\left(\frac{1}{\delta}\right)^{K+1} + \mathcal{L}\left(\frac{1}{\delta}\right)\left(\frac{1}{1-\delta}\right)^{K}, \tag{4.69}$$

where $\mathcal{I}$ and $\mathcal{L}$ are defined as

$$\mathcal{I} = \frac{1}{2}\left(\frac{\alpha_z}{2\beta_z}\right)^{K+1} \frac{4N_0}{\sigma_h^2 E_{\text{tot}}} \left(\frac{2N_0}{\sigma_a^2 \lambda_{T_1R} E_{\text{tot}}} + \frac{2N_0}{\sigma_b^2 \lambda_{T_2R} E_{\text{tot}}}\right)^{K}, \tag{4.70}$$

$$\mathcal{L} = \frac{\Psi_K}{2}\frac{2N_0}{\sigma_h^2 E_{\text{tot}}} \left(\frac{N_0}{\sigma_a^2 \lambda_{T_1R} E_{\text{tot}}} + \frac{N_0}{\sigma_b^2 \lambda_{T_2R} E_{\text{tot}}}\right) \times \left(\frac{\sigma_a^2 \lambda_{T_1R} + \sigma_b^2 \lambda_{T_2R}}{\sigma_a^2 \sigma_b^2 \lambda_{T_1R} \lambda_{T_2R}} \frac{N_0}{E_{\text{tot}}}\right)^{K-1}. \tag{4.71}$$

By taking the second derivative of (4.69) with respect to δ, it is easily observed that the objective function is strictly a convex function of δ in the interval $(0, 1)$. Thus, taking the first derivative of (4.69) with respect to δ and equating it to zero, the following expression is obtained

$$\mathcal{I}(K+1)\left(\frac{1}{\delta}\right)^{K+2} - \mathcal{L}\frac{(K+1)\delta - 1}{\delta^2}\left(\frac{1}{1-\delta}\right)^{K+1} = 0. \tag{4.72}$$

The optimum values of δ, δ^*, can be determined using simple iterative techniques such as bisection method and hence the optimum values E_T^* and E_R^*.

4.3.3 Optimizing Source Power Allocation under Fixed Relay Power and Position

Optimum E_T^*, obtained using OPA, can be used to find the optimal source power allocation (OSA) (i.e. $E_{T_1}^*$, $E_{T_2}^*$) assuming fixed relay power (E_R) and position (d_{T_1R}, d_{T_2R}). The source power optimization problem can be mathematically stated as

$$\begin{aligned} \min_{E_{T_1}, E_{T_1}} \quad & \mathcal{P}_{\text{sym}}^{e2e}(e) \\ \text{subject to} \quad & E_{T_1} + E_{T_2} \leq E_{TS}, \\ & E_{T_1},\ E_{T_2} > 0, \end{aligned} \tag{4.73}$$

where E_{TS} is the total power allocated to both terminals of the system. By defining ρ such that $0 < \rho < 1$, the optimum values of the power allocated to both terminals can be represented as $E_{T_1} = \rho E_{TS}$ and $E_{T_2} = (1-\rho)E_{TS}$. Substituting these values into (4.57), the following expression is obtained

$$\mathcal{P}_{\text{sym}}^{e2e}(e) = \mathcal{B}\left(\frac{1}{\rho} + \frac{1}{1-\rho}\right)\left(\frac{\mathcal{V}}{\rho} + \frac{\mathcal{X}}{1-\rho}\right)^K + \mathcal{Y}\left(\frac{\mathcal{V}}{\rho} + \frac{\mathcal{X}}{1-\rho}\right), \tag{4.74}$$

where

$$\mathcal{B} = \frac{1}{2}\left(\frac{\alpha_z}{2\beta_z}\right)^{K+1} \frac{N_0}{\sigma_h^2 E_{TS}}, \tag{4.75}$$

$$\mathcal{V} = \frac{N_0}{\sigma_a^2 \lambda_{T_1R} E_{TS}}, \tag{4.76}$$

$$\mathcal{X} = \frac{N_0}{\sigma_b^2 \lambda_{T_2R} E_{TS}}, \tag{4.77}$$

$$\mathcal{Y} = \frac{\Psi_K}{2} \frac{N_0}{\sigma_h^2 E_R} \left(\frac{\sigma_a^2 \lambda_{T_1R} + \sigma_b^2 \lambda_{T_2R}}{\sigma_a^2 \sigma_b^2 \lambda_{T_1R} \lambda_{T_2R}} \frac{N_0}{E_R}\right)^{K-1}. \tag{4.78}$$

The expression for $\mathcal{P}_{\text{sym}}^{e2e}(e)$, given by (4.74), is found to be strictly a convex function of ρ in the interval $(0, 1)$. Thus, taking the first derivative of (4.74) with respect to ρ and equating it to zero, the following expression is obtained

$$\mathcal{B}\frac{(2\rho-1)}{\rho^2(1-\rho)^2}\left(\frac{\mathcal{V}}{\rho}+\frac{\mathcal{X}}{1-\rho}\right)^K+\mathcal{Y}\left[\frac{\mathcal{X}}{(1-\rho)^2}-\frac{\mathcal{V}}{\rho^2}\right] + \mathcal{B}K\frac{1}{\rho(1-\rho)}\left[\frac{\mathcal{X}}{(1-\rho)^2}-\frac{\mathcal{V}}{\rho^2}\right]\left(\frac{\mathcal{V}}{\rho}+\frac{\mathcal{X}}{1-\rho}\right)^{K-1}=0. \tag{4.79}$$

The optimum value of ρ (ρ^*) can be obtained from the previous expression using simple iterative techniques such as bisection method, and hence, the optimum values of the power allocated to both terminals (i.e. $E_{T_1}^*$, $E_{T_2}^*$) can be calculated.

4.4 Outage Probability Analysis

In this section, the overall outage performance of the 2W-SSC system is evaluated over Rayleigh fading channel. A closed-form expression for the asymptotic approximation of the outage probability is also derived.

4.4.1 Exact Outage Probability

For the transmission scenario presented in Section 4.1, system outage occurs either when $\mathsf{T}_1 \to \mathsf{T}_2$, $\mathsf{T}_2 \to \mathsf{T}_1$, $\mathsf{T}_1 \to \mathsf{R}_i$ and $\mathsf{T}_2 \to \mathsf{R}_i$ links are in outage, or when the cooperative links are in outage assuming no outage in $\mathsf{T}_1 \to \mathsf{R}_i$ and $\mathsf{T}_2 \to \mathsf{R}_i$ links. Thus, the outage probability for the signal received from T_1 can be expressed as

$$\mathcal{P}_{\text{out}}^{T_1}=\left(\mathcal{P}_{\text{out}}^{\text{off}}\right)^K\mathcal{P}_{\text{out}}^{T_1T_2}+\left(1-\mathcal{P}_{\text{out}}^{\text{off}}\right)^K\mathcal{P}_{\text{out}}^{T_1,\text{coop}}, \tag{4.80}$$

where $\mathcal{P}_{\text{out}}^{T_1T_2}$ denotes the outage probability of the $\mathsf{T}_1 \to \mathsf{T}_2$ link, $\mathcal{P}_{\text{out}}^{T_1,\text{coop}}$ the outage probability of the cooperative link, and $\mathcal{P}_{\text{out}}^{\text{off}}$ denotes the outage probability when a relay link to both terminals has failed. $\mathcal{P}_{\text{out}}^{\text{off}}$ can be written as

$$\mathcal{P}_{\text{out}}^{\text{off}} = 1 - \left(1 - \mathcal{P}_{\text{out}}^{T_1R}\right)\left(1 - \mathcal{P}_{\text{out}}^{T_2R}\right), \tag{4.81}$$

where $\mathcal{P}_{\text{out}}^{T_1R}$ and $\mathcal{P}_{\text{out}}^{T_2R}$ represent outage probabilities of $\mathsf{T}_1 \to \mathsf{R}_i$ and $\mathsf{T}_2 \to \mathsf{R}_i$ links, respectively. For a given target rate R_0 bits/s/Hz, the event that an outage happens in the $\mathsf{T}_1 \to \mathsf{R}_i$ link corresponds to the event $(1/3)\log_2(1+\gamma_{sa_i}) < R_0$, or equivalently $\gamma_{sa_i} < \mu_{th}$, where $\mu_{th} = 2^{3R_0} - 1$. The reason for the factor 1/3 is that there are 3 time slots used in the system. Thus, $\mathcal{P}_{\text{out}}^{T_1R}$ can be expressed as

$$\mathcal{P}_{\text{out}}^{T_1R} \triangleq \Pr\left\{\frac{1}{3}\log_2\left(1+\gamma_{sa_i}\right) < R_0\right\}, \tag{4.82}$$

$$\mathcal{P}_{\text{out}}^{T_1R} = 1 - \exp\left(-\frac{\mu_{th}}{\overline{\gamma}_{sa}}\right). \tag{4.83}$$

Similarly, $\mathcal{P}_{\text{out}}^{T_2R}$ and $\mathcal{P}_{\text{out}}^{T_1T_2}$ can be obtained as

$$\mathcal{P}_{\text{out}}^{T_2R} = 1 - \exp\left(-\frac{\mu_{th}}{\overline{\gamma}_{sb}}\right), \tag{4.84}$$

and

$$\mathcal{P}_{\text{out}}^{T_1T_2} = 1 - \exp\left(-\frac{\mu_{th}}{\overline{\gamma}_{h_1}}\right). \tag{4.85}$$

When no outage happens in $\mathsf{T}_1 \to \mathsf{R}_i$ and $\mathsf{T}_2 \to \mathsf{R}_i$ links and the relay successfully decodes both source signals, the best relay transmits different symbols using $\mathsf{R}_t \to \mathsf{T}_1$ and $\mathsf{R}_t \to \mathsf{T}_2$ links to both terminals in the third time slot. Thus, the average mutual information for the cooperative link at T_2, for the signal received from

T_1, is given by

$$I_{T_1}^{\text{coop}} \triangleq \frac{1}{3}\log_2(1+\gamma_{h_1}) + \frac{1}{3}\log_2(1+\gamma_{b_t}). \tag{4.86}$$

Assuming γ_{h_1} and γ_{b_t} to be independent random variables, the outage probability of the cooperative link at T_2, for the signal received from T_1, can be expressed as

$$\mathcal{P}_{\text{out}}^{T_1,\text{coop}} = \Pr\left\{I_{T_1}^{\text{coop}} < R_0\right\} = \iint\limits_{\Lambda} f\left(\gamma_{h_1},\gamma_{b_t}\right) d\gamma_{h_1} d\gamma_{b_t}, \tag{4.87}$$

where $\Lambda \triangleq \{(\gamma_{h_1},\gamma_{b_t})|(1+\gamma_{h_1})(1+\gamma_{b_t}) < 2^{3R_0},\ \ \gamma_{h_1} \geq 0,\ \ \gamma_{b_t} \geq 0\}$ and $f(\gamma_{h_1},\gamma_{b_t}) = f_{\gamma_{h_1}}(\gamma_{h_1})\, f_{\gamma_{b_t}}(\gamma_{b_t})$ is the joint PDF of γ_{h_1} and γ_{b_t}. Thus,

$$\mathcal{P}_{\text{out}}^{T_1,\text{coop}} = \int_0^{\mu_{th}} \int_0^{\frac{1+\mu_{th}}{1+\gamma_{h_1}}-1} f_{\gamma_{h_1}}(\gamma_{h_1})\, f_{\gamma_{b_t}}(\gamma_{b_t}) d\gamma_{h_1} d\gamma_{b_t}. \tag{4.88}$$

Using the Taylor series to approximate terms such as $\exp\{-(\mu_{th}-\gamma_{h_1})/(\overline{\gamma}_b(1+\gamma_{h_1}))\}$ and solving the integral in the previous expression, $\mathcal{P}_{\text{out}}^{T_1,\text{coop}}$ is obtained as

$$\begin{aligned}
\mathcal{P}_{\text{out}}^{T_1,\text{coop}} &= \sum_{k=1}^{K} \binom{K}{k} \frac{(-1)^{k-1}}{\overline{\gamma}_a} \frac{\overline{\gamma}_m}{k\overline{\gamma}_b - \overline{\gamma}_m} \left[1 - \exp\left(-\frac{\mu_{th}}{\overline{\gamma}_{h_1}}\right)\right] \\
&\left[k\overline{\gamma}_b \left\{1 - \exp\left(-\frac{\mu_{th}}{\overline{\gamma}_b}\right)\right\} - \overline{\gamma}_m \left\{1 - \exp\left(-\frac{k\mu_{th}}{\overline{\gamma}_m}\right)\right\}\right] \\
&+ \sum_{k=1}^{K} \binom{K}{k} \frac{(-1)^{k-1}}{\overline{\gamma}_b} \overline{\gamma}_m \left[1 - \exp\left(-\frac{\mu_{th}}{\overline{\gamma}_{h_1}}\right)\right] \left[1 - \exp\left(-\frac{k\mu_{th}}{\overline{\gamma}_m}\right)\right].
\end{aligned} \tag{4.89}$$

From (4.80), (4.81), (4.83), (4.84), (4.85) and (4.89), the outage probability for the signal received from T_1, $\mathcal{P}_{\text{out}}^{T_1}$, can be obtained. Similarly, the outage probability for the signal received from T_2, $\mathcal{P}_{\text{out}}^{T_2}$, can be obtained by replacing $\overline{\gamma}_{h_1}$ with $\overline{\gamma}_{h_2}$, and by interchanging $\overline{\gamma}_b$ and $\overline{\gamma}_a$ in $\mathcal{P}_{\text{out}}^{T_1}$. Thus, the overall outage probability of the

system is given by

$$\mathcal{P}_{\text{out}} = \frac{\mathcal{P}_{\text{out}}^{T_1} + \mathcal{P}_{\text{out}}^{T_2}}{2}. \tag{4.90}$$

4.4.2 Asymptotic Outage Probability

In the following, the asymptotic approximation for the overall outage probability is evaluated for high SNR to obtain an insight of the system performance. Using the fact that $(1 - \mathcal{P}_{\text{out}}^{\text{off}}) \to 1$ for high SNR, the asymptotic outage probability of T_1 can be expressed as

$$\mathcal{P}_{\text{out}}^{T_1} \simeq \left(\mathcal{P}_{\text{out}}^{\text{off}}\right)^K \mathcal{P}_{\text{out}}^{T_1 T_2} + \mathcal{P}_{\text{out}}^{T_1,\text{coop}}, \tag{4.91}$$

where $\mathcal{P}_{\text{out}}^{\text{off}}$ can be approximated as

$$\mathcal{P}_{\text{out}}^{\text{off}} \approx \mathcal{P}_{\text{out}}^{T_1 R} + \mathcal{P}_{\text{out}}^{T_2 R}. \tag{4.92}$$

Using (4.44), $\mathcal{P}_{\text{out}}^{T_1 R}$ can be approximated as

$$\mathcal{P}_{\text{out}}^{T_1 R} \simeq \frac{\mu_{th}}{\overline{\gamma}_{sa}}. \tag{4.93}$$

Similarly, the other outage probabilities can be written as

$$\mathcal{P}_{\text{out}}^{T_2 R} \simeq \frac{\mu_{th}}{\overline{\gamma}_{sb}}, \tag{4.94}$$

and

$$\mathcal{P}_{\text{out}}^{T_1 T_2} \simeq \frac{\mu_{th}}{\overline{\gamma}_{h_1}}. \tag{4.95}$$

Substituting (4.48) and (4.49) into (4.88), and solving the integration, $\mathcal{P}_{\text{out}}^{T_1,\text{coop}}$

is approximated as

$$\mathcal{P}_{\text{out}}^{T_1,\text{coop}} \simeq \frac{1}{\overline{\gamma}_{h_1}\overline{\gamma}_b}\left(\frac{1}{\overline{\gamma}_m}\right)^{K-1}\frac{\mu_{th}^{K+1}}{K+1}. \tag{4.96}$$

Thus, using (4.91)–(4.96), the asymptotic outage probability of T_1 can be written as

$$\mathcal{P}_{\text{out}}^{T_1} \simeq \left(\frac{\mu_{th}}{\overline{\gamma}_{sa}}+\frac{\mu_{th}}{\overline{\gamma}_{sb}}\right)^{K}\frac{\mu_{th}}{\overline{\gamma}_{h_1}} + \frac{1}{\overline{\gamma}_{h_1}\overline{\gamma}_b}\left(\frac{1}{\overline{\gamma}_m}\right)^{K-1}\frac{\mu_{th}^{K+1}}{K+1}. \tag{4.97}$$

In a similar manner, the asymptotic outage probability of T_2, $\mathcal{P}_{\text{out}}^{T_2}$, can be obtained by replacing $\overline{\gamma}_{h_1}$ with $\overline{\gamma}_{h_2}$, and by interchanging $\overline{\gamma}_b$ and $\overline{\gamma}_a$ in (4.97). The overall asymptotic outage probability of the system can be written as

$$\begin{aligned}\mathcal{P}_{\text{out}} \simeq &\left(\frac{\mu_{th}}{\overline{\gamma}_{sa}}+\frac{\mu_{th}}{\overline{\gamma}_{sb}}\right)^{K}\left(\frac{\mu_{th}}{\overline{\gamma}_{h_1}}+\frac{\mu_{th}}{\overline{\gamma}_{h_2}}\right)\\ &+\left(\frac{1}{\overline{\gamma}_{h_1}\overline{\gamma}_b}+\frac{1}{\overline{\gamma}_{h_2}\overline{\gamma}_a}\right)\left(\frac{1}{\overline{\gamma}_m}\right)^{K-1}\frac{\mu_{th}^{K+1}}{K+1}.\end{aligned} \tag{4.98}$$

4.5 Channel Capacity Analysis

In this section, the average channel capacity of the system, which is also an important performance metric, is evaluated.

4.5.1 Average Channel Capacity

The average channel capacity, in the Shannon's sense, can be evaluated by averaging the instantaneous capacity for an AWGN channel over the fading distribution for optimal rate adaptation with constant transmit power and receiver channel state information [68, 70]. The average channel capacity of the 2W-SSC system can be expressed as

$$\overline{C} = \overline{C}_{T_1T_2} + \overline{C}_{T_2T_1} + \overline{C}_{R_tT_1} + \overline{C}_{R_tT_2}, \tag{4.99}$$

where $\overline{C}_{T_1T_2}$, $\overline{C}_{T_2T_1}$, $\overline{C}_{R_tT_1}$ and $\overline{C}_{R_tT_2}$ denote the average channel capacities of $\mathsf{T}_1 \rightarrow \mathsf{T}_2$, $\mathsf{T}_2 \rightarrow \mathsf{T}_1$, $\mathsf{R}_t \rightarrow \mathsf{T}_1$ and $\mathsf{R}_t \rightarrow \mathsf{T}_2$ links, respectively. The average channel capacity of the $\mathsf{T}_1 \rightarrow \mathsf{T}_2$ link can be written as

$$\overline{C}_{T_1T_2} = B\,\frac{1}{3}\int_0^{\infty} \log_2\left(1+\gamma_{h_1}\right) f_{\gamma_{h_1}}(\gamma_{h_1}) d\gamma_{h_1}, \tag{4.100}$$

where B is the bandwidth of the channel. The reason for the factor 1/3 is that 1 symbol is transmitted over the $\mathsf{T}_1 \rightarrow \mathsf{T}_2$ link in 3 time slots. In order to simplify (4.100), the following expression is formulated using [69, 3.352.4]

$$\int_0^{\infty} \ln(1+x) e^{-x/c} dx = c\, e^{1/c}\, E_1\left(\frac{1}{c}\right), \tag{4.101}$$

where $E_1(\cdot)$ represents the exponential integral, defined as $E_1(u) = \int_u^{\infty} (\exp(-t)/t)\, dt$ [67, 5.1.1]. Substituting $f_{\gamma_{h_1}}(\gamma_{h_1})$ into (4.100), and solving the integration using (4.101), $\overline{C}_{T_1T_2}$ can be written as

$$\overline{C}_{T_1T_2} = B\,\frac{1}{3\ln 2} e^{1/\overline{\gamma}_{h_1}} E_1\left(\frac{1}{\overline{\gamma}_{h_1}}\right). \tag{4.102}$$

Similarly, the following expression is obtained

$$\overline{C}_{T_2T_1} = B\,\frac{1}{3\ln 2} e^{1/\overline{\gamma}_{h_2}} E_1\left(\frac{1}{\overline{\gamma}_{h_2}}\right). \tag{4.103}$$

The average channel capacity of the $\mathsf{R}_t \rightarrow \mathsf{T}_2$ link can be written as

$$\overline{C}_{R_tT_2} = B\,\frac{1}{3}\int_0^{\infty} \log_2\left(1+\gamma_{b_t}\right) f_{\gamma_{b_t}}(\gamma_{b_t}) d\gamma_{b_t}. \tag{4.104}$$

Substituting (4.38) into (4.104), and solving the integration using (4.101), $\overline{C}_{R_tT_2}$ can be expressed as

$$\begin{aligned}\overline{C}_{R_tT_2} = &\frac{B}{3\ln 2}\sum_{k=1}^{K}\binom{K}{k}\frac{(-1)^{k-1}}{\overline{\gamma}_a}\frac{k\overline{\gamma}_m}{k\overline{\gamma}_b-\overline{\gamma}_m}\times\\ &\left[\overline{\gamma}_b e^{1/\overline{\gamma}_b}E_1\left(\frac{1}{\overline{\gamma}_b}\right)-\frac{\overline{\gamma}_m}{k}e^{k/\overline{\gamma}_m}E_1\left(\frac{k}{\overline{\gamma}_m}\right)\right]\\ &+\frac{B}{3\ln 2}\sum_{k=1}^{K}\binom{K}{k}\frac{(-1)^{k-1}}{\overline{\gamma}_b}\overline{\gamma}_m e^{k/\overline{\gamma}_m}E_1\left(\frac{k}{\overline{\gamma}_m}\right).\end{aligned} \tag{4.105}$$

Similarly, the average channel capacity of the $\mathsf{R}_t \rightarrow \mathsf{T}_1$ link, $\overline{C}_{R_tT_1}$, can be obtained by interchanging $\overline{\gamma}_b$ and $\overline{\gamma}_a$ in (4.105). Using the above results, the closed-form expression for the average channel capacity of the system can be expressed as

$$\begin{aligned}\frac{\overline{C}}{B} = &\frac{1}{3\ln 2}\sum_{k=1}^{K}\binom{K}{k}\frac{(-1)^{k-1}}{\overline{\gamma}_a}\frac{k\overline{\gamma}_m}{k\overline{\gamma}_b-\overline{\gamma}_m}\left[\overline{\gamma}_b e^{1/\overline{\gamma}_b}E_1\left(\frac{1}{\overline{\gamma}_b}\right)-\frac{\overline{\gamma}_m}{k}e^{k/\overline{\gamma}_m}E_1\left(\frac{k}{\overline{\gamma}_m}\right)\right]\\ &+\frac{1}{3\ln 2}\sum_{k=1}^{K}\binom{K}{k}\frac{(-1)^{k-1}}{\overline{\gamma}_b}\frac{k\overline{\gamma}_m}{k\overline{\gamma}_a-\overline{\gamma}_m}\left[\overline{\gamma}_a e^{1/\overline{\gamma}_a}E_1\left(\frac{1}{\overline{\gamma}_a}\right)-\frac{\overline{\gamma}_m}{k}e^{k/\overline{\gamma}_m}E_1\left(\frac{k}{\overline{\gamma}_m}\right)\right]\\ &+\frac{1}{3\ln 2}\sum_{k=1}^{K}\binom{K}{k}(-1)^{k-1}e^{k/\overline{\gamma}_m}E_1\left(\frac{k}{\overline{\gamma}_m}\right)\\ &+\frac{1}{3\ln 2}\left[e^{1/\overline{\gamma}_{h_1}}E_1\left(\frac{1}{\overline{\gamma}_{h_1}}\right)+e^{1/\overline{\gamma}_{h_2}}E_1\left(\frac{1}{\overline{\gamma}_{h_2}}\right)\right].\end{aligned} \tag{4.106}$$

4.5.2 Upper Bound on the Capacity

Using Jensen's Inequality, the average channel capacity of a link can be upper bounded as

$$\overline{C} \leq B\frac{1}{3}\log_2\left(1+\mathbb{E}\{\gamma\}\right), \tag{4.107}$$

where $\mathbb{E}\{\cdot\}$ denotes the expectation operator, evaluated by $\mathbb{E}\{\gamma\} = \int_0^\infty \gamma f_\gamma(\gamma) d\gamma$ and can be simplified using $\int_0^\infty t\, e^{-t/c} dt = c^2$. Thus, the upper bounds on the capacities of the links are obtained as

$$\overline{C}_{T_1T_2} \leq B\frac{1}{3}\log_2\left(1+\overline{\gamma}_{h_1}\right), \tag{4.108}$$

$$\overline{C}_{T_2T_1} \leq B\frac{1}{3}\log_2\left(1+\overline{\gamma}_{h_2}\right), \tag{4.109}$$

and

$$\overline{C}_{R_tT_2} \leq B\frac{1}{3}\log_2\left(1+\mathbb{E}\{\gamma_{b_t}\}\right), \tag{4.110}$$

where

$$\begin{aligned}\mathbb{E}\{\gamma_{b_t}\} = &\sum_{k=1}^{K}\binom{K}{k}\frac{(-1)^{k-1}}{\overline{\gamma}_a}\frac{k\overline{\gamma}_m}{k\overline{\gamma}_b-\overline{\gamma}_m}\left[\overline{\gamma}_b^2-\left(\frac{\overline{\gamma}_m}{k}\right)^2\right]\\ &+\sum_{k=1}^{K}\binom{K}{k}\frac{(-1)^{k-1}}{\overline{\gamma}_b}\frac{\overline{\gamma}_m^2}{k}.\end{aligned} \tag{4.111}$$

In a similar manner, $\overline{C}_{R_tT_1}$ can be obtained by interchanging $\overline{\gamma}_b$ and $\overline{\gamma}_a$ in (4.111) and hence an upper bound on the capacity of the system.

4.6 Results and Discussion

In this section, the numerical results are presented to illustrate the performance of the 2W-SSC system using analytical expressions and numerical simulations. These include average bit error probability (BEP), outage probability and channel capacity of the 2W-SSC system over a slow Rayleigh fading channel for different system parameters such as the number of relays (K), average signal-to-noise ratio (E_b/N_0), information rate (R_0), equal power allocation (EPA), optimal power allocation (OPA),

and optimal relay position (ORP). Also, the Monte Carlo simulations to illustrate the performance of the system were performed with 10^9 trials for each simulation point for accuracy and correctness. The SSD used in the system is 4-QAM with a rotation angle of 26.6°. The path loss exponent is set to $\nu = 3$ and the variances of the channel coefficients are $\sigma_h^2 = \sigma_a^2 = \sigma_b^2 = 1$. The 2W-SSC system is assumed to have K relays located at the middle of both terminals, unless otherwise stated. For the fair analysis, the total power budget to exchange four symbols in the 2W-SSC system is same as used for the case of the direct transmission, i.e. $E_{T_1} = E_{T_2} = 1$ for first and second time slots and $E_R = 2$ for the third time slot, making the total power budget equals to 4 units.

Figure 4.2 shows the average BEP of the system as a function of the average SNR (E_b/N_0) for different number of relays (K). The simulation results in this plot are represented by $\diamond$ markers while analytical and asymptotic results are shown by solid and dashed lines, respectively. It is clear from the figure that analytical results for the error probability, given by (4.41), are in perfect agreement with the simulation results, thus validating the mathematical expressions. Also, the asymptotic behaviour of the system for medium and high SNRs, given by (4.54), is in close agreement with the analytical and simulation results at medium and high SNRs. It is observed that as the number of relays (K) in the system increases, the slope of the BEP curve becomes steeper, indicating the increase in cooperative diversity gain. This indicates that the diversity gain achieved is $K + 1$, given by (4.55), due to the cooperation in the system. For example, BEP= 10^{-5} is achieved at $E_b/N_0 = 26$ dB with one relay ($K = 1$), or at $E_b/N_0 = 17.7$ dB with two relays ($K = 2$), or at $E_b/N_0 = 13.5$ dB with three relays ($K = 3$) in the system. Thus, compared to a single relay in the system, an E_b/N_0 gain of about 8.3 dB and 12.5 dB can be achieved if two and three relays, respectively, are used in the system.

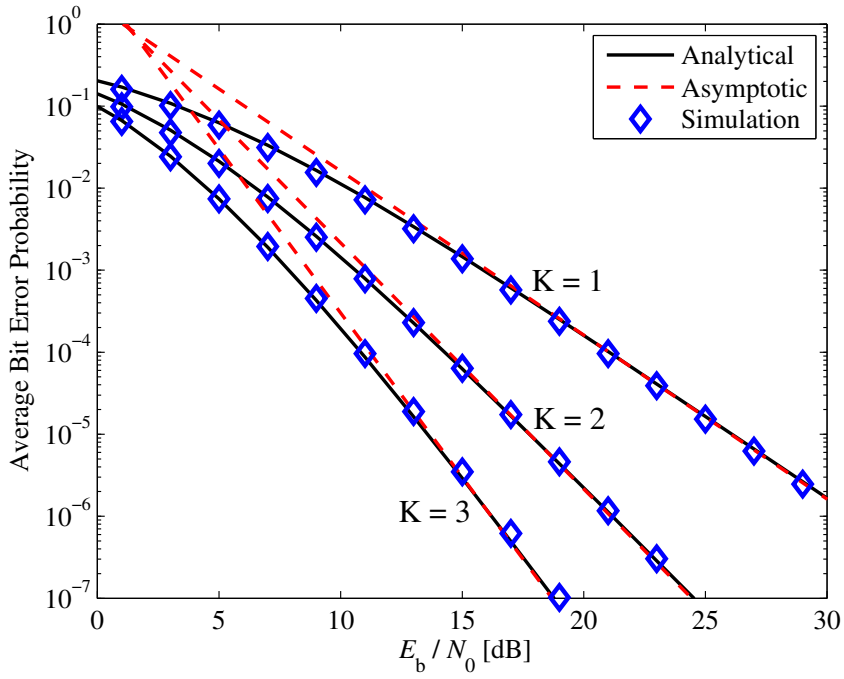

Figure 4.2: Error probability of the 2W-SSC system as a function of E_b/N_0, when $K = 1$, 2 and 3.

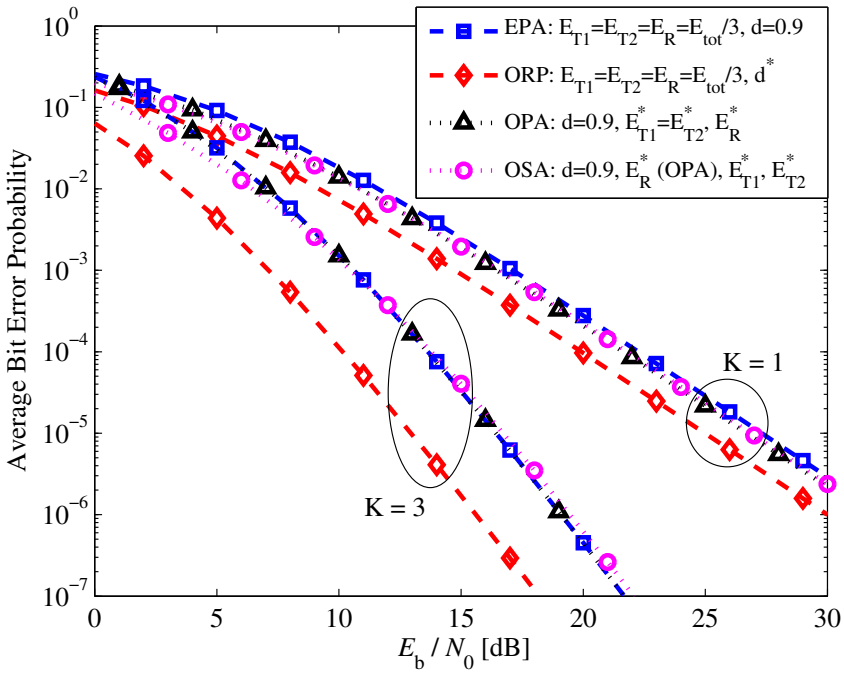

Figure 4.3: Error probability of the 2W-SSC system as a function of E_b/N_0, with different optimization schemes when $d_{T_1R} = 0.9$, and $K = 1, 3$.

Figure 4.3 compares the error performance of the system for different optimization schemes when relays are placed close to T_2 and far away from T_1 (i.e. $d_{T_1R} = 0.9$). The figure also shows the average BEP of the system for equal power allocation (EPA), optimal relay position (ORP), optimal power allocation (OPA), and optimal source power allocation (OSA). It is clear that the performance enhancement can be achieved with optimal relay position scheme over other optimization schemes and about 4 dB gain in E_b/N_0 can be achieved. The optimum placement of relays is obtained using (4.67), which is at the middle of both terminals ($d^* = 0.5$), due to the two-way communication. It is observed that when relays are close to either terminal, the optimal power scheme allocates more power to the terminal farther from the relays, which supports to maintain the error performance.

The outage performance of the system as a function of E_b/N_0 is shown in Figure 4.4. The simulation results perfectly match with the analytical results for the outage probability, given by (4.90), which confirms the accuracy of the mathematical expressions derived for the outage probability. Also, it is noted that the asymptotic outage performance of the system, derived in (4.98), is in good agreement with both simulation and analytical results, at medium and high SNRs. The slope of the outage probability curve becomes steeper with the increase in the number of relays, indicating an increase in the diversity order of the system.

Figure 4.5 depicts the outage probability of the system as a function of the information rate (R_0) at $E_b/N_0 = 20$ dB. Again, it is noted that both exact and asymptotic outage probability results, (4.90) and (4.98), are in close agreement with the simulation results.

Figure 4.6 is plotted to demonstrate the average channel capacity of the system as a function of E_b/N_0. The figure also shows the upper bound on the capacity of the system with dashed lines. Channel capacity results for $K = 1$ and $K = 3$ are

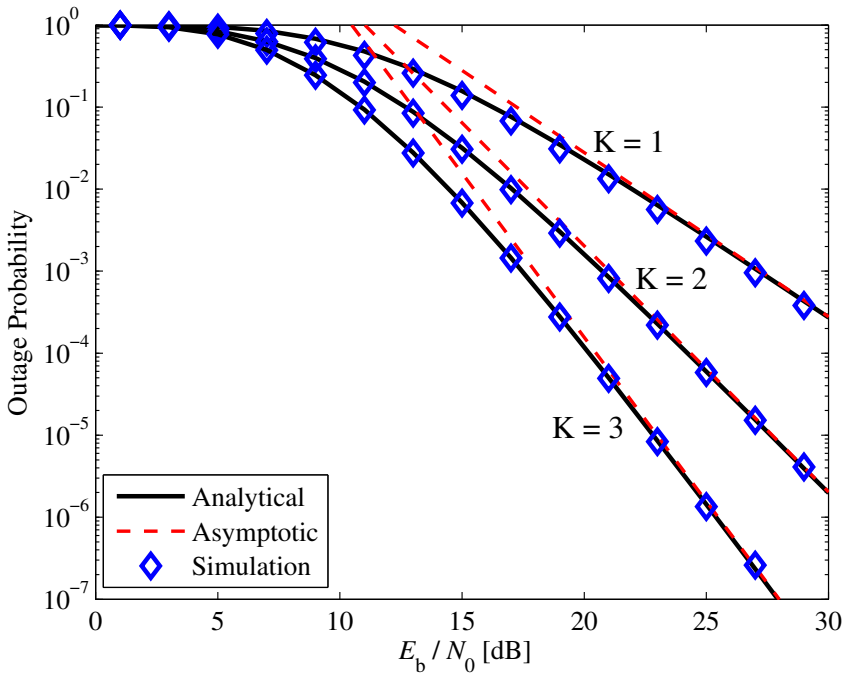

Figure 4.4: Outage probability of the 2W-SSC system as a function of E_b/N_0 when $R_0 = 2$, and $K = 1, 2, 3$.

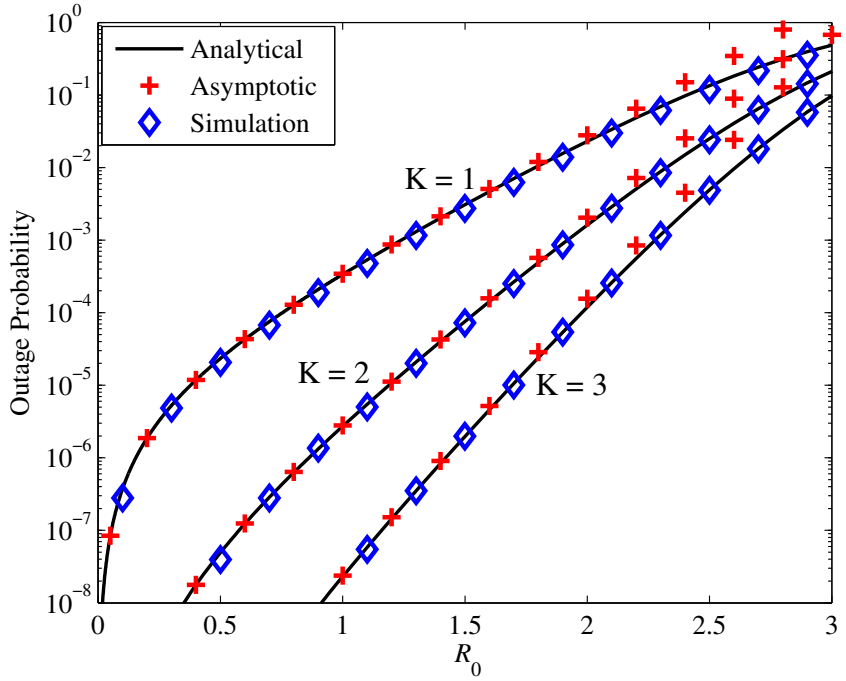

Figure 4.5: Outage probability of the 2W-SSC system as a function of information rate (R_0) when $E_b/N_0 = 20$ dB, and $K = 1, 2, 3$.

shown in the figure and also the channel capacity for the case of direct transmission is plotted for comparison. It is evident that the analytical expression for the capacity of the system, given by (4.106), are in excellent agreement with their corresponding simulation results, thus validating the analytical work for channel capacity of the system. The figure shows the significant capacity improvement for the 2W-SSC system, as the system exchanges four symbols in three time slots, while direct transmission system requires four time slots to exchange the same four symbols. It is observed that the capacity of the system improves with the increase in the number of relays. For example, the average channel capacity of 10 bits/s/Hz can be achieved at $E_b/N_0 = 14.4$ dB with three relays as compared to $E_b/N_0 = 15.8$ dB with one relay, thus providing an E_b/N_0 gain of about 1.4 dB.

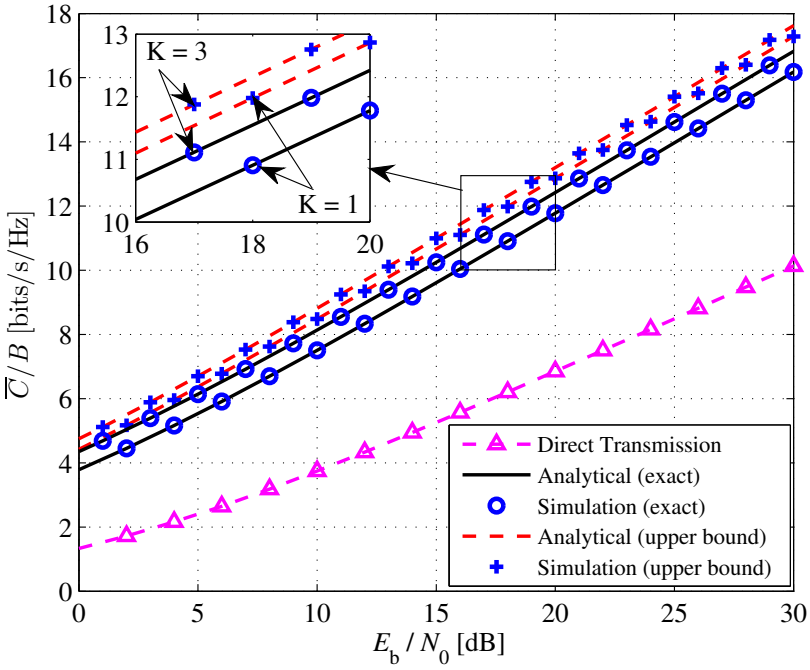

Figure 4.6: Channel capacity of the 2W-SSC system as a function of E_b/N_0, when $K = 1$ and 3.

4.7 Summary

In this chapter, a two-way signal space cooperative system using the best relay is presented and its performance was analyzed. The error probability expression of the 2W-SSC system was derived over the Rayleigh fading channel. It was shown that the 2W-SSC system enhances the performance and doubles the spectral efficiency of the conventional two-way cooperative system. The closed-form expression for the asymptotic error probability was obtained, which showed that the 2W-SSC system can achieve a diversity order equal to one higher than the number of cooperating relays. A detailed analysis of system optimization, including relay placement and power allocation, was additionally conducted. It was shown that the power allocation is affected by the relays position, especially when the relays are close to either terminal. Moreover, the system optimization was shown to enhance the performance significantly. Exact and asymptotic outage probability expressions were also derived. Lastly, closed-form expressions for average channel capacity as well as an upper bound on channel capacity were obtained. The validity of all of the aforementioned analysis and derivations was confirmed through extensive Monte Carlo simulations.

Chapter 5

Dual-Hop Signal Space Cooperative Relaying System using Single Relay

The dual-hop relaying plays an important role when a direct link between source and destination is not practical for various reasons and constraints [34, 65]. In a dual-hop relaying system, operating in half-duplex mode without a direct link between source and destination, the source broadcasts information signal to the relay and in turn relay repeats it to the destination using its own subchannel in the next phase [46]. This strategy of relaying decreases the overall system spectral efficiency and restricts the achievable data rate [48]. However, if signal space diversity (SSD) [25] is used in the dual-hop relaying system, it is possible to improve its spectral efficiency and performance. Thus, a dual-hop DF relaying system with signal space diversity using a single relay is proposed. Hereafter, the proposed system will be referred to as DH-SSC-1R.

In the conventional dual-hop DF relaying system, the transmission of one symbol takes one transmission cycle with two transmission phases and the transmission of two symbols takes two transmission cycles with a total of four phases. The DH-SSC-1R system uses two transmission cycles with a total of three phases for the transmission of two symbols.

In the DH-SSC-1R system, the first symbol from the expanded constellation is transmitted to the relay in the first phase. This symbol is decoded and two symbols, first and second symbols, from the rotated constellation are recovered at the relay, due to the SSD technique. The relay then forwards the first and second symbols to the destination in the second and third phases, respectively. Thus, in the DH-SSC system, two symbols are transmitted in three phases while in the conventional dual-hop DF relaying system four phases are required to achieve the same. Therefore, the DH-SSC system is more spectrally efficient than the conventional system, as the number of transmission phases is less than that required in the conventional system. Also, the DH-SSC system offers superior performance relative to the comparable dual-hop relaying systems.

In this chapter, the system model of the proposed DH-SSC-1R system is described in Section 5.1. Closed-form expression for the average symbol error probability (SEP) and its asymptotic approximation are derived in Section 5.2. The performance of the DH-SSC-1R system is compared with the relevant dual-hop relaying systems in Section 5.3. The chapter is concluded in Section 5.4.

5.1 System Model

The proposed dual-hop signal space cooperative relaying system is shown in Figure 5.1, which consists of a source (S), a destination (D), and a relay (R), without a direct link between the source and the destination. It is assumed that each node is equipped with a single omni-directional antenna and the system operates in half-duplex mode. All the channels in the system are assumed to slow Rayleigh fading channels. It is also assumed that the channel information is available at all the receiving nodes, and channels are mutually independent.

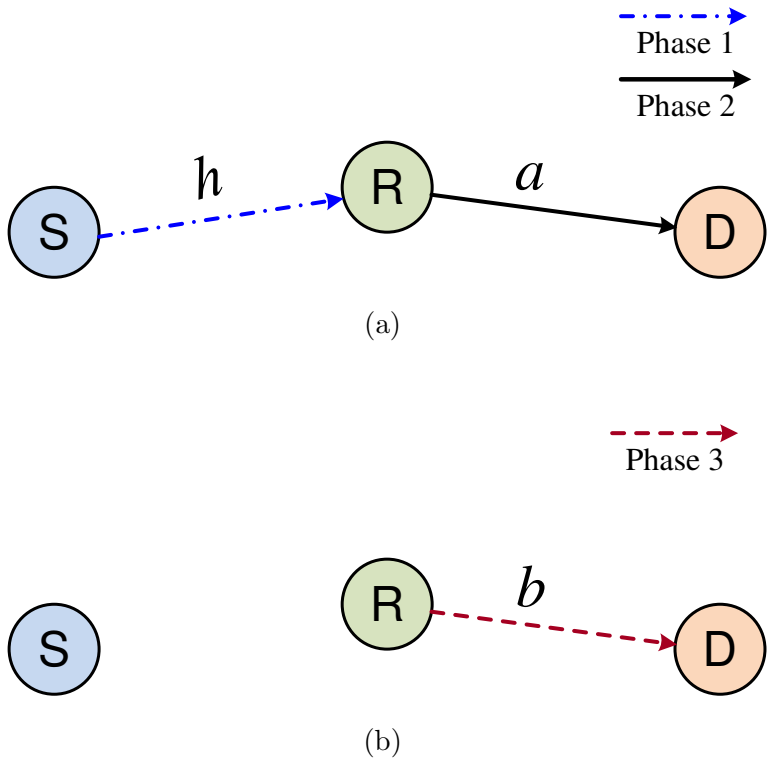

Figure 5.1: System model of a dual-hop signal space cooperative relaying system with a single relay (DH-SSC-1R). (a) First transmission cycle (b) Second transmission cycle

In the DH-SSC-1R system, SSD is used at the source, the destination and the relay with signal points rotated and interleaved before transmission. At the source, each $m = \log_2(M)$ group of information bits is mapped to a point in the ordinary constellation either M-QAM or M-PSK. For simplicity, two original source symbols $\mathbf{s} = (s_1, s_2)$ from the ordinary constellation Φ (e.g. 4-QAM) are considered. These symbols are denoted as $s_1 = \Re\{s_1\} + j\Im\{s_1\}$ and $s_2 = \Re\{s_2\} + j\Im\{s_2\}$, where $j = \sqrt{-1}$, and $\Re\{\cdot\}$ and $\Im\{\cdot\}$ are in-phase (I) and quadrature (Q) components of the symbols, respectively. The original symbols are then rotated, i.e. $x_1 = s_1\, e^{j\theta}$ and $x_2 = s_2\, e^{j\theta}$, which then belong to the rotated constellation Φ_r. The Q components of the rotated symbols are interleaved to transmit signal components over different

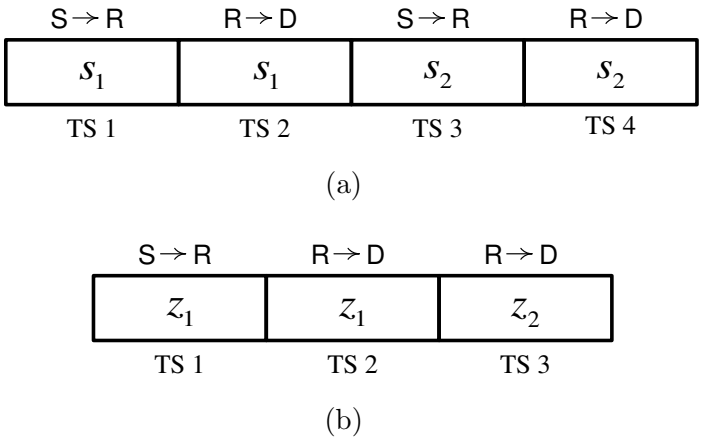

Figure 5.2: Time slots (TS) allocation to: (a) the conventional dual-hop relaying system, and (b) the DH-SSC-1R system.

fading paths, as

$$z_1 = \Re\{x_1\} + j\Im\{x_2\}, \tag{5.1}$$

$$z_2 = \Re\{x_2\} + j\Im\{x_1\}. \tag{5.2}$$

The transmitted SSD symbols, $z = (z_1, z_2)$, correspond to an expanded constellation Υ. It is important to note that three transmission phases are used to transmit these two symbols in the DH-SSC-1R system. The total power budget of the system for the transmission of every two symbols in three phases is restricted to E_{tot}, which is equal to the total power of two symbols. In the first phase, the source transmits only one of the two symbols (i.e. z_1) to the relay with an energy of E_S, as shown in Figure 5.2. The received signal at the relay can be expressed as

$$y_{SR}^{(1)} = \sqrt{E_S \lambda_{SR}}\, h\, z_1 + w_R, \tag{5.3}$$

where w_R represents zero-mean additive white Gaussian noise (AWGN) with a variance of N_0 at the relay and h represents the channel coefficient of $\mathsf{S}-\mathsf{R}$ link with a

variance of σ_h^2. Moreover, $\lambda_{SR} = 1/d_{SR}^{\nu}$ represents the geometric gain with d_{SR} as the $\mathsf{S}-\mathsf{R}$ distance and ν as the path loss exponent. Then, the rotated symbols, x_1 and x_2, are detected at the relay from the received expanded symbol, $z_1 = \Re\{x_1\} + j\Im\{x_2\}$, using maximum likelihood technique as

$$\hat{x}_1 = \arg\min_{x \in \Phi_r} \left| \Re\{h^* \, y_{SR}\} - \sqrt{E_S \lambda_{SR}} \, |h|^2 \, \Re\{x_1\} \right|^2, \tag{5.4}$$

$$\hat{x}_2 = \arg\min_{x \in \Phi_r} \left| \Im\{h^* \, y_{SR}\} - \sqrt{E_S \lambda_{SR}} \, |h|^2 \, \Im\{x_2\} \right|^2, \tag{5.5}$$

where $*$ denotes complex conjugation. If the source symbol is correctly detected by the relay, the relay is able to recover both symbols, x_1 and x_2, from the received expanded symbol z_1. In case of error in detection, the relay sends an indication of its failure to the source through a reliable feedback channel. The channel coefficients of relay-to-destination link in the second phase ($\mathsf{R}^{(2)} - \mathsf{D}$) and relay-to-destination link in the third phase ($\mathsf{R}^{(3)} - \mathsf{D}$) are denoted as a and b, with their variances as σ_a^2 and σ_b^2, respectively.

The relay (R) forwards both z_1 and z_2 with symbol energy of E_R to the destination in the second and third phases, respectively, as shown in Figure 5.2. Thus, the received signals at the destination can be expressed as

$$y_{RD}^{(2)} = \sqrt{E_R \lambda_{RD}} \, a \, [\Re\{x_1\} + j\Im\{x_2\}] + w_{D_1}, \tag{5.6}$$

$$y_{RD}^{(3)} = \sqrt{E_R \lambda_{RD}} \, b \, [\Re\{x_2\} + j\Im\{x_1\}] + w_{D_2}, \tag{5.7}$$

where w_{D_1} and w_{D_2} represent zero-mean AWGN with a variance of N_0 at the destination, and $\lambda_{RD} = 1/d_{RD}^{\nu}$ represents the geometric gain of $\mathsf{R}-\mathsf{D}$ links with d_{RD} as the $\mathsf{R}-\mathsf{D}$ distance. Let $\mathbf{r} = (r_1, r_2)$ represent the signal at the destination after

component de-interleaver, given by

$$r_1 = \Re\{a^* \, y_{RD}^{(2)}\} + j\Im\{b^* \, y_{RD}^{(3)}\}, \tag{5.8}$$

$$r_2 = \Re\{b^* \, y_{RD}^{(3)}\} + j\Im\{a^* \, y_{RD}^{(2)}\}. \tag{5.9}$$

The maximum likelihood detection is again used at the destination to detect the source message using

$$\hat{x}_1 = \arg \min_{x \in \Phi_r} \left[\left| \Re\{r_1\} - \sqrt{E_R \lambda_{RD}} |a|^2 \Re\{x_1\} \right|^2 + \left| \Im\{r_1\} - \sqrt{E_R \lambda_{RD}} |b|^2 \Im\{x_1\} \right|^2 \right], \tag{5.10}$$

$$\hat{x}_2 = \arg \min_{x \in \Phi_r} \left[\left| \Re\{r_2\} - \sqrt{E_R \lambda_{RD}} |b|^2 \Re\{x_2\} \right|^2 + \left| \Im\{r_2\} - \sqrt{E_R \lambda_{RD}} |a|^2 \Im\{x_2\} \right|^2 \right]. \tag{5.11}$$

After de-rotating, i.e. $\hat{s}_1 = \hat{x}_1 \, e^{-j\theta}$ and $\hat{s}_2 = \hat{x}_2 \, e^{-j\theta}$, original transmitted signal points can be obtained.

It is significant to highlight that the DH-SSC-1R system transmits two symbols in three phases while the conventional dual-hop DF relaying system uses two phases to transmit one symbol, thus, resulting in improved data rate and spectral efficiency compared to the conventional dual-hop DF relaying system, without extra bandwidth, complexity, or transmit power.

5.2 Error Probability Analysis

In this section, a closed-form expression for the error probability of the DH-SSC-1R system over Rayleigh fading channel is derived. Also, an asymptotic approximation

of the error probability of the system is presented.

5.2.1 Average Error Probability

The average symbol error probability (SEP) of the system depends upon the probability that the relay detects the signal received from the source with or without an error, and hence can be written as

$$\mathcal{P}_{\text{sym}}(e) = \mathcal{P}_{\text{sym}}^{\text{SR}}(e) + \left[1 - \mathcal{P}_{\text{sym}}^{\text{SR}}(e)\right] \mathcal{P}_{\text{sym}}^{\text{coop}}(e), \tag{5.12}$$

where $\mathcal{P}_{\text{sym}}^{\text{coop}}(e)$ denotes the conditional probability of the cooperative link between $\mathsf{R}^{(2)} - \mathsf{D}$ and $\mathsf{R}^{(3)} - \mathsf{D}$ when the relay correctly detects the signal received from the source. Also, $\mathcal{P}_{\text{sym}}^{\text{SR}}(e)$ denotes the average SEP of the $\mathsf{S} - \mathsf{R}$ link, i.e. the probability that the relay is unable to detect the signal received from the source correctly.

The conditional SEP for a given SNR γ_h over the $\mathsf{S} - \mathsf{R}$ link can be written as

$$\mathcal{P}_{\text{sym}}^{\text{SR}}(e|\gamma_h) \leq \alpha_z Q\left(\sqrt{\beta_z \gamma_h}\right), \tag{5.13}$$

where $Q(x) = \frac{1}{\sqrt{2\pi}} \int_x^\infty e^{-t^2/2} dt$ denotes the Gaussian Q-function [67, 26.2.3]. Also, $\gamma_h = |h|^2 E_S/N_0$ denotes the instantaneous SNR of the $\mathsf{S} - \mathsf{R}$ link with the average SNR $\overline{\gamma}_h = \sigma_h^2 E_S/N_0$. Moreover, α_z and β_z are obtained by the expanded constellation and its size $|\Upsilon|$. For instance, $\alpha_z = 4$ and $\beta_z = 3/(|\Upsilon| - 1)$ for M-QAM; and $\alpha_z = 2$ and $\beta_z = 2\sin^2(\pi/|\Upsilon|)$ for M-PSK [5]. It is important to mention that all derived results in this chapter are applicable to any modulation scheme which has instantaneous SEP of the form $\alpha\, Q(\sqrt{\beta\,\gamma})$. Thus, $\mathcal{P}_{\text{sym}}^{\text{SR}}(e)$ over Rayleigh fading

channel can be expressed as

$$\mathcal{P}_{\text{sym}}^{\text{SR}}(e) = \int_0^\infty \alpha_z Q\left(\sqrt{\beta_z \gamma_h}\right) f_{\gamma_h}(\gamma_h)\, d\gamma_h, \tag{5.14}$$

where $f_{\gamma_h}(\gamma_h) = \frac{1}{\overline{\gamma}_h} e^{-\gamma_h/\overline{\gamma}_h}$ is the PDF of the SNR γ_h [68]. The integration in (5.14) is solved using (A.12), thus $\mathcal{P}_{\text{sym}}^{\text{SR}}(e)$ can be written as

$$\mathcal{P}_{\text{sym}}^{\text{SR}}(e) = \frac{\alpha_z}{2}\left(1 - \sqrt{\frac{\beta_z \overline{\gamma}_h}{\beta_z \overline{\gamma}_h + 2}}\right). \tag{5.15}$$

The SEP of the cooperative link between $\mathsf{R}^{(2)} - \mathsf{D}$ and $\mathsf{R}^{(3)} - \mathsf{D}$ for given SNRs γ_a and γ_b can be represented as

$$\mathcal{P}_{\text{sym}}^{\text{coop}}(e|\gamma_a, \gamma_b) = \alpha_x Q\left(\sqrt{\beta_x \gamma_t}\right), \tag{5.16}$$

where $\alpha_x = 2(|\Phi_r| - 1)/|\Phi_r|$, $\beta_x = 3/(|\Phi_r|^2 - 1)$ [5], and γ_t is the SNR of the cooperative link ($\gamma_t = \gamma_a + \gamma_b$). Therefore, $\mathcal{P}_{\text{sym}}^{\text{coop}}(e)$ over a fading channel can be expressed as

$$\mathcal{P}_{\text{sym}}^{\text{coop}}(e) = \int_0^\infty \alpha_x Q\left(\sqrt{\beta_x \gamma_t}\right) f_{\gamma_t}(\gamma_t)\, d\gamma_t, \tag{5.17}$$

where $f_{\gamma_t}(\gamma_t)$ is the PDF of the SNR γ_t. $f_{\gamma_t}(\gamma_t)$ can be evaluated using the PDFs of γ_a and γ_b, that are $f_{\gamma_a}(\gamma_a) = \frac{1}{\overline{\gamma}_a} e^{-\gamma_a/\overline{\gamma}_a}$ and $f_{\gamma_b}(\gamma_b) = \frac{1}{\overline{\gamma}_b} e^{-\gamma_b/\overline{\gamma}_b}$, respectively, where $\gamma_a = |a|^2 E_R/N_0$, $\gamma_b = |b|^2 E_R/N_0$, $\overline{\gamma}_a = \sigma_a^2 E_R/N_0$, and $\overline{\gamma}_b = \sigma_b^2 E_R/N_0$. Thus, using (C.6), $f_{\gamma_t}(\gamma_t)$ can be written as

$$f_{\gamma_t}(\gamma) = \frac{1}{\overline{\gamma}_b - \overline{\gamma}_a}\left(e^{-\gamma/\overline{\gamma}_b} - e^{-\gamma/\overline{\gamma}_a}\right) \tag{5.18}$$

Upon substituting (5.18) into (5.17) and solving the integration using (A.12), $\mathcal{P}_{\text{sym}}^{\text{coop}}(e)$ can be written as

$$\mathcal{P}_{\text{sym}}^{\text{coop}}(e) = \frac{\alpha_x}{2}\frac{1}{\overline{\gamma}_b - \overline{\gamma}_a}\left[\overline{\gamma}_b\left(1 - \sqrt{\frac{\beta_x\overline{\gamma}_b}{\beta_x\overline{\gamma}_b + 2}}\right) - \overline{\gamma}_a\left(1 - \sqrt{\frac{\beta_x\overline{\gamma}_a}{\beta_x\overline{\gamma}_a + 2}}\right)\right] \tag{5.19}$$

Finally, a closed-form expression for the average SEP of the system can be easily obtained by substituting (5.19) and (5.15) into (5.12).

5.2.2 Asymptotic Error Probability

An asymptotic SEP expression is straightforward compared to the average SEP expression, to quantify the diversity gain and analyzing the effects of system parameters. Also, the asymptotic SEP expression is valid for moderate to high SNR region. The asymptotic SEP of the system can be written as

$$\mathcal{P}_{\text{sym}}(e) \simeq \mathcal{P}_{\text{sym}}^{\text{SR}}(e) + \mathcal{P}_{\text{sym}}^{\text{coop}}(e). \tag{5.20}$$

The PDF of γ_h can be approximated using the Taylor series expansion and neglecting the higher order terms, as

$$f_{\gamma_h}(\gamma) \simeq \frac{1}{\overline{\gamma}_h}. \tag{5.21}$$

Thus,

$$\mathcal{P}_{\text{sym}}^{\text{SR}}(e) \simeq \frac{\alpha_z}{2\beta_z}\frac{1}{\overline{\gamma}_h}. \tag{5.22}$$

From (5.18), $f_{\gamma_t}(\gamma)$ can be approximated as

$$f_{\gamma_t}(\gamma) \simeq \frac{1}{\overline{\gamma}_a\overline{\gamma}_b}. \tag{5.23}$$

Upon substituting (5.23) into (5.17) and solving the integration, the following expression is obtained

$$\mathcal{P}_{\text{sym}}^{\text{coop}}(e) \simeq \frac{\alpha_x}{2\beta_x}\frac{1}{\overline{\gamma}_a\overline{\gamma}_b}, \tag{5.24}$$

Upon substituting (5.22) and (5.24) into (5.20), the asymptotic SEP can be expressed as

$$\mathcal{P}_{\text{sym}}(e) \simeq \frac{\alpha_z}{2\beta_z}\frac{1}{\overline{\gamma}_h} + \frac{\alpha_x}{2\beta_x}\frac{1}{\overline{\gamma}_a\overline{\gamma}_b}, \tag{5.25}$$

5.3 Results and Discussion

The performance of the DH-SSC-1R system is illustrated using the analytical expressions derived in the previous section. The variances of channel coefficients are assumed to be $\sigma_h^2 = \sigma_a^2 = \sigma_b^2 = 1$ and the path loss exponent to be $\nu = 3$. In the system, the relay is located at the middle of S and D. For the fair analysis of the system, the total power budget to transmit two symbols is same as that required for a direct transmission system, i.e. $E_S = 1$ and $E_R = 0.5$, making the total power budget equals to 2 units to transmit two symbols. For accuracy of Monte Carlo simulations, 10^9 iterations are used for each simulation point.

The performance of the DH-SSC-1R system is compared with other relevant dual-hop DF relaying and direct transmission systems, as shown in Figure 5.3. The SSD used in the system is 4-QAM with a rotation angle of 26.6°. There are two relevant dual-hop DF relaying systems that are of great importance to compare with the DH-SSC-1R system. One is SSD-based dual-hop DF relaying system, and the other is conventional dual-hop DF relaying system. In SSD-based dual-hop system, one SSD symbol from the expanded constellation is transmitted from the source to the relay and the relay decodes the symbol and forwards the same symbol to the

destination. Due to SSD, the destination recovers two symbols, and thus SSD-based dual-hop system transmits two symbols in two phases. However, it has poor error performance, as shown in Figure 5.3 with the $\triangle$ markers. Since the SSD-based dual-hop system uses a single instance of link between the relay and the destination, error in one SSD symbol leads to the error in two original symbols. The conventional dual-hop system, on the other hand, transmits one symbol in two phases and its performance is shown in Figure 5.3 with the $\square$ markers. The average bit error probabilities of the DH-SSC-1R system and the direct transmission system are also shown in the figure with the solid lines and the $\circ$ markers, respectively. It is observed from the figure that the DH-SSC-1R system has the same error performance as that of the direct transmission system and is superior to SSD-based dual-hop system. The advantage of the DH-SSC-1R system is that it saves one phase while maintaining the same performance compared to the conventional dual-hop system. The major advantage of the DH-SSC-1R system is that it is better in terms of system performance and spectral efficiency compared to the relevant dual-hop systems.

Figure 5.4 shows the average bit error probability (BEP) of the DH-SSC-1R system using 4-QAM as a function of the average SNR (E_b/N_0). The simulation result in this figure is represented by $\circ$ markers while analytical and asymptotic results are shown by solid and dashed lines, respectively. It is evident that analytical result for the error probability is in good agreement with the simulation results, thus confirming the derived mathematical expressions. Also, the asymptotic result, given by (5.25), has a good match with the analytical and simulation results at medium and high SNRs.

In a similar fashion, the average BEP of the DH-SSC-1R system using 16-QAM with $\theta = 13.8^\circ$ is obtained and shown in Figure 5.5. Therefore, the DH-SSC-1R system can be used with any order of M-QAM and M-PSK modulation schemes.

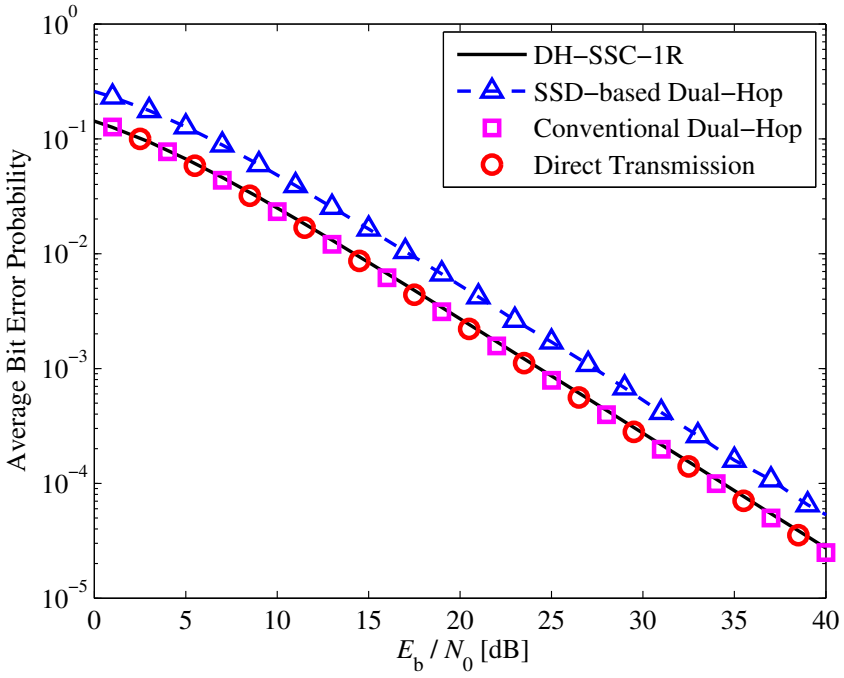

Figure 5.3: Performance comparison of the DH-SSC-1R system using 4-QAM with relevant dual-hop systems.

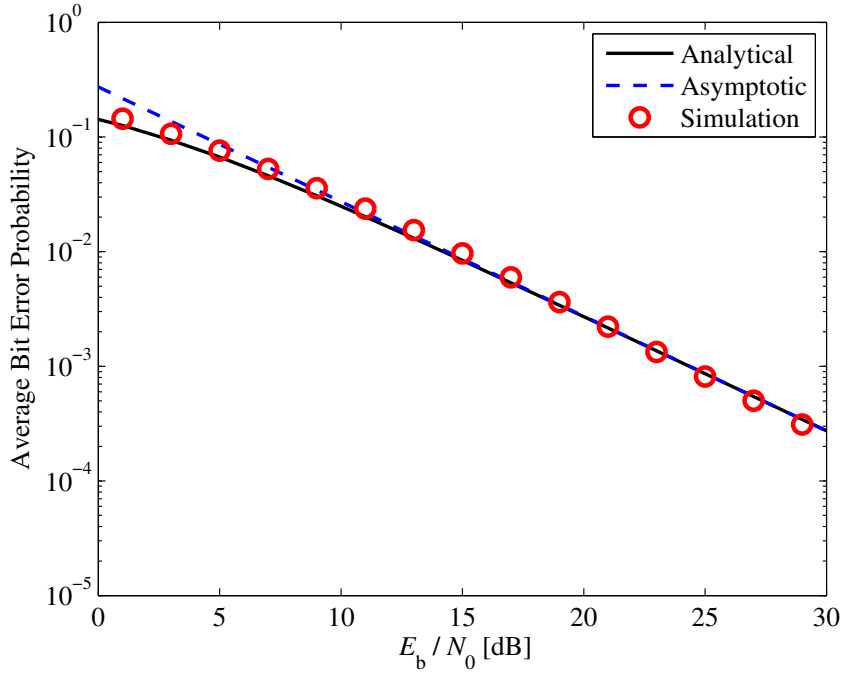

Figure 5.4: Error probability of the DH-SSC-1R system using 4-QAM.

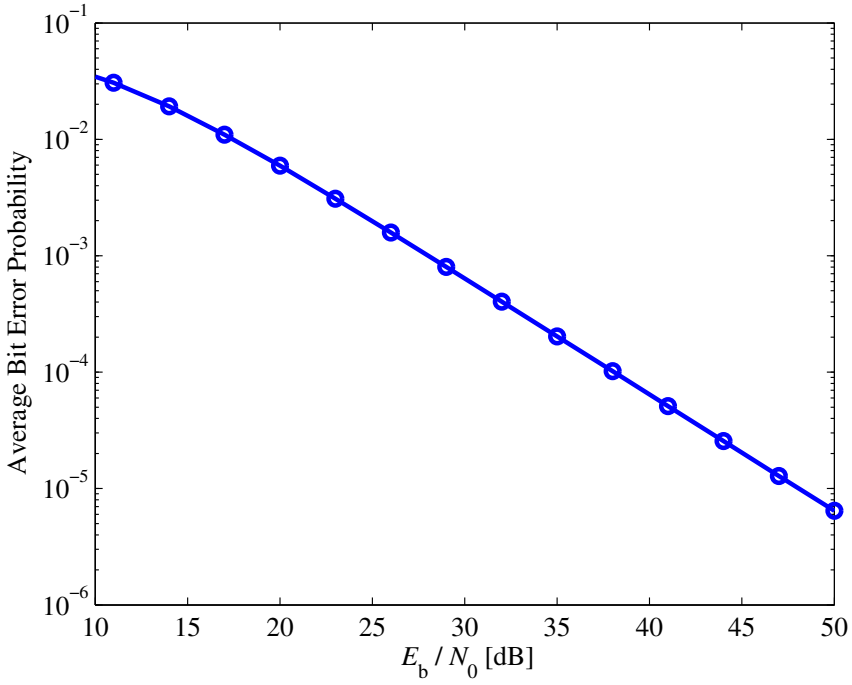

Figure 5.5: Error probability of the DH-SSC-1R system using 16-QAM.

5.4 Summary

This chapter has introduced a dual-hop DF relaying system with a single relay using signal space diversity (SSD) where no direct link exists between the source and the destination. The error performance of the DH-SSC system was analyzed over Rayleigh fading channel. It was shown that the proposed DH-SSC-1R system improves the spectral efficiency of the conventional dual-hop DF relaying system. The DH-SSC-1R system was compared with other relevant dual-hop systems and showed its superiority in terms of system performance and spectral efficiency. Exact and asymptotic expressions for the error probability were derived. All of the analysis and mathematical derivations were validated through Monte Carlo simulations.

Chapter 6

Dual-Hop Signal Space Cooperative Relaying System using Multiple Relays

In this chapter, the concept of SSD into a dual-hop DF relaying system is extended to the case of K intermediate relays in the system. Analysis of various performance metrics and system optimization of the system is carried out and the best relay selection and relay location are examined. The proposed system will be referred to as DH-SSC.

In the DH-SSC system, the first symbol from the expanded constellation is transmitted to the relays in the first phase. This symbol is decoded at the relays to recover the first and second rotated symbols. Based on the quality of links between the relays and the destination, the best relay is chosen from the set of relays that have decoded the symbols correctly. The best relay then forwards the first and second symbols to the destination in the second and third phases, respectively. Thus, the DH-SSC system transmits two symbols in three phases while the conventional dual-hop DF relaying system requires four phases to transmit the same two symbols. Therefore, the DH-SSC system enhances the spectral efficiency by reducing the number of phases for transmission and improves the system performance. The DH-SSC system shows superior performance compared to the well-known dual-hop relaying systems.

The chapter is organized as follows: The system model of the DH-SSC system is described in Section 6.1. Closed-form expressions for the average symbol error probability (SEP), asymptotic approximation of SEP and the diversity gain of the system are derived in Section 6.2. The optimizations of power allocation and relay position as well as the joint optimization of the two are examined in Section 6.3. Exact and asymptotic outage probabilities are derived in Section 6.4. Average channel capacity and its upper bound are derived in Section 6.5. The analytical and simulation results are presented and discussed in Section 6.6. The chapter is concluded in Section 6.7.

6.1 System Model

The system model of the dual-hop signal space cooperative relaying system is shown in Figure 6.1. The DH-SSC system consists of a source (S), a destination (D), and K number of relays (R_i, $i = 1, 2, ..., K$) without a direct link between the source and the destination. Each node in the system is equipped with a single omni-directional antenna and operates in half-duplex mode. The system is assumed to operate in slow Rayleigh fading channels. It is also assumed that the channel information is available at all the receiving nodes, and all channels are mutually independent.

In the DH-SSC system, SSD is applied at the source, the destination and the relays, where the signal points are rotated and interleaved before transmission. At the source, each group of $m = \log_2(M)$ information bits is mapped to a signal point in the ordinary constellation using M-QAM or M-PSK. For simplicity, two original source symbols $\mathbf{s} = (s_1, s_2)$ are considered from the ordinary constellation Φ (e.g. 4-QAM). These original complex symbols are denoted as $s_1 = \Re\{s_1\} + j\Im\{s_1\}$ and $s_2 = \Re\{s_2\} + j\Im\{s_2\}$, where $j = \sqrt{-1}$, and $\Re\{\cdot\}$ and $\Im\{\cdot\}$ are in-phase (I) and

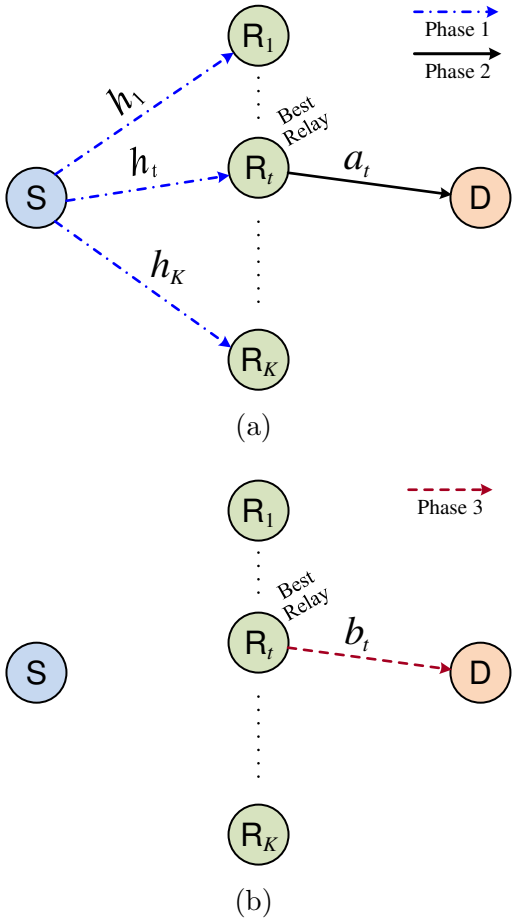

Figure 6.1: System model of a dual-hop signal space cooperative relaying system (DH-SSC) with K relays. (a) First transmission cycle (b) Second transmission cycle

quadrature (Q) components of the symbols, respectively. The original symbols are then rotated, i.e. $x_1 = s_1\, e^{j\theta}$ and $x_2 = s_2\, e^{j\theta}$, which then belong to the rotated constellation Φ_r. The Q components of the rotated symbols are interleaved in order to transmit signal components through different fading paths, as

$$z_1 = \Re\{x_1\} + j\Im\{x_2\}, \tag{6.1}$$

$$z_2 = \Re\{x_2\} + j\Im\{x_1\}. \tag{6.2}$$

The transmitted SSD symbols, $z = (z_1, z_2)$, correspond to an expanded con-

stellation Υ. It is important to note that two transmission cycles to transmit two symbols consists of three phases in the DH-SSC system. The total power budget for the transmission of every two symbols in three phases at the source and the best relay is restricted to E_{tot}. For a fair study and analysis, the total power budget E_{tot} is equal to the total energy of two symbols. In the first phase, the source transmits only one of the two symbols (i.e. z_1) to the relays with symbol energy of E_S, thus the received signal at the ith relay can be expressed as

$$y_{SR_i}^{(1)} = \sqrt{\lambda_{SR} E_S}\, h_i\, z_1 + w_{R_i}, \tag{6.3}$$

where w_{R_i} represents zero-mean additive white Gaussian noise (AWGN) with a variance of N_0 at the ith relay and h_i represents the channel coefficients of $\mathsf{S} - \mathsf{R}_i$ links with a variance of σ_h^2. Moreover, $\lambda_{SR} = 1/d_{SR}^{\nu}$ represents the geometric gain with d_{SR} as the $\mathsf{S} - \mathsf{R}_i$ distance and ν as the path loss exponent. Then, the rotated symbols, x_1 and x_2, are detected at the ith relay from the transmitted expanded symbol, $z_1 = \Re\{x_1\} + j\Im\{x_2\}$, using the maximum likelihood technique as

$$\hat{x}_1 = \arg \min_{x \in \Phi_r} \left| \Re\{h_i^*\, y_{SR_i}\} - \sqrt{\lambda_{SR} E_S}\, |h_i|^2\, \Re\{x_1\} \right|^2, \tag{6.4}$$

$$\hat{x}_2 = \arg \min_{x \in \Phi_r} \left| \Im\{h_i^*\, y_{SR_i}\} - \sqrt{\lambda_{SR} E_S}\, |h_i|^2\, \Im\{x_2\} \right|^2, \tag{6.5}$$

where $*$ denotes complex conjugation. If the source symbol is successfully detected by the relay, then the relay is able to recover both symbols, x_1 and x_2, from the transmitted expanded symbol z_1. In case of error in detection, the relay sends an indication of its failure to the source through a reliable feedback channel. The decoding set of relays is denoted as $\mathcal{C}$ that correctly decodes the source message and $|\mathcal{C}|$ as its cardinality. The channel coefficients of relay-to-destination links in the second phase

($\mathsf{R}_i^{(2)} - \mathsf{D}$) and relay-to-destination links in the third phase ($\mathsf{R}_i^{(3)} - \mathsf{D}$) are denoted as a_i and b_i with their variances as σ_a^2 and σ_b^2, respectively. Based on the channel quality of both a_i and b_i, the relay selection criteria to choose the best relay R_t [71], among all the relays that are members of $\mathcal{C}$, can be written as

$$\mathsf{R}_t = \arg\max_{i \in \mathcal{C}} \left\{ \min \left(\gamma_{a_i}, \gamma_{b_i} \right) \right\}. \tag{6.6}$$

where γ_{a_i} and γ_{b_i} denote the instantaneous signal-to-noise ratios (SNRs) of $\mathsf{R}_i^{(2)} - \mathsf{D}$ and $\mathsf{R}_i^{(3)} - \mathsf{D}$ links, respectively. The best relay, R_t, forwards both z_1 and z_2 with symbol energy of E_R to the destination in the second and third phases, respectively. Thus, the received signals at the destination can be expressed as

$$y_{R_tD}^{(2)} = \sqrt{\lambda_{RD} E_R}\, a_t \, [\Re\{x_1\} + j\Im\{x_2\}] + w_{D_1}, \tag{6.7}$$

$$y_{R_tD}^{(3)} = \sqrt{\lambda_{RD} E_R}\, b_t \, [\Re\{x_2\} + j\Im\{x_1\}] + w_{D_2}, \tag{6.8}$$

where w_{D_1} and w_{D_2} represent zero-mean AWGN with a variance of N_0 at the destination, and $\lambda_{RD} = 1/d_{RD}^{\nu}$ represents the geometric gain of $\mathsf{R}_i - \mathsf{D}$ links with d_{RD} as the $\mathsf{R}_i - \mathsf{D}$ distance. $\mathbf{r} = (r_1, r_2)$ denotes the signal at the destination after component de-interleaver, and can be expressed as

$$r_1 = \Re\{a_t^* \, y_{R_tD}^{(2)}\} + j\Im\{b_t^* \, y_{R_tD}^{(3)}\}, \tag{6.9}$$

$$r_2 = \Re\{b_t^* \, y_{R_tD}^{(3)}\} + j\Im\{a_t^* \, y_{R_tD}^{(2)}\}. \tag{6.10}$$

The maximum likelihood detection is used at the destination to detect the

source message using

$$\hat{x}_1 = \arg\min_{x\in\Phi_r} \left[\left| \Re\{r_1\} - \sqrt{\lambda_{RD}E_R}|a_t|^2\Re\{x_1\} \right|^2 + \left| \Im\{r_1\} - \sqrt{\lambda_{RD}E_R}|b_t|^2\Im\{x_1\} \right|^2 \right], \tag{6.11}$$

$$\hat{x}_2 = \arg\min_{x\in\Phi_r} \left[\left| \Re\{r_2\} - \sqrt{\lambda_{RD}E_R}|b_t|^2\Re\{x_2\} \right|^2 + \left| \Im\{r_2\} - \sqrt{\lambda_{RD}E_R}|a_t|^2\Im\{x_2\} \right|^2 \right]. \tag{6.12}$$

After de-rotating, i.e. $\hat{s}_1 = \hat{x}_1\, e^{-j\theta}$ and $\hat{s}_2 = \hat{x}_2\, e^{-j\theta}$, original transmitted signal points can be obtained.

It is significant to highlight that the DH-SSC system transmits two symbols in three phases. On the other hand, the conventional dual-hop DF relaying system uses two phases to transmit one symbol, thus using four phases for the same two symbols. Therefore, the DH-SSC system significantly improves the data rate and the spectral efficiency when compared with the conventional dual-hop DF relaying system without extra bandwidth, complexity, or transmit power.

6.2 Error Probability Analysis

In this section, a closed-form expression for the error probability of the DH-SSC system over Rayleigh fading channel is derived. An asymptotic approximation of the error probability and diversity gain of the system are also examined.

6.2.1 Average Error Probability

The average symbol error probability (SEP) of the system depends on the ability of the relays to detect the signal received from the source with or without an error, and

therefore can be written as

$$\mathcal{P}_{\text{sym}}(e) = \Pr\{|\mathcal{C}| = 0\} + \sum_{k=1}^{K} \Pr\{|\mathcal{C}| = k\} \mathcal{P}_{\text{sym}}^{\text{coop}}(e|k), \tag{6.13}$$

where $\mathcal{P}_{\text{sym}}^{\text{coop}}(e|k)$ denotes the conditional probability of the cooperative link between $\mathsf{R}_i^{(2)} - \mathsf{D}$ and $\mathsf{R}_i^{(3)} - \mathsf{D}$ when k relays detect the signal received from the source correctly. Also, $\Pr\{|\mathcal{C}| = 0\}$ denotes the probability that none of the relays detects the signal received from the source correctly, and $\Pr\{|\mathcal{C}| = k\}$ the probability that k relays detect the signal received from the source correctly. These probabilities can be expressed as

$$\Pr\{|\mathcal{C}| = 0\} = \left[\mathcal{P}_{\text{sym}}^{\text{SR}_i}(e)\right]^K, \tag{6.14}$$

$$\Pr\{|\mathcal{C}| = k\} = \binom{K}{k} \left[\mathcal{P}_{\text{sym}}^{\text{SR}_i}(e)\right]^{K-k} \left[1 - \mathcal{P}_{\text{sym}}^{\text{SR}_i}(e)\right]^k. \tag{6.15}$$

The average SEP can then be written as

$$\mathcal{P}_{\text{sym}}(e) = \left[\mathcal{P}_{\text{sym}}^{\text{SR}_i}(e)\right]^K + \sum_{k=1}^{K} \binom{K}{k} \left[\mathcal{P}_{\text{sym}}^{\text{SR}_i}(e)\right]^{K-k} \times \left[1 - \mathcal{P}_{\text{sym}}^{\text{SR}_i}(e)\right]^k \mathcal{P}_{\text{sym}}^{\text{coop}}(e|k), \tag{6.16}$$

where $\mathcal{P}_{\text{sym}}^{\text{SR}_i}(e)$ is the average SEP over the $\mathsf{S} - \mathsf{R}_i$ link. The conditional SEP for a given SNR γ_{h_i} over the $\mathsf{S} - \mathsf{R}_i$ link can be written as

$$\mathcal{P}_{\text{sym}}^{\text{SR}_i}(e|\gamma_{h_i}) \leq \alpha_z Q\left(\sqrt{\beta_z \gamma_{h_i}}\right), \tag{6.17}$$

where $Q(x) = \frac{1}{\sqrt{2\pi}} \int_x^\infty e^{-t^2/2} dt$ denotes the Gaussian Q-function [67, 26.2.3]. Also, $\gamma_{h_i} = |h_i|^2 \lambda_{SR} E_S/N_0$ denotes the instantaneous SNR of $\mathsf{S}-\mathsf{R}_i$ links with the average

SNR $\overline{\gamma}_h = \sigma_h^2 \lambda_{SR} E_S/N_0$. Moreover, α_z and β_z are determined by the expanded constellation and its size $|\Upsilon|$. For instance, $\alpha_z = 4$ and $\beta_z = 3/(|\Upsilon|-1)$ for M-QAM; and $\alpha_z = 2$ and $\beta_z = 2\sin^2(\pi/|\Upsilon|)$ for M-PSK [5]. It is important to mention that all derived results in this chapter are applicable to any modulation scheme which has instantaneous SEP of the form $\alpha\, Q(\sqrt{\beta\,\gamma})$. Thus, $\mathcal{P}_{\text{sym}}^{\text{SR}_i}(e)$ over Rayleigh fading channel can be expressed as

$$\mathcal{P}_{\text{sym}}^{\text{SR}_i}(e) = \int_0^\infty \alpha_z Q\left(\sqrt{\beta_z \gamma_{h_i}}\right) f_{\gamma_{h_i}}\left(\gamma_{h_i}\right) d\gamma_{h_i}, \tag{6.18}$$

where $f_{\gamma_{h_i}}(\gamma_{h_i}) = \frac{1}{\overline{\gamma}_h} e^{-\gamma_{h_i}/\overline{\gamma}_h}$ is the PDF of the SNR γ_{h_i} [68]. Upon solving the integration in (6.18) using (A.12), $\mathcal{P}_{\text{sym}}^{\text{SR}_i}(e)$ can be written as

$$\mathcal{P}_{\text{sym}}^{\text{SR}_i}(e) = \frac{\alpha_z}{2}\left(1 - \sqrt{\frac{\beta_z \overline{\gamma}_h}{\beta_z \overline{\gamma}_h + 2}}\right). \tag{6.19}$$

The SEP of the cooperative link between $\mathsf{R}_i^{(2)} - \mathsf{D}$ and $\mathsf{R}_i^{(3)} - \mathsf{D}$ for given SNRs γ_{a_i}, γ_{b_i} and k active relays can be represented as

$$\mathcal{P}_{\text{sym}}^{\text{coop}}(e|k, \gamma_{a_i}, \gamma_{b_i}) = \alpha_x Q\left(\sqrt{\beta_x \gamma_t}\right), \tag{6.20}$$

where $\alpha_x = 2(|\Phi_r| - 1)/|\Phi_r|$, $\beta_x = 3/(|\Phi_r|^2 - 1)$ [5], and γ_t is the SNR of the best relay obtained through the relay selection criterion, expressed in (6.6). Therefore, $\mathcal{P}_{\text{sym}}^{\text{coop}}(e|k)$ over a fading channel can be expressed as

$$\mathcal{P}_{\text{sym}}^{\text{coop}}(e|k) = \int_0^\infty \alpha_x Q\left(\sqrt{\beta_x \gamma_t}\right) f_{\gamma_t}\left(\gamma_t\right) d\gamma_t, \tag{6.21}$$

where $f_{\gamma_t}(\gamma_t)$ is the PDF of the SNR γ_t and can be evaluated using PDFs of γ_{a_i} and γ_{b_i}, that are $f_{\gamma_{a_i}}(\gamma_{a_i}) = \frac{1}{\overline{\gamma}_a} e^{-\gamma_{a_i}/\overline{\gamma}_a}$ and $f_{\gamma_{b_i}}(\gamma_{b_i}) = \frac{1}{\overline{\gamma}_b} e^{-\gamma_{b_i}/\overline{\gamma}_b}$, respectively, where $\gamma_{a_i} = |a_i|^2 \lambda_{RD} E_R/N_0$, $\gamma_{b_i} = |b_i|^2 \lambda_{RD} E_R/N_0$, $\overline{\gamma}_a = \sigma_a^2 \lambda_{RD} E_R/N_0$, and $\overline{\gamma}_b = \sigma_b^2 \lambda_{RD} E_R/N_0$. Thus, using (B.21), $f_{\gamma_t}(\gamma_t)$ can be written as

$$
\begin{aligned}
f_{\gamma_t}(\gamma) = & \sum_{k=1}^{|\mathcal{C}|} \binom{|\mathcal{C}|}{k} \frac{(-1)^{k-1}}{\overline{\gamma}_a} \frac{k\overline{\gamma}_m}{k\overline{\gamma}_b - \overline{\gamma}_m} \left(e^{-\gamma/\overline{\gamma}_b} - e^{-k\gamma/\overline{\gamma}_m} \right) \\
& + \sum_{k=1}^{|\mathcal{C}|} \binom{|\mathcal{C}|}{k} \frac{(-1)^{k-1}}{\overline{\gamma}_b} k\, e^{-k\gamma/\overline{\gamma}_m},
\end{aligned} \tag{6.22}
$$

where $\overline{\gamma}_m$ is the harmonic mean of $\overline{\gamma}_a$ and $\overline{\gamma}_b$, i.e. $\overline{\gamma}_m = \overline{\gamma}_a \overline{\gamma}_b / (\overline{\gamma}_a + \overline{\gamma}_b)$. Upon substituting (6.22) into (6.21) and solving the integration using (A.12), $\mathcal{P}_{\text{sym}}^{\text{coop}}(e|k)$ can be written as

$$
\begin{aligned}
\mathcal{P}_{\text{sym}}^{\text{coop}}(e|k) = & \frac{\alpha_x}{2} \sum_{i=1}^{k} \binom{k}{i} \frac{(-1)^{i-1}}{\overline{\gamma}_a} \frac{i\overline{\gamma}_m}{i\overline{\gamma}_b - \overline{\gamma}_m} \times \\
& \left[\overline{\gamma}_b \left(1 - \sqrt{\frac{\beta_x \overline{\gamma}_b}{\beta_x \overline{\gamma}_b + 2}} \right) - \frac{\overline{\gamma}_m}{i} \left(1 - \sqrt{\frac{\beta_x \overline{\gamma}_m}{\beta_x \overline{\gamma}_m + 2\, i}} \right) \right] \\
& + \frac{\alpha_x}{2} \sum_{i=1}^{k} \binom{k}{i} \frac{(-1)^{k-1}}{\overline{\gamma}_b} \overline{\gamma}_m \left(1 - \sqrt{\frac{\beta_x \overline{\gamma}_m}{\beta_x \overline{\gamma}_m + 2\, i}} \right).
\end{aligned} \tag{6.23}
$$

Finally, a closed-form expression for the average SEP of the system can be easily obtained by substituting (6.23) and (6.19) into (6.16).

6.2.2 Asymptotic Error Probability

An asymptotic SEP expression is simple and straightforward compared to the average SEP expression, which clearly quantifies the diversity gain and analyzes the effects of system parameters. Also, the asymptotic SEP expression is valid for moderate to

high SNR region. The asymptotic SEP of the system can be written as

$$\mathcal{P}_{\text{sym}}(e) \simeq \left[\mathcal{P}_{\text{sym}}^{\text{SR}_i}(e)\right]^K + \sum_{k=1}^{K} \binom{K}{k} \left[\mathcal{P}_{\text{sym}}^{\text{SR}_i}(e)\right]^{K-k} \mathcal{P}_{\text{sym}}^{\text{coop}}(e|k). \tag{6.24}$$

The PDF of γ_{h_i} can be approximated using the Taylor series expansion and neglecting the higher order terms, as

$$f_{\gamma_{h_i}}(\gamma) \simeq \frac{1}{\overline{\gamma}_{h_i}}. \tag{6.25}$$

Thus,

$$\mathcal{P}_{\text{sym}}^{\text{SR}_i}(e) \simeq \frac{\alpha_z}{2\beta_z} \frac{1}{\overline{\gamma}_h}. \tag{6.26}$$

From (6.22), $f_{\gamma_t}(\gamma)$ can be approximated as

$$f_{\gamma_t}(\gamma) \simeq k\gamma^{k-1} \frac{1}{\overline{\gamma}_b} \left(\frac{1}{\overline{\gamma}_g}\right)^{k-1}. \tag{6.27}$$

Upon substituting (6.27) into (6.21) and solving the integration using [69, 3.351.2], the following expression is obtained

$$\mathcal{P}_{\text{sym}}^{\text{coop}}(e|k) \simeq \frac{\alpha_x 2^{k-1} \Gamma(k+\frac{1}{2})}{\beta_x^k \sqrt{\pi}} \frac{1}{\overline{\gamma}_b} \left(\frac{1}{\overline{\gamma}_g}\right)^{k-1}, \tag{6.28}$$

where $\Gamma(\cdot)$ is the gamma function, i.e. $\Gamma(u) = \int_0^\infty e^{-t} t^{u-1} dt$ [67, 6.1.1]. Upon substituting (6.26) and (6.28) into (6.24), the asymptotic SEP can be expressed as

$$\mathcal{P}_{\text{sym}}(e) \simeq \left(\frac{\alpha_z}{2\beta_z} \frac{1}{\overline{\gamma}_h}\right)^K + \sum_{k=1}^{K} \binom{K}{k} \Lambda_k \left(\frac{\alpha_z}{2\beta_z} \frac{1}{\overline{\gamma}_h}\right)^{K-k} \frac{1}{\overline{\gamma}_b} \left(\frac{1}{\overline{\gamma}_g}\right)^{k-1}, \tag{6.29}$$

where Λ_k is defined as

$$\Lambda_k = \frac{\alpha_x 2^{k-1}\Gamma(k+\frac{1}{2})}{\beta_x^k \sqrt{\pi}}. \tag{6.30}$$

6.2.3 Diversity Gain Analysis

The asymptotic SEP, given by (6.29), can be used to find the diversity gain of the DH-SSC system. Thus, using equal power allocation (EPA) and substituting $E_S = E_R = E_e$ into (6.29), the following expression is obtained

$$\mathcal{P}_{\text{sym}}(e) = \left(\frac{E_e}{N_0}\right)^{-K} \left[\left(\frac{\alpha_z}{2\beta_z \sigma_h^2 \lambda_{SR}}\right)^K + \sum_{k=1}^{K} \binom{K}{k} \Lambda_k \times \left(\frac{\alpha_z}{2\beta_z \sigma_h^2 \lambda_{SR}}\right)^{K-k} \left(\frac{1}{\sigma_b^2 \lambda_{RD}}\right) \left(\frac{1}{\sigma_g^2 \lambda_{RD}}\right)^{k-1}\right]. \tag{6.31}$$

It is evident from (6.31) that the DH-SSC system offers a diversity gain of K, which is equal to the number of relay nodes in the system.

6.3 System Optimization

6.3.1 Optimizing Power Allocation under Fixed Relay Position

In this section, the optimal power allocation (OPA) is obtained at the source and the relay under the condition of fixed relay placement (d_{SR}, d_{RD}), assuming a total power budget of the system as E_{tot}. When no relay is able to correctly decode the signal received from the source, i.e. $|\mathcal{C}| = 0$, the optimization problem would be useless, thus it is assumed that at least one relay correctly decodes the signal received

from the source. The power optimization problem with the goal of minimizing the average SEP can be formulated as

$$\begin{aligned} \min_{E_S, E_R} \quad & \mathcal{P}_{\text{sym}}(e) \\ \text{subject to} \quad & E_S + 2E_R \leq E_{\text{tot}}, \\ & E_S,\ E_R > 0, \end{aligned} \tag{6.32}$$

The reason of using $2E_R$ is that the relay participates in the transmission for two phases over two transmission cycles, while the source for one phase. A more tractable form of (6.29) is required to find closed-form expressions for system optimization, which can be obtained after applying the binomial expansion [69] on (6.29) as

$$\mathcal{P}_{\text{sym}}(e) \simeq \left(\frac{\alpha_z}{2\beta_z}\frac{1}{\overline{\gamma}_h}\right)^K + \Lambda_K \frac{1}{\overline{\gamma}_b}\left(\frac{1}{\overline{\gamma}_m}\right)^{K-1}, \tag{6.33}$$

By defining ξ such that $0 < \xi < 1$, the optimum values of the power allocated to the source and the relay can be represented as $E_S = \xi E_{\text{tot}}$ and $E_R = (1-\xi)E_{\text{tot}}/2$. Upon substituting these values into (6.33), the following expression is obtained

$$\mathcal{P}_{\text{sym}}(e) = \mathcal{A}_K \left(\frac{1}{\xi}\right)^K + \mathcal{I}_K \Lambda_K \left(\frac{1}{1-\xi}\right)^K, \tag{6.34}$$

where $\mathcal{A}_K$ and $\mathcal{I}_K$ are defined as

$$\mathcal{A}_K = \left(\frac{\alpha_z}{2\beta_z}\frac{N_0 d_{SR}^{\nu}}{\sigma_h^2 E_{\text{tot}}}\right)^K \text{ and } \mathcal{I}_K = \frac{\sigma_g^2}{\sigma_b^2}\left(\frac{2N_0 d_{RD}^{\nu}}{\sigma_g^2 E_{\text{tot}}}\right)^K. \tag{6.35}$$

The second derivative of $\mathcal{P}_{\text{sym}}(e)$ with respect to ξ is evaluated to check the the convexity of $\mathcal{P}_{\text{sym}}(e)$. It can be easily noticed that $\partial^2 \mathcal{P}_{\text{sym}}(e)/\partial \xi^2$ is positive in the interval $(0, 1)$, indicating that the objective function is strictly a convex function of

ξ in the interval $(0, 1)$. Taking the first derivative of $\mathcal{P}_{\text{sym}}(e)$ with respect to ξ and equating it to zero, the optimum ξ can be obtained as

$$\xi^* = \left[\left(\frac{\mathcal{I}_K \Lambda_K}{\mathcal{A}_K} \right)^{1/(K+1)} + 1 \right]^{-1}. \tag{6.36}$$

Using (6.36), optimal values of the power allocated to the source (E_S^*) and the relays (E_R^*) at a given relay location can be determined. If the set of relays are assumed to be located near the middle of the source and the destination i.e. $d_{SR} = 0.5$, (6.36) is approximated to $\xi = 1/(K+1)$. Thus, the optimal power allocation can be approximated as $E_S^* = E_{\text{tot}}/(K+1)$ and $E_R^* = K\,E_{\text{tot}}/2(K+1)$. It is observed that the optimal power allocated to the relays (E_R^*) rises with the increase in the number of relays (K), while optimal power allocated to the source decreases.

6.3.2 Optimizing Relay Position under Fixed Power Allocation

For optimizing the relay position, the normalized distance between the source and the destination (i.e. $d_{SD} = 1$) is used. It is assumed that the relays are placed on the straight-line that joins the source and the destination (i.e. $d_{SR} = d$ and $d_{RD} = 1-d$), which minimizes the effect of path loss. When fixed power is allocated to the source (E_S) and the relays (E_R), the relay location optimization problem can be written as

$$\begin{aligned} \min_{d} \quad & \mathcal{P}_{\text{sym}}(e) \\ \text{subject to} \quad & 0 \leq d \leq 1, \end{aligned} \tag{6.37}$$

Then, (6.33) can be written as

$$\mathcal{P}_{\text{sym}}(e) = \mathcal{U}_K d^{\nu K} + \mathcal{V}_K \Lambda_K \left(1-d\right)^{\nu K}, \tag{6.38}$$

where $\mathcal{U}_K$ and $\mathcal{V}_K$ are defined as

$$\mathcal{U}_K = \left(\frac{\alpha_z}{2\beta_z}\frac{N_0}{\sigma_h^2 E_S}\right)^K \text{ and } \mathcal{V}_K = \frac{\sigma_g^2}{\sigma_b^2}\left(\frac{N_0}{\sigma_g^2 E_R}\right)^K. \tag{6.39}$$

Upon taking the second derivative of $\mathcal{P}_{\text{sym}}(e)$ with respect to d, it is easily found that the objective function is strictly a convex function of d in the interval $[0,1]$. Now, taking the first derivative of $\mathcal{P}_{\text{sym}}(e)$ with respect to d and equating it to zero, the closed-form expression for the optimal relay location (d^*) is obtained as

$$d^* = \left[\left(\frac{\mathcal{U}_K}{\mathcal{V}_K \Lambda_K}\right)^{1/(\nu K-1)} + 1\right]^{-1}. \tag{6.40}$$

6.3.3 Jointly Optimizing Power Allocation and Relay Location

In this section, the power allocation and the relay position are jointly optimized to further enhance the system performance. It is assumed that the relays are placed on the straight-line (i.e. $d_{SR} = d$ and $d_{RD} = 1-d$), and the power allocated to the source and the relays is related to the total power budget of the system as $E_S = \delta E_{\text{tot}}$ and $E_R = (1-\delta)E_{\text{tot}}/2$ such that $0 < \delta < 1$. The joint optimization problem can be

formulated as

$$\begin{aligned} \min_{E_S,E_R,d} \quad & \mathcal{P}_{\text{sym}}(e) \\ \text{subject to} \quad & E_S + 2E_R \leq E_{\text{tot}}, \\ & E_S, E_R > 0, \\ & 0 \leq d \leq 1. \end{aligned} \tag{6.41}$$

Then, (6.33) can be written as

$$\mathcal{P}_{\text{sym}}(e) = \mathcal{H}_K \left(\frac{d^\nu}{\delta}\right)^K + \mathcal{J}_K \Lambda_K \left[\frac{(1-d)^\nu}{(1-\delta)}\right]^K, \tag{6.42}$$

where $\mathcal{H}_K$ and $\mathcal{J}_K$ are defined as

$$\mathcal{H}_K = \left(\frac{\alpha_z}{2\beta_z}\frac{N_0}{\sigma_h^2 E_{\text{tot}}}\right)^K \text{ and } \mathcal{J}_K = \frac{\sigma_g^2}{\sigma_b^2}\left(\frac{2N_0}{\sigma_g^2 E_{\text{tot}}}\right)^K. \tag{6.43}$$

The expression of $\mathcal{P}_{\text{sym}}(e)$ is found to be a strict convex function of δ and d in the interval $(0,1)$ and $[0,1]$, respectively. Thus, taking the first derivative of $\mathcal{P}_{\text{sym}}(e)$ with respect to δ and d, respectively, equating them to zero, and solving them simultaneously, the closed-form expressions for d^* and δ^* are obtained as

$$d^* = \left[\left(\frac{\mathcal{J}_K \Lambda_K}{\mathcal{H}_K}\right)^{1/(K-\nu K+1)} + 1\right]^{-1}, \tag{6.44}$$

$$\delta^* = \left[\left(\frac{\mathcal{J}_K \Lambda_K}{\mathcal{H}_K}\right)^{1/(K-\nu K+1)} + 1\right]^{-1}. \tag{6.45}$$

The optimal relay location can be found from (6.44) and the optimal power allocation can be calculated using (6.45). It is observed from (6.44) and (6.45) that as the number of relays increases, the optimal position of the relays will be closer to the destination, thus increasing the optimal power allocated to the source and

decreasing the optimal power allocated to the relays.

6.4 Outage Probability Analysis

First, the CDF of $f_{\gamma_t}(\gamma)$ is obtained, and then closed-form expressions for the exact and asymptotic outage probabilities of the system are derived.

6.4.1 CDF of $f_{\gamma_t}(\gamma)$

From (6.22), the CDF of $f_{\gamma_t}(\gamma)$ can be written as

$$F_{\gamma_t}(\gamma_0) = \sum_{k=1}^{K} \binom{K}{k} \frac{(-1)^{k-1}}{\overline{\gamma}_a} \frac{k\overline{\gamma}_m}{k\overline{\gamma}_b - \overline{\gamma}_m} \left[\overline{\gamma}_b \left(1 - e^{-\gamma_0/\overline{\gamma}_b}\right) - \frac{\overline{\gamma}_m}{k} \left(1 - e^{-k\gamma_0/\overline{\gamma}_m}\right) \right] + \sum_{k=1}^{K} \binom{K}{k} \frac{(-1)^{k-1}}{\overline{\gamma}_b} \overline{\gamma}_m \left(1 - e^{-k\gamma_0/\overline{\gamma}_m}\right). \quad (6.46)$$

6.4.2 Exact Outage Probability

In the DH-SSC system, the overall system outage happens either when all $\mathsf{S}-\mathsf{R}_i$ links are in outage or when both $\mathsf{R}_t - \mathsf{D}$ links are in outage with no outage in the $\mathsf{S}-\mathsf{R}_i$ link. Thus, the overall outage probability of the system can be written as

$$\mathcal{P}_{\text{out}} = \left(\mathcal{P}_{\text{out}}^{\text{SR}}\right)^K + \left(1 - \mathcal{P}_{\text{out}}^{\text{SR}}\right)^K \mathcal{P}_{\text{out}}^{\text{RD}}, \quad (6.47)$$

where $\mathcal{P}_{\text{out}}^{\text{SR}}$ and $\mathcal{P}_{\text{out}}^{\text{RD}}$ represent the outage probabilities of the $\mathsf{S}-\mathsf{R}_i$ link and the cooperative $\mathsf{R}_t - \mathsf{D}$ links, respectively. Let R_0 bits/s/Hz denotes the given target rate, the outage in the $\mathsf{S}-\mathsf{R}_i$ link would correspond to the event $(1/3)\log_2(1+\gamma_{h_i}) < R_0$, or equivalently $\gamma_{h_i} < \mu_{th}$, where $\mu_{th} = 2^{3R_0} - 1$. The factor $1/3$ is used because of 3

phases for transmission in the system. Thus, $\mathcal{P}_{\text{out}}^{\text{SR}}$ can be written as

$$\mathcal{P}_{\text{out}}^{\text{SR}} \triangleq \Pr\left\{\frac{1}{3}\log_2\left(1+\gamma_{h_i}\right) < R_0\right\}, \tag{6.48}$$

$$\mathcal{P}_{\text{out}}^{\text{SR}} = 1 - \exp\left(-\frac{\mu_{th}}{\overline{\gamma}_h}\right). \tag{6.49}$$

When the relay decodes the source signal correctly with no outage in the $\mathsf{S}-\mathsf{R}_i$ link, the best relay transmits two different symbols through $\mathsf{R}_t-\mathsf{D}$ links in two phases. Thus, the average mutual information for $\mathsf{R}_t-\mathsf{D}$ links can be obtained as

$$I_{\text{RD}} \triangleq \frac{1}{3}\log_2(1+\gamma_t) + \frac{1}{3}\log_2(1+\gamma_t), \tag{6.50}$$

$$I_{\text{RD}} = \frac{2}{3}\log_2(1+\gamma_t). \tag{6.51}$$

Therefore, the outage probability of $\mathsf{R}_t-\mathsf{D}$ links can be written as

$$\mathcal{P}_{\text{out}}^{\text{RD}} \triangleq \Pr\left\{I_{\text{RD}} < R_0\right\} = F_{\gamma_t}(2^{3R_0/2}-1). \tag{6.52}$$

From (6.46), (6.47), (6.49) and (6.52), the exact overall outage probability of the system can be obtained.

6.4.3 Asymptotic Outage Probability

The asymptotic outage probability is valid for moderate to high SNR region. For high SNR, $(1-\mathcal{P}_{\text{out}}^{\text{SR}})$ equals to 1, then the asymptotic outage probability of the system can be written as

$$\mathcal{P}_{\text{out}} \simeq \left(\mathcal{P}_{\text{out}}^{\text{SR}}\right)^K + \mathcal{P}_{\text{out}}^{\text{RD}}. \tag{6.53}$$

From (6.25), $\mathcal{P}_{\text{out}}^{\text{SR}}$ can be approximated as

$$\mathcal{P}_{\text{out}}^{\text{SR}} \simeq \frac{2^{3R_0}-1}{\overline{\gamma}_h}. \tag{6.54}$$

From (6.27), the CDF of $f_{\gamma_t}(\gamma)$ can be approximated as

$$F_{\gamma_t}(\gamma_0) \simeq \frac{\gamma_0^K}{\overline{\gamma}_b}\left(\frac{1}{\overline{\gamma}_m}\right)^{K-1}. \tag{6.55}$$

From (6.53), (6.54) and (6.55), the asymptotic outage probability can be written as

$$\mathcal{P}_{\text{out}} \simeq \left(\frac{2^{3R_0}-1}{\overline{\gamma}_h}\right)^K + \frac{(2^{3R_0/2}-1)^K}{\overline{\gamma}_b}\left(\frac{1}{\overline{\gamma}_m}\right)^{K-1}. \tag{6.56}$$

6.5 Channel Capacity Analysis

In this section, the closed-form expressions for the channel capacity of the system and its upper bound are derived.

6.5.1 Average Channel Capacity

The average channel capacity, in the Shannon's sense, can be evaluated by averaging the instantaneous capacity for an AWGN channel over the fading distribution when transmit power is constant and the channel state information is available at the receiver [68, 70]. The average channel capacity of the DH-SSC system can be written as

$$\overline{C} = B\,\frac{2}{3}\int_0^\infty \log_2(1+\gamma)\, f_{\gamma_t}(\gamma)d\gamma, \tag{6.57}$$

where B denotes the channel bandwidth and factor $2/3$ is due to the transmission of two symbols in three phases. In order to solve the preceding integration, the following

relation is formulated using [69, 3.352.4]

$$\int_0^{\infty} \ln(1+t)e^{-t/c}dt = c\,e^{1/c}\,E_1\left(\frac{1}{c}\right), \tag{6.58}$$

where $E_1(x) = \int_x^{\infty}(\exp(-t)/t)\,dt$ denotes the exponential integral [67, 5.1.1]. Upon substituting (6.22) into (6.57), and solving the integration using (6.58), the average channel capacity in closed-form can be written as

$$\begin{aligned}\frac{\overline{C}}{B} = &\frac{2}{3\ln 2}\sum_{k=1}^{K}\binom{K}{k}\frac{(-1)^{k-1}}{\overline{\gamma}_a}\frac{k\overline{\gamma}_m}{k\overline{\gamma}_b-\overline{\gamma}_m}\left[\overline{\gamma}_b e^{1/\overline{\gamma}_b}E_1\left(\frac{1}{\overline{\gamma}_b}\right) - \frac{\overline{\gamma}_m}{k}e^{k/\overline{\gamma}_m}E_1\left(\frac{k}{\overline{\gamma}_m}\right)\right]\\ &+\frac{2}{3\ln 2}\sum_{k=1}^{K}\binom{K}{k}\frac{(-1)^{k-1}}{\overline{\gamma}_b}\,\overline{\gamma}_m e^{k/\overline{\gamma}_m}E_1\left(\frac{k}{\overline{\gamma}_m}\right).\end{aligned} \tag{6.59}$$

6.5.2 Upper Bound on the Capacity

The average channel capacity, using Jensen's Inequality, is upper bounded as

$$\overline{C} \le B\frac{2}{3}\log_2\left(1+\mathbb{E}\{\gamma_t\}\right), \tag{6.60}$$

where $\mathbb{E}\{\gamma_t\} = \int_0^{\infty}\gamma f_{\gamma_t}(\gamma)d\gamma$ represents the expectation operator and can be simplified using $\int_0^{\infty} t\,e^{-t/c}dt = c^2$. Thus, the following expression is obtained

$$\begin{aligned}\mathbb{E}\{\gamma_t\} = &\sum_{k=1}^{K}\binom{K}{k}\frac{(-1)^{k-1}}{\overline{\gamma}_a}\frac{k\overline{\gamma}_m}{k\overline{\gamma}_b-\overline{\gamma}_m}\left[\overline{\gamma}_b^2 - \left(\frac{\overline{\gamma}_m}{k}\right)^2\right]\\ &+\sum_{k=1}^{K}\binom{K}{k}\frac{(-1)^{k-1}\overline{\gamma}_m^2}{k\overline{\gamma}_b}.\end{aligned} \tag{6.61}$$

Upon substituting (6.61) into (6.60), a closed-form expression for the upper bound on the capacity can be easily obtained.

6.6 Results and Discussions

In this section, the performance of the DH-SSC system is illustrated for different system parameters. In addition, the accuracy of the derived analytical expressions is validated through computer simulations. To illustrate numerical results, 4-QAM SSD with a rotation angle of 26.6° is used in the system. The path loss exponent is set to $\nu = 3$ and the variances of channel coefficients are assumed to be $\sigma_h^2 = \sigma_a^2 = \sigma_b^2 = 1$. The DH-SSC system is assumed to have K relays located at the middle of the source (S) and the destination (D), unless otherwise stated. For the fair comparison of the system, the total power budget of the system to transmit two symbols is equivalent to that of the direct transmission system, i.e. $E_S = 1$ and $E_R = 0.5$, making the total power budget equals to 2 units to transmit two symbols. In all Monte Carlo simulations, 10^9 iterations are used for each simulation point to obtain accurate results.

Figure 6.2 demonstrates the average bit error probability (BEP) performance of the DH-SSC system with respect to the average SNR (E_b/N_0), for one, two and three relay nodes in the system. This figure illustrates the simulation results with □ markers while analytical and asymptotic results with solid and dashed lines, respectively. The figure validates the analytical and asymptotic BEP results, given by (6.16) and (6.29), through computer simulations, where analytical and asymptotic results are in good agreement with the simulation results. The error performance of the system improves as the number of cooperating relays increases in the system. This implies that the increase in the number of relays contributes to the diversity enhancement, which confirms the diversity gain analysis, given by (6.31). For example, BEP= 10^{-5} is achieved at $E_b/N_0 = 44$ dB with one relay node ($K = 1$), or at $E_b/N_0 = 24$ dB with two relay nodes ($K = 2$), or at $E_b/N_0 = 18.5$ dB with three relay nodes ($K = 3$).

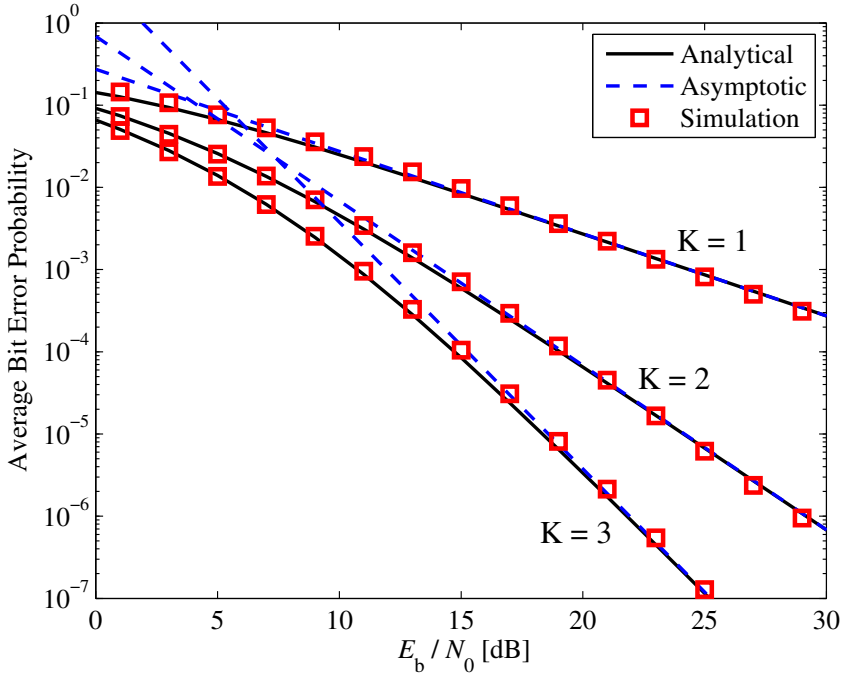

Figure 6.2: Error performance of the DH-SSC system with respect to E_b/N_0, when $K = 1, 2, 3$.

When the BEP results for different number of relay nodes are compared, it is observed that the DH-SSC system achieves an E_b/N_0 gain of about 20 dB, and 25.5 dB with two and three relay nodes, respectively, compared to the single relay system.

Figures 6.3 and 6.4 illustrate the outage performance of the system with respect to the average SNR (E_b/N_0), and the information rate (R_0) at $E_b/N_0 = 20$ dB, respectively. These figures also show the simulation results with □ markers while analytical and asymptotic outage probabilities with solid and dashed lines, respectively. It is observed that both simulation and analytical results are in excellent agreement, and asymptotic outage probability has a good match with both simulation and analytical results at medium and high SNRs. Thus, these figures verify the accuracy of the derived analytical work for the outage probability, given by (6.47) and (6.56). It is also noticed that the outage probability of the system significantly improves when

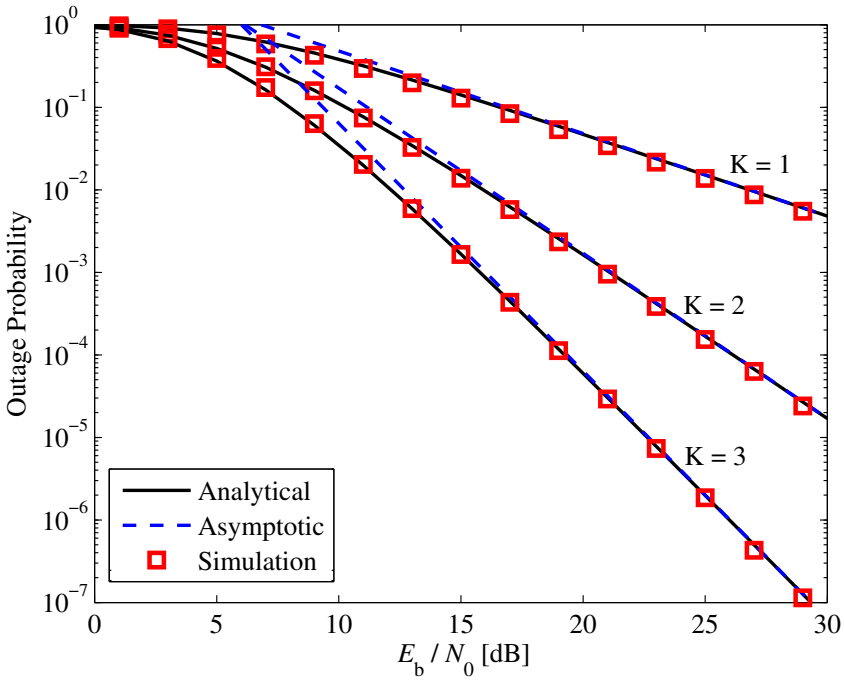

Figure 6.3: Outage performance of the DH-SSC system with respect to E_b/N_0, when $R_0 = 2$ and $K = 1, 2, 3$.

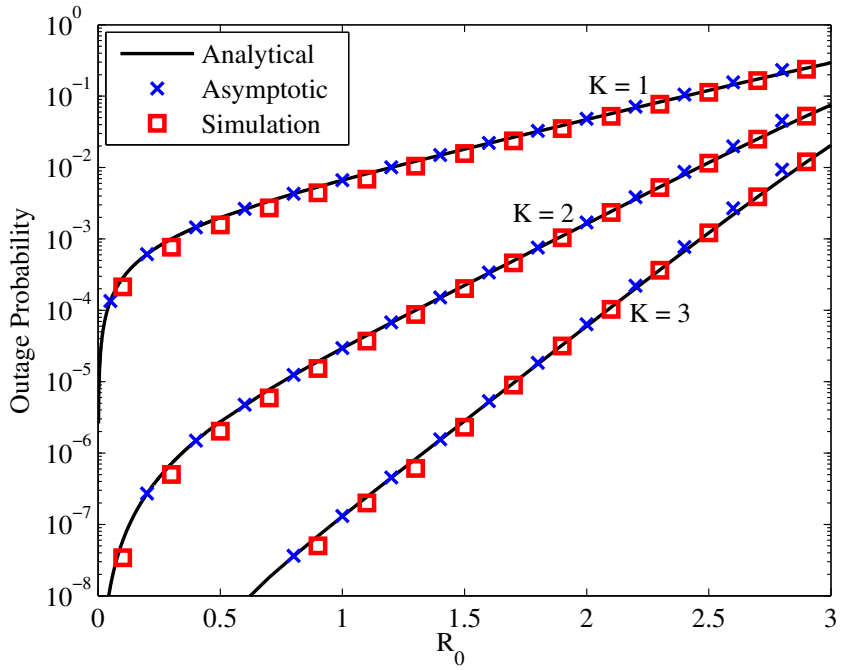

Figure 6.4: Outage performance of the DH-SSC system with respect to information rate (R_0), when $E_b/N_0 = 20$ dB and $K = 1, 2, 3$.

the number of relays in the system is increased, which clearly shows the diversity enhancement.

Figures 6.5 and 6.6 describe the effect of relay placement on system's error and outage performances, respectively. These figures also illustrate performance results for both equal power allocation (EPA) and optimal power allocation (OPA), where the optimal power allocated to the source and the destination is obtained using (6.36). Figure 6.5 shows the average SNR (E_b/N_0) required to achieve BEP of 10^{-3} with respect to $\mathsf{S} - \mathsf{R}_i$ distance (d_{SR}). Figure 6.6 portrays the outage probability with respect to d_{SR} at $E_b/N_0 = 15$ dB. It is observed that when the relay nodes are placed near the middle location of the source and the destination, the performance of the system due to OPA is similar to that of EPA. For near-to-source relays location, the performance gap between OPA and EPA is small, and the highest performance gain is noticed for near-to-destination relays location. The reason for this behaviour is that for near-to-destination relays location, the power allocated to the source based on EPA is not enough to guarantee correct data transmission to the relays during the first phase. Thus, OPA provides the solution of increasing the power allocated to the source and decreasing the power allocated to the relays to enhance the system performance. On the other hand, for near-to-source relays location scenario, OPA decreases the power allocated to the source and increases the power allocated to the relays to improve system performance. In Figure 6.5 at $d_{SR} = 0.9$, OPA with $K = 2$ provides the same performance as that by EPA with $K = 3$, thus demonstrating the benefits of OPA. Figure 6.6 illustrates that the outage probability is optimum when relays are placed in the middle location. In Figure 6.6 at $d_{SR} = 0.9$, the outage probability for $K = 3$ due to OPA is more than 10 times better than that for $K = 3$ due to EPA.

Figures 6.7 and 6.8 show the error and outage performances of the system with

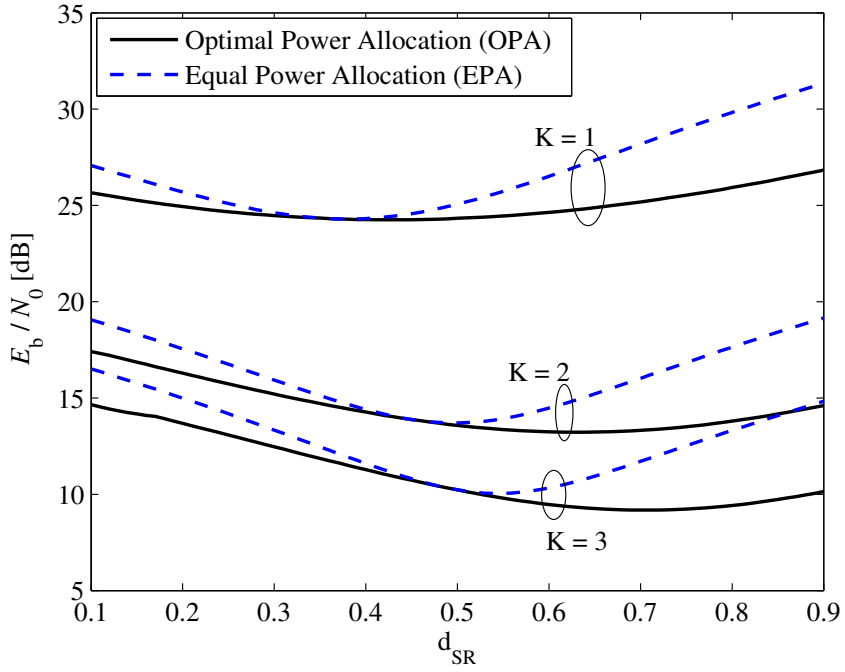

Figure 6.5: E_b/N_0 required to achieve BEP of 10^{-3} in DH-SSC with respect to $\mathsf{S} - \mathsf{R}_i$ distance (d_{SR}) for OPA and EPA.

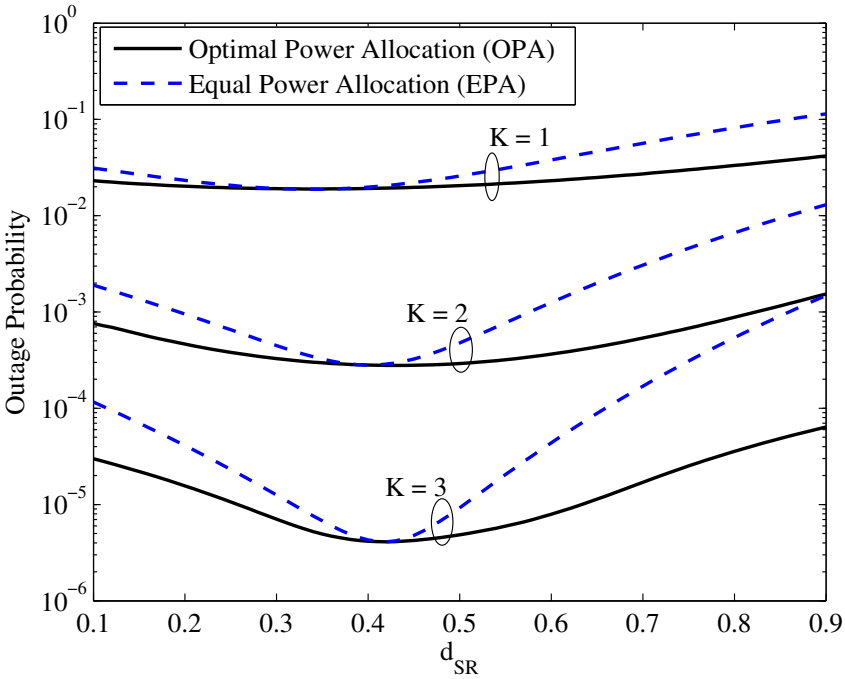

Figure 6.6: Outage probability of the DH-SSC system with respect to $\mathsf{S} - \mathsf{R}_i$ distance (d_{SR}) for OPA and EPA when $E_b/N_0 = 15$ dB and $R_0 = 1$.

respect to E_b/N_0 for different optimization schemes, respectively. It is considered that the relay nodes are located close to the destination and far away from the source (i.e. $d_{SR} = 0.9$) and information rate R_0 is 2 bits/s/Hz. These figures illustrate the average BEP and outage probability for EPA, OPA, optimal relay position (ORP), and joint optimization of PA and relay location. The significant performance improvement is noticed using different optimization schemes compared to EPA. It is also observed that the joint optimization scheme provides the optimum performance of the system compared to all other optimization schemes considered. The joint optimization with $K = 3$ provides about 6 dB gain of E_b/N_0 in BEP performance and about 7 dB gain of E_b/N_0 in outage performance.

Figure 6.9 illustrates the average channel capacity of the system with respect to E_b/N_0, for one and three relay nodes in the system. In addition, this figure shows an upper bound on the capacity of the DH-SSC system with dashed lines and the capacity of the direct transmission system with ○ markers for comparison. It is clearly observed that the analytical results for exact and upper bound capacities, given by (6.59) and (6.60), perfectly match with their corresponding simulation results, which validates the derived mathematical expressions of channel capacity. Thus, the channel capacity increases as the number of relay nodes increases in the system.

6.7 Summary

In this chapter, a dual-hop DF relaying system using signal space diversity (SSD) was introduced, where no direct link exists between the source and the destination. The performance analysis of the DH-SSC system was carried out over Rayleigh fading channel. It was shown that the DH-SSC system improves the spectral efficiency of the conventional dual-hop DF relaying system. Exact and asymptotic expressions

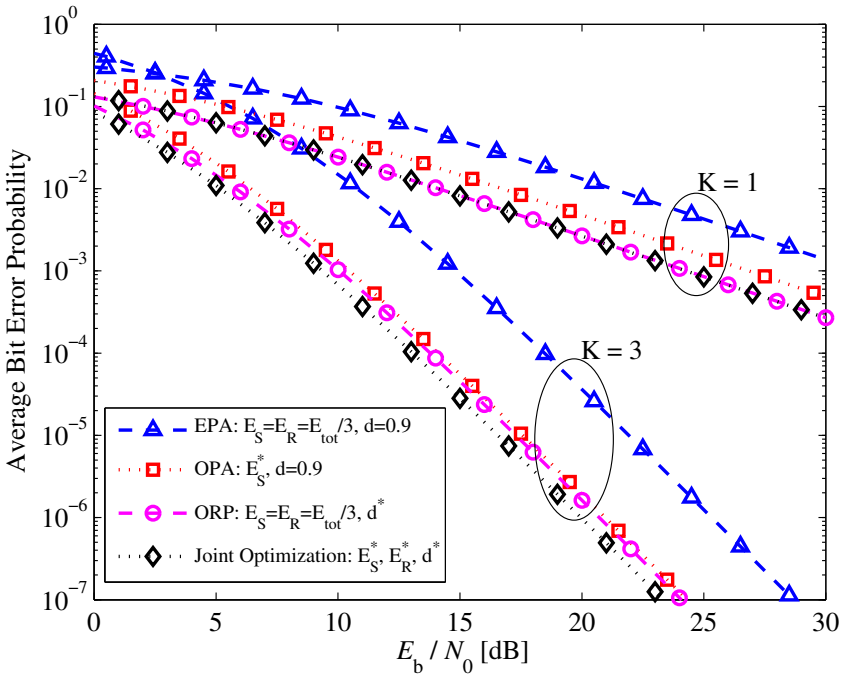

Figure 6.7: Error performance of the DH-SSC system with respect to E_b/N_0 for different optimization schemes when $d_{SR} = 0.9$.

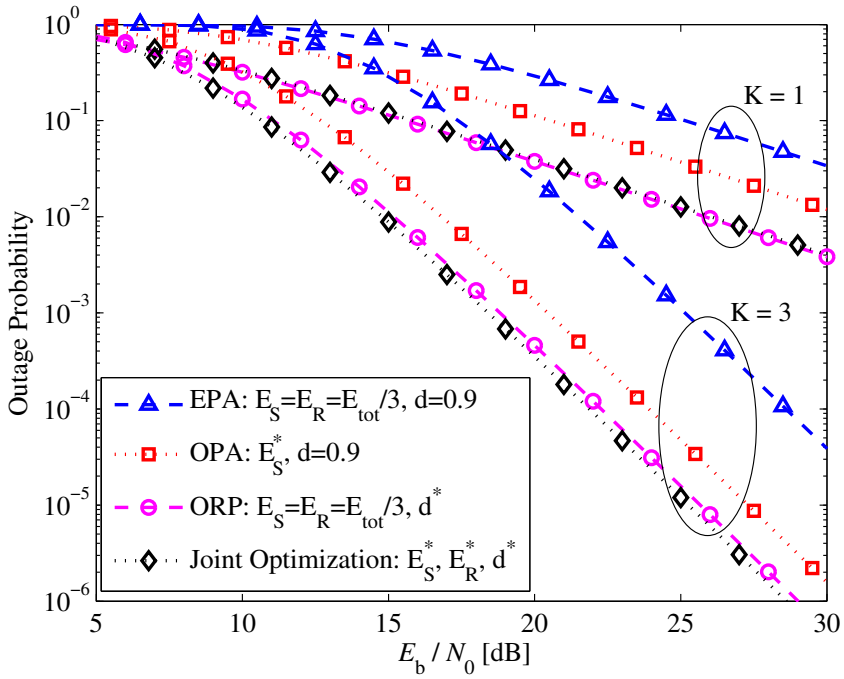

Figure 6.8: Outage probability performance of the DH-SSC system with respect to E_b/N_0 for different optimization schemes when $R_0 = 2$ and $d_{SR} = 0.9$.

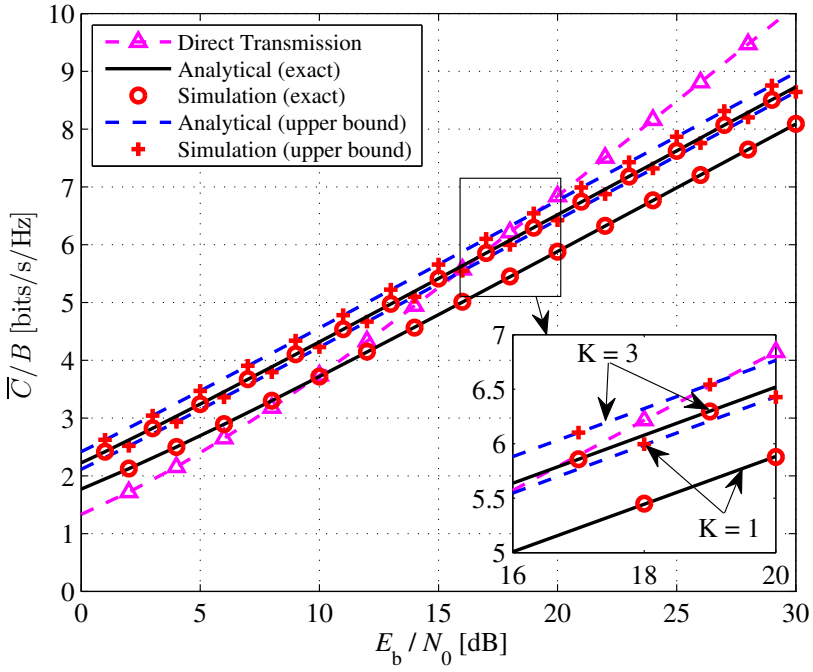

Figure 6.9: Channel capacity of the DH-SSC system with respect to E_b/N_0 when $K = 1, 3$.

for the error probability, outage probability and channel capacity were derived. All of the analysis and mathematical derivations were validated through Monte Carlo simulations. The diversity gain of the system was evaluated and it was shown that the DH-SSC system can achieve a diversity order equal to the number of relay nodes. In addition, the system optimization was carried out, including power allocation, relay placement as well as the joint optimization of the two. It was noticed that the system performance is optimum when relays are located in the middle of the source and the destination. It was also observed that the joint optimization of PA and relay position enhances the system performance significantly when the relays are placed close to either source or destination.

Chapter 7

Conclusions and Future Work

In this thesis, the spectrally efficient cooperative relay systems were proposed and investigated. In these systems, the signal space diversity (SSD) was combined with the conventional cooperative relay networks and it was shown that these systems significantly enhanced the spectral efficiency and the data transmission of the conventional cooperative relay networks.

7.1 Conclusions

This thesis can be concluded in the following points.

- In chapter 3, the concept of incorporating SSD into the conventional two-way cooperative system was introduced. The proposed two-way signal space cooperative system using a single a DF relay was referred to as 2W-SSC-1R. It was shown that the 2W-SSC-1R system exchanges four symbols in three time slots while the conventional two-way cooperative system uses six time slots to exchange the same four symbols. Thus, the 2W-SSC system has doubled the spectral efficiency and the data transmission of the conventional two-way cooperative system without adding extra bandwidth, complexity or transmit power. The closed-form expression for the error probability of the system was derived over Rayleigh fading channels. The error performance of the system

was compared with the conventional system and it was found that the 2W-SSC-1R system provides high spectral efficiency without decreasing the error performance.

- In chapter 4, the two-way signal space cooperative system (2W-SSC-1R), proposed and analyzed in chapter 3, was extended with multiple intermediate relays and was referred to as 2W-SSC. The best relay out of K relays was chosen in the system. The comprehensive analysis of the 2W-SSC system was carried out in this chapter and closed-form expressions for various performance metrics, including error probability, outage probability and channel capacity, were derived. It was shown that the 2W-SSC system provides a diversity gain equal to one higher than the number of relays. The system optimization was investigated to enhance the system performance and it was found that optimum relay position significantly improves the performance of the system. It was also observed that the system provides higher channel capacity compared to the direct transmission system. All of the mathematical analysis and derivations were confirmed through Monte Carlo simulations.

- In chapter 5, the idea of combining SSD with a dual-hop DF relaying system without a direct link between the source and the destination was presented. The proposed dual-hop signal space relaying system was referred to as DH-SSC-1R. It was shown that the DH-SSC-1R system transmits two symbols in three transmission phases while the conventional dual-hop DF relaying system uses four phases to transmit the same two symbols. Therefore, the DH-SSC-1R system improves the spectral efficiency and the data transmission without additional complexity, bandwidth or transmit power. The DH-SSC-1R system was analyzed over Rayleigh fading channels and error probability performance

was derived. The performance of the DH-SSC-1R system was compared with the other dual-hop relaying systems and it was found that the DH-SSC-1R system improves the spectral efficiency without loosing performance of the system.

- chapter 6, the dual-hop signal space cooperative system was extended with multiple intermediate relays and referred to as DH-SSC. The best relay is selected based on the channel conditions to forward the received data to the destination. The closed-form expressions for the exact and asymptotic error probability, outage probability and channel capacity were derived and validated through Monte Carlo simulations. It was shown that the DH-SSC system provides diversity gain of equal to the number of relays. In addition, the system optimization of the DH-SSC system was carried out and it was observed that the system performance is optimum when relays were located in the middle of the source and the destination. It was also noticed that joint optimization of power allocation and relay position improves the system performance significantly if relays are placed close to either source or destination.

7.2 Future Prospects

Cooperative relaying is a key enabling technology for future 5G wireless networks and thus, provides opportunities for research to incorporate into the future 5G wireless networks. Cooperative relaying has been included in several standards such as 3GPP LTE-Advanced, IEEE 802.11j and IEEE 802.11m, and more sophisticated cooperative relaying techniques are highly expected to be employed in 5G standards. The concept of cooperative relaying has several challenges and issues, which are required to be addressed. The following is a brief list of some interesting suggestions for possible future extensions of this work.

- In this thesis, two-dimensional ordinary constellation such as M-QAM or M-PSK is rotated and expanded to obtain signal space diversity. It would be very interesting if other types of modulation schemes is utilized to achieve signal space diversity and employed in cooperative relay networks to increase spectral efficiency.

- The 2W-SSC system in this thesis doubles the spectral efficiency and the data transmission of the conventional two-way cooperative system (i.e. time-division broadcast channel, TDBC). The introduction of signal space diversity in other two-way cooperative protocols such as multiple-access broadcast channel (MABC) or the naive four-phase, can be explored to improve the spectral efficiency of the conventional two-phase two-way or the conventional naive four-phase two-way cooperative systems.

- This thesis has combined signal space diversity (SSD) with the decode-and-forward (DF) relay. The introduction of SSD into other types of relays, such as compress-and-forward and filter-and-forward, can be explored to enhance the system performance.

- In past, signal space diversity has been combined with some coding schemes and therefore SSD can also be introduced in cooperative relay networks with coded cooperation.

- In this thesis, two-hop relay networks were considered, it would be interesting to incorporate SSD into multi-hop relay networks.

References

[1] M. Castells, *The rise of the network society: The information age: Economy, society, and culture*. John Wiley & Sons, 2011, vol. 1.

[2] J. Gozalvez, "5G Tests and Demonstrations [Mobile Radio]," *IEEE Vehicular Technology Magazine*, vol. 10, no. 2, pp. 16–25, Jun. 2015.

[3] A. Osseiran, F. Boccardi, V. Braun, K. Kusume, P. Marsch, M. Maternia, O. Queseth, M. Schellmann, H. Schotten, H. Taoka, H. Tullberg, M. A. Uusitalo, B. Timus, and M. Fallgren, "Scenarios for 5G mobile and wireless communications: the vision of the METIS project," *IEEE Communications Magazine*, vol. 52, no. 5, pp. 26–35, May 2014.

[4] T. S. Rappaport, *Wireless Communications: Principles and Practice*, 2nd ed. Upper Saddle River, NJ: Prentice-Hall, 2002.

[5] J. Proakis and M. Salehi, *Digital communications*, 5th ed. McGraw-Hill New York, 2008.

[6] B. Sklar, *Digital Communications: Fundamentals and Applications*, 2nd ed. Upper Saddle River, New Jersey: Prentice Hall, 2001.

[7] A. Sendonaris, E. Erkip, and B. Aazhang, "User cooperation diversity. Part I. System description," *IEEE Transactions on Communications*, vol. 51, no. 11, pp. 1927–1938, Nov. 2003.

[8] K. J. Rayliu, A. K. Sadek, W. Su, and A. Kwasinksi, *Cooperative Communications and Networking*. Cambridge, UK: Cambrdige University Press, 2009.

[9] J. Laneman, D. Tse, and G. W. Wornell, "Cooperative diversity in wireless networks: Efficient protocols and outage behavior," *IEEE Transactions on Information Theory,*, vol. 50, no. 12, pp. 3062–3080, Dec. 2004.

[10] T. E. Hunter and A. Nosratinia, "Diversity through coded cooperation," *IEEE Transactions on Wireless Communications*, vol. 5, no. 2, pp. 283–289, Feb. 2006.

[11] G. Kramer, M. Gastpar, and P. Gupta, "Cooperative strategies and capacity theorems for relay networks," *IEEE Transactions on Information Theory*, vol. 51, no. 9, pp. 3037–3063, Sep. 2005.

[12] H. Chen, A. Gershman, and S. ShahbazPanahi, "Filter-and-forward distributed beamforming in relay networks with frequency selective fading," *IEEE Transactions on Signal Processing*, vol. 58, no. 3, pp. 1251–1262, Mar. 2010.

[13] E. C. van der Meulen, "Transmission of Information in a T-Terminal Discrete Memoryless Channel," Department of Statistics, University of California, Berkeley, CA, Tech. Rep., 1968.

[14] ——, "Three-terminal communication channels," *Advances in applied Probability*, vol. 3, no. 1, pp. 120–154, 1971.

[15] T. M. Cover and A. El Gamal, "Capacity theorems for the relay channel," *IEEE Transactions on Information Theory*, vol. 25, no. 5, pp. 572–584, 1979.

[16] T. M. Cover and J. A. Thomas, *Elements of information theory*. John Wiley & Sons, New York, 2012.

[17] A. Sendonaris, E. Erkip, and B. Aazhang, "Increasing uplink capacity via user cooperation diversity," in *IEEE International Symposium on Information Theory*, Aug. 1998, p. 156.

[18] ——, "User cooperation diversity. Part II. Implementation aspects and performance analysis," *IEEE Transactions on Communications*, vol. 51, no. 11, pp. 1939–1948, Nov. 2003.

[19] T. E. Hunter, S. Sanayei, and A. Nosratinia, "Outage analysis of coded cooperation," *IEEE Transactions on Information Theory*, vol. 52, no. 2, pp. 375–391, Feb. 2006.

[20] E. G. Larsson and B. R. Vojcic, "Cooperative transmit diversity based on superposition modulation," *IEEE Communications Letters*, vol. 9, no. 9, pp. 778–780, Sep. 2005.

[21] K. Zheng, L. Wang, and W. Wang, "Performance analysis of coded cooperation with hierarchical modulation," in *IEEE International Conference on Communications*, May 2008, pp. 4978–4982.

[22] H. Samra, Z. Ding, and P. M. Hahn, "Symbol mapping diversity design for multiple packet transmissions," *IEEE Transactions on Communications*, vol. 53, no. 5, pp. 810–817, May 2005.

[23] K. G. Seddik, A. S. Ibrahim, and K. J. R. Liu, "Trans-modulation in wireless relay networks," *IEEE Communications Letters*, vol. 12, no. 3, pp. 170–172, Mar. 2008.

[24] K. Boull and J. Belfiore, "Modulation scheme designed for the rayleigh fading channel," in *CISS*, vol. 92, 1992, pp. 288–293.

[25] J. Boutros and E. Viterbo, "Signal space diversity: a power- and bandwidth-efficient diversity technique for the Rayleigh fading channel," *IEEE Transactions on Information Theory*, vol. 44, no. 4, pp. 1453–1467, Jul. 1998.

[26] F. Oggier, "Algebraic methods for channel coding," Ph.D. dissertation, Ecole Polytechnique Federale de Lausanne (EPFL), 2005.

[27] F. Oggier and E. Viterbo, "Table of algebraic rotations," 2005, (Last Accessed: 2016-04-09). [Online]. Available: http://ecse.monash.edu.au/staff/eviterbo/rotations/rotations.html

[28] Q. Xie, J. Song, K. Peng, F. Yang, and Z. Wang, "Coded modulation with signal space diversity," *IEEE Transactions on Wireless Communications*, vol. 10, no. 2, pp. 660–669, Feb. 2011.

[29] K. Pappi, N. Chatzidiamantis, and G. Karagiannidis, "Error performance of multidimensional lattice constellations Part II: Evaluation over fading channels," *IEEE Transactions on Communications*, vol. 61, no. 3, pp. 1099–1110, Mar. 2013.

[30] M. Z. A. Khan and B. S. Rajan, "Space-time block codes from co-ordinate interleaved orthogonal designs," in *IEEE International Symposium on Information Theory*, 2002, p. 275.

[31] Y.-H. Kim and M. Kaveh, "Coordinate-interleaved space-time coding with rotated constellation," in *IEEE Vehicular Technology Conference*, vol. 1, Apr. 2003, pp. 732–735.

[32] J. Harshan and B. S. Rajan, "Co-ordinate interleaved distributed space-time coding for two-antenna-relays networks," *IEEE Transactions on Wireless Communications*, vol. 8, no. 4, pp. 1783–1791, Apr. 2009.

[33] E. S. Lo and K. B. Letaief, "Coded cooperation for improved distance spectrum and diversity in wireless systems," in *IEEE Global Telecommunications Conference*, Nov. 2007, pp. 4344–4348.

[34] M. Hasna and M.-S. Alouini, "End-to-end performance of transmission systems with relays over Rayleigh-fading channels," *IEEE Transactions on Wireless Communications*, vol. 2, no. 6, pp. 1126–1131, Nov. 2003.

[35] ——, "A performance study of dual-hop transmissions with fixed gain relays," *IEEE Transactions on Wireless Communications*, vol. 3, no. 6, pp. 1963–1968, Nov. 2004.

[36] J. Boyer, D. D. Falconer, and H. Yanikomeroglu, "Multihop diversity in wireless relaying channels," *IEEE Transactions on Communications*, vol. 52, no. 10, pp. 1820–1830, Oct. 2004.

[37] S. J. Kim, N. Devroye, P. Mitran, and V. Tarokh, "Achievable rate regions and performance comparison of half duplex bi-directional relaying protocols," *IEEE Transactions on Information Theory*, vol. 57, no. 10, pp. 6405–6418, Oct. 2011.

[38] S. Ghasemi-Goojani and H. Behroozi, "Lattice-coded cooperation protocol for the half-duplex gaussian two-way relay channel," *EURASIP Journal on Wireless Communications and Networking*, vol. 2015, no. 1, pp. 1–18, 2015.

[39] I. Avram, N. Aerts, and M. Moeneclaey, "Low-complexity quantize-and-forward cooperative communication using two-way relaying," *EURASIP Journal on Wireless Communications and Networking*, vol. 2014, no. 1, pp. 1–10, 2014.

[40] P. Larsson, N. Johansson, and K.-E. Sunell, "Coded bi-directional relaying," in *IEEE 63rd Vehicular Technology Conference*, vol. 2, May 2006, pp. 851–855.

[41] K. Song, B. Ji, Y. Huang, M. Xiao, and L. Yang, "Performance analysis of antenna selection in two-way relay networks," *IEEE Transactions on Signal Processing*, vol. 63, no. 10, pp. 2520–2532, May 2015.

[42] T. Oechtering, C. Schnurr, I. Bjelakovic, and H. Boche, "Broadcast capacity region of two-phase bidirectional relaying," *IEEE Transactions on Information Theory*, vol. 54, no. 1, pp. 454–458, Jan. 2008.

[43] R. Ahlswede, N. Cai, S.-Y. Li, and R. Yeung, "Network information flow," *IEEE Transactions on Information Theory*, vol. 46, no. 4, pp. 1204–1216, Jul. 2000.

[44] T. Vu, P. Duhamel, and M. Di Renzo, "On the diversity of network-coded cooperation with decode-and-forward relay selection," *IEEE Transactions on Wireless Communications*, vol. 14, no. 8, pp. 4369–4378, Aug. 2015.

[45] Y. Liu and C. W. Sung, "Network-coded retransmissions in wireless demodulate-and-forward relay channels," *EURASIP Journal on Wireless Communications and Networking*, vol. 2013, no. 1, pp. 1–14, 2013.

[46] B. Rankov and A. Wittneben, "Spectral efficient protocols for half-duplex fading relay channels," *IEEE Journal on Selected Areas in Communications*, vol. 25, no. 2, pp. 379–389, Feb. 2007.

[47] G. Farhadi and N. Beaulieu, "On the ergodic capacity of wireless relaying systems over rayleigh fading channels," *IEEE Transactions on Wireless Communications*, vol. 7, no. 11, pp. 4462–4467, Nov. 2008.

[48] K. Azarian, H. El Gamal, and P. Schniter, "On the achievable diversity-multiplexing tradeoff in half-duplex cooperative channels," *IEEE Transactions on Information Theory*, vol. 51, no. 12, pp. 4152–4172, Dec. 2005.

[49] M. T. O. El Astal, A. M. Abu-Hudrouss, B. P. Salmon, and J. C. Olivier, "An adaptive transmission protocol for exploiting diversity and multiplexing gains in wireless relaying networks," *EURASIP Journal on Wireless Communications and Networking*, vol. 2015, no. 1, pp. 1–15, 2015.

[50] M. Noori and M. Ardakani, "On the achievable rates of symmetric gaussian multi-way relay channels," *EURASIP Journal on Wireless Communications and Networking*, vol. 2013, no. 1, pp. 1–8, 2013.

[51] S. A. Ahmadzadeh, S. A. Motahari, and A. K. Khandani, "Signal space cooperative communication," *IEEE Transactions on Wireless Communications*, vol. 9, no. 4, pp. 1266–1271, Apr. 2010.

[52] T. Lu, J. Ge, Y. Yang, and Y. Gao, "BEP analysis for DF cooperative systems combined with signal space diversity," *IEEE Communications Letters*, vol. 16, no. 4, pp. 486–489, Apr. 2012.

[53] B. Zhao and M. Valenti, "Distributed turbo coded diversity for relay channel," *Electronics Letters*, vol. 39, no. 10, pp. 786–787, May 2003.

[54] Y. Cao and B. Vojcic, "Cooperative coding using serial concatenated convolutional codes," in *IEEE Wireless Communications and Networking Conference*, vol. 2, Mar. 2005, pp. 1001–1006.

[55] M. Müller, M. Taranetz, and M. Rupp, "Providing current and future cellular services to high speed trains," *IEEE Communications Magazine*, vol. 53, no. 10, pp. 96–101, Oct. 2015.

[56] D. Hwang, S.-G. Hong, and T.-J. Lee, "Multiuser two way relaying schemes in the future cellular network," *IEEE Transactions on Wireless Communications*, vol. 12, no. 10, pp. 5200–5207, Oct. 2013.

[57] X. Tao, X. Xu, and Q. Cui, "An overview of cooperative communications," *IEEE Communications Magazine*, vol. 50, no. 6, pp. 65–71, June 2012.

[58] Y. Yang, H. Hu, J. Xu, and G. Mao, "Relay technologies for WiMax and LTE-advanced mobile systems," *IEEE Communications Magazine*, vol. 47, no. 10, pp. 100–105, Oct. 2009.

[59] T.-T. Tran, Y. Shin, and O.-S. Shin, "Overview of enabling technologies for 3GPP LTE-advanced," *EURASIP Journal on Wireless Communications and Networking*, vol. 2012, no. 1, pp. 1–12, 2012.

[60] Q. Li, R. Q. Hu, Y. Qian, and G. Wu, "Cooperative communications for wireless networks: techniques and applications in LTE-advanced systems," *IEEE Wireless Communications*, vol. 19, no. 2, pp. 22–29, Apr. 2012.

[61] F. Boccardi, R. W. Heath, A. Lozano, T. L. Marzetta, and P. Popovski, "Five disruptive technology directions for 5G," *IEEE Communications Magazine*, vol. 52, no. 2, pp. 74–80, Feb. 2014.

[62] W. Zhuang and M. Ismail, "Cooperation in wireless communication networks," *IEEE Wireless Communications*, vol. 19, no. 2, pp. 10–20, Apr. 2012.

[63] A. Nosratinia, T. Hunter, and A. Hedayat, "Cooperative communication in wireless networks," *IEEE Communications Magazine*, vol. 42, no. 10, pp. 74–80, Oct. 2004.

[64] A. Nosratinia and T. E. Hunter, "Grouping and partner selection in cooperative wireless networks," *IEEE Journal on Selected Areas in Communications*, vol. 25, no. 2, pp. 369–378, Feb. 2007.

[65] M. R. Avendi and H. H. Nguyen, "Differential dual-hop relaying under user mobility," *IET Communications*, vol. 8, no. 17, pp. 3161–3169, 2014.

[66] IEEE, "IEEE 802.16 Standard: Air Interface for Fixed Broadband Wireless Access Systems," 2004.

[67] M. Abramowitz and I. A. Stegun, *Handbook of Mathematical Functions with Formulas, Graphs, and Mathematical Tables*, 10th ed. Washington, DC: National Bureau of Standards, U.S. Governement Printing Office, 1972.

[68] M. K. Simon and M.-S. Alouini, *Digital Communications over Fading Channels*, 2nd ed. New Jersey, USA: John Wiley & Sons, 2004.

[69] I. S. Gradshteyn and I. M. Ryzhik, *Table of Integrals, Series, and Products*, 7th ed. San Diego, California: Elsevier Inc., 2007.

[70] M. R. Bhatnagar, "On the capacity of decode-and-forward relaying over rician fading channels," *IEEE Communications Letters*, vol. 17, no. 6, pp. 1100–1103, June 2013.

[71] K. Tourki, H.-C. Yang, and M.-S. Alouini, "Error-rate performance analysis of incremental decode-and-forward opportunistic relaying," *IEEE Transactions on Communications*, vol. 59, no. 6, pp. 1519–1524, Jun. 2011.

Appendix A

Error Probability over a Rayleigh Fading Channel

In this appendix, the derivation of the error probability over Rayleigh fading channel is shown. This closed-form expression of error probability is applicable to any digital modulation scheme which has the instantaneous symbol error probability of the following form:

$$\mathcal{P}_{\text{sym}}(e|\gamma) = \alpha\, Q\left(\sqrt{\beta\gamma}\right), \tag{A.1}$$

where $Q(u) = \frac{1}{\sqrt{2\pi}} \int_u^\infty e^{-t^2/2} dt$ is the Gaussian Q-function [67, 26.2.3], γ is the instantaneous signal-to-noise (SNR) ratio per symbol, and α and β are determined by the type of the digital modulation scheme. Therefore, the average symbol error probability (SEP) over a fading channel, $\mathcal{P}_{\text{sym}}(e)$, can be written as

$$\mathcal{P}_{\text{sym}}(e) = \int_0^\infty \alpha\, Q\left(\sqrt{\beta\gamma}\right) f_\gamma(\gamma)\, d\gamma, \tag{A.2}$$

where $f_\gamma(\gamma)$ is the PDF of the SNR γ. The PDF of the Rayleigh fading channel, $f_\gamma(\gamma)$, is given by

$$f_\gamma(\gamma) = \frac{1}{\overline{\gamma}}\, e^{-\gamma/\overline{\gamma}}, \quad \gamma \geq 0 \tag{A.3}$$

where $\overline{\gamma}$ is the average SNR per symbol. Thus, the average symbol error probability over the Rayleigh fading channel can be expressed as

$$\mathcal{P}_{\text{sym}}(e) = \int_0^\infty \alpha\, Q\left(\sqrt{\beta\gamma}\right) \frac{1}{\overline{\gamma}}\, e^{-\gamma/\overline{\gamma}} d\gamma, \tag{A.4}$$

Let

$$u = Q\left(\sqrt{\beta\gamma}\right) \qquad \text{and} \qquad dv = \frac{1}{\overline{\gamma}}\, e^{-\gamma/\overline{\gamma}} dt, \tag{A.5}$$

Then,

$$du = -\frac{1}{\sqrt{2\pi}} e^{-\beta\gamma/2} \sqrt{\frac{\beta}{4\gamma}}\, dt \qquad \text{and} \qquad v = -e^{-\gamma/\overline{\gamma}}. \tag{A.6}$$

Using substitution from (A.6) and integrating (A.4)

$$\mathcal{P}_{\text{sym}}(e) = \frac{1}{2}\,\alpha - \alpha \int_0^\infty \frac{1}{\sqrt{2\pi}} \sqrt{\frac{\beta}{4\gamma}} e^{-\gamma(\frac{1}{\overline{\gamma}}+\frac{\beta}{2})} dt. \tag{A.7}$$

Let

$$\frac{x^2}{2} = \gamma\left(\frac{1}{\overline{\gamma}} + \frac{\beta}{2}\right) \qquad \Rightarrow \qquad x = \sqrt{2\gamma\left(\frac{1}{\overline{\gamma}} + \frac{\beta}{2}\right)}, \tag{A.8}$$

Then,

$$xdx = \left(\frac{1}{\overline{\gamma}} + \frac{\beta}{2}\right) dx \qquad \Rightarrow \qquad \sqrt{\frac{\beta}{4\gamma}}\, dt = \sqrt{\frac{\beta\overline{\gamma}}{\beta\overline{\gamma}+2}}\, dx \tag{A.9}$$

Substituting (A.9) into (A.7)

$$\mathcal{P}_{\text{sym}}(e) = \frac{1}{2}\,\alpha - \alpha\sqrt{\frac{\beta\overline{\gamma}}{\beta\overline{\gamma}+2}}\int_{0}^{\infty}\frac{1}{\sqrt{2\pi}}\,e^{-u^2/2}dt, \tag{A.10}$$

$$\mathcal{P}_{\text{sym}}(e) = \frac{1}{2}\,\alpha - \alpha\sqrt{\frac{\beta\overline{\gamma}}{\beta\overline{\gamma}+2}}\,Q(0). \tag{A.11}$$

Thus, the closed-form expression for the average symbol error probability of a digital modulation scheme over a Rayleigh fading channel can be written as

$$\mathcal{P}_{\text{sym}}(e) = \int_{0}^{\infty}\alpha\,Q\left(\sqrt{\beta\gamma}\right)\frac{1}{\overline{\gamma}}\,e^{-\gamma/\overline{\gamma}}dt = \frac{1}{2}\,\alpha\left(1-\sqrt{\frac{\beta\overline{\gamma}}{\beta\overline{\gamma}+2}}\right). \tag{A.12}$$

Appendix B

PDF of the SNR of the Best Relay

In this appendix, the analysis for the PDF of the SNR, γ_t, of the best relay over Rayleigh fading channel is shown using [71]. The criteria to choose the best relay based on channel SNRs, γ_{a_i} and γ_{b_i}, is expressed as

$$\mathsf{R}_t = \arg\max_{i \in K} \left\{ \min\left(\gamma_{a_i}, \gamma_{b_i}\right) \right\}. \tag{B.1}$$

The PDF of the SNR of the best relay, γ_t, can be expressed as

$$f_{\gamma_{b_t}}(\gamma) = \int_0^\infty f_{\gamma_{b_i}|U_i=u}(\gamma)\ f_V(u)\, du, \tag{B.2}$$

where $U_i = \min\left(\gamma_{a_i}, \gamma_{b_i}\right)$ and $V = \max_{i \in K} U_i$. The conditional PDF can be written, using the Bayes rule, as

$$f_{\gamma_{b_i}|U_i=u}(\gamma) = \frac{f_{\gamma_{b_i},U_i}(\gamma, u)}{f_{U_i}(u)}. \tag{B.3}$$

The CDF of U_i can be obtained as

$$F_{U_i}(u) = \Pr\left\{ \min\left(\gamma_{a_i}, \gamma_{b_i}\right) < u \right\}, \tag{B.4}$$

$$F_{U_i}(u) = 1 - \Pr\left\{\gamma_{a_i} \geq u\right\} \Pr\left\{\gamma_{b_i} \geq u\right\}. \tag{B.5}$$

For Rayleigh fading channels,

$$F_{U_i}(u) = 1 - e^{-u/\overline{\gamma}_a} e^{-u/\overline{\gamma}_b}, \tag{B.6}$$

$$F_{U_i}(u) = 1 - e^{-u/\overline{\gamma}_m}, \tag{B.7}$$

where $\overline{\gamma}_m = \overline{\gamma}_a \overline{\gamma}_b / (\overline{\gamma}_a + \overline{\gamma}_b)$. Thus, the PDF of U_i is obtained as

$$f_{U_i}(u) = \frac{d}{du} F_{U_i}(u), \tag{B.8}$$

$$f_{U_i}(u) = \frac{1}{\overline{\gamma}_m} e^{-u/\overline{\gamma}_m}. \tag{B.9}$$

The joint CDF $F_{\gamma_{b_i}, U_i}(\gamma, u)$ can be obtained as [71]

$$F_{\gamma_{b_i}, U_i}(\gamma, u) = \Pr\left\{\gamma_{b_i} < \gamma, \min\left(\gamma_{a_i}, \gamma_{b_i}\right) < u\right\}, \tag{B.10}$$

$$F_{\gamma_{b_i}, U_i}(\gamma, u) = F_{\gamma_{a_i}}(u) F_{\gamma_{b_i}}(\gamma) + F_{\gamma_{b_i}}(u)\left[1 - F_{\gamma_{a_i}}(u)\right]. \tag{B.11}$$

Thus, the joint PDF $f_{\gamma_{b_i}, U_i}(\gamma, u)$ can be written as

$$f_{\gamma_{b_i}, U_i}(\gamma, u) = f_{\gamma_{a_i}}(u) f_{\gamma_{b_i}}(\gamma) + f_{\gamma_{b_i}}(u)\left[1 - F_{\gamma_{a_i}}(u)\right]. \tag{B.12}$$

Using (B.3), (B.9) and (B.12), the PDF of the SNR of the best relay can be represented as

$$f_{\gamma_{b_t}}(\gamma) = \int_0^{\gamma} \frac{f_{\gamma_{b_i}}(\gamma)\, f_{\gamma_{a_i}}(u)}{f_{U_i}(u)} f_V(u) du + \frac{f_{\gamma_{b_i}}(\gamma)\left[1 - F_{\gamma_{a_i}}(\gamma)\right]}{f_{U_i}(\gamma)} f_V(\gamma), \tag{B.13}$$

where $f_{\gamma_{a_i}}(\gamma_{a_i}) = \frac{1}{\overline{\gamma}_a} e^{-\gamma_{a_i}/\overline{\gamma}_a}$ and $f_{\gamma_{b_i}}(\gamma_{b_i}) = \frac{1}{\overline{\gamma}_b} e^{-\gamma_{b_i}/\overline{\gamma}_b}$ for Rayleigh fading chan-

nels. Then, the CDF of $V = \max_{i \in K} U_i$, $F_V(\gamma)$, is derived as follows:

$$F_V(u) = \Pr\{V \leq u\}, \tag{B.14}$$

$$F_V(u) = \Pr\left\{\max_{i \in K} U_i \leq u\right\}, \tag{B.15}$$

$$F_V(u) = \prod_{i=1}^{K} \Pr\left\{U_i \leq u\right\}, \tag{B.16}$$

$$F_V(u) = \prod_{i=1}^{K} F_{U_i}(u), \tag{B.17}$$

$$F_V(u) = \left(1 - e^{-u/\overline{\gamma}_m}\right)^K. \tag{B.18}$$

Thus, the PDF of $V = \max_{i \in K} U_i$ can be written as

$$f_V(u) = \frac{K}{\overline{\gamma}_m} e^{-u/\overline{\gamma}_m} \left(1 - e^{-u/\overline{\gamma}_m}\right)^{K-1}. \tag{B.19}$$

Using the binomial expansion [69], the PDF, $f_V(u)$, can also be written as

$$f_V(u) = \sum_{i=1}^{K} \binom{K}{i} (-1)^{i-1} \frac{i}{\overline{\gamma}_m} e^{-iu/\overline{\gamma}_m}. \tag{B.20}$$

Substituting all the expressions into (B.13) and then integrating, the PDF of the SNR of the best relay over Rayleigh fading channels can be written as

$$\begin{aligned} f_{\gamma_{b_t}}(\gamma) = &\sum_{k=1}^{K} \binom{K}{k} \frac{(-1)^{k-1}}{\overline{\gamma}_a} \frac{k\overline{\gamma}_m}{k\overline{\gamma}_b - \overline{\gamma}_m} \left(e^{-\gamma/\overline{\gamma}_b} - e^{-k\gamma/\overline{\gamma}_m}\right) \\ &+ \sum_{k=1}^{K} \binom{K}{k} \frac{(-1)^{k-1}}{\overline{\gamma}_b} k\, e^{-k\gamma/\overline{\gamma}_m}. \end{aligned} \tag{B.21}$$

Appendix C

PDF of the SNR of Dual Cooperative Link

In this appendix, the PDF of the SNR of the dual cooperative link is derived. Let γ_a and γ_b be the SNRs of the two independent and non-identical Rayleigh fading channels, and hence their PDFs can be written as

$$f_{\gamma_a}(\gamma_a) = \frac{1}{\overline{\gamma}_a} e^{-\gamma_a/\overline{\gamma}_a}, \tag{C.1}$$

$$f_{\gamma_b}(\gamma_b) = \frac{1}{\overline{\gamma}_b} e^{-\gamma_b/\overline{\gamma}_b}. \tag{C.2}$$

where $\overline{\gamma}_a$ and $\overline{\gamma}_b$ are average SNRs of the links. The SNR of the cooperative link can be expressed as

$$\gamma_t = \gamma_a + \gamma_b \tag{C.3}$$

Thus, the PDF of γ_t can be derived by convolving the PDFs of γ_a and γ_b, which can be obtained as

$$f_{\gamma_t}(\gamma_t) = \int_0^{\gamma_t} f_{\gamma_a}(\gamma) f_{\gamma_b}(\gamma_t - \gamma) d\gamma \tag{C.4}$$

$$f_{\gamma_t}(\gamma_t) = \frac{1}{\overline{\gamma_a}\,\overline{\gamma_b}} e^{-\gamma_t/\overline{\gamma}_b} \int_0^{\gamma_t} e^{-\left(\frac{1}{\overline{\gamma}_a} - \frac{1}{\overline{\gamma}_b}\right)\gamma} d\gamma \tag{C.5}$$

After integrating, $f_{\gamma_t}(\gamma_t)$ can be written as

$$f_{\gamma_t}(\gamma) = \frac{1}{\overline{\gamma}_b - \overline{\gamma}_a}\left(e^{-\gamma/\overline{\gamma}_b} - e^{-\gamma/\overline{\gamma}_a}\right) \tag{C.6}$$

Curriculum Vitae

Name: Muhammad Ajmal Khan

Education:

Ph.D. Candidate Sep 2010 - Jun 2016 *Major*	The University of Western Ontario, London, Canada Department of Electrical and Computer Engineering Communication Systems and Data Networks
M.S., 2001	King Fahd Univ. of Petroleum & Minerals (KFUPM), Department of Electrical Engineering, Dhahran, Saudi Arabia
B.E., 1997	N.E.D. University of Engineering & Technology, Department of Electrical Engineering, Karachi, Pakistan

Experience:

Assistant Professor (Tenure-track) Joining Aug. 2016	Ohio Northern University, Ohio, USA Department of Electrical & Computer Engineering and Computer Science (ECCS)
Lecturer 2001 - 2009	King Fahd Univ. of Petroleum & Minerals (KFUPM), Department of Electrical Engineering
Lecturer 1997 - 1999	N.E.D. University of Engineering & Technology, Department of Electrical Engineering

Awards and Honours: (during Doctoral Studies)

- 3MT Thesis Presentation Competition, 1st Winner, in ECE Department Heat, UWO, Jan 2016
- Teaching Assistant Award, UWO, June 2014

- NSERC-CGSD, Govt. of Canada, 2012 - 2014
- Outstanding Research Contribution Scholarship, PSAC Local 610, UWO, 2014
- Academic Achievement Scholarship, PSAC Local 610, UWO, May 2013
- Ontario Graduate Scholarship (OGS), Sep 2010 - Aug 2011
- OGS, Approved but Declined due to NSERC-CGSD scholarship, 2012
- Western Graduate Research Scholarship (WGRS) for Doctorial Studies, UWO

Publications: (during Doctoral Studies)

[1] **M. A. Khan**, R. K. Rao, and X. Wang, "Outage Probability and System Optimization of SSD-based Dual-Hop Relaying System," *Wireless Personal Communications*, submission: June 2016 (under review)

[2] **M. A. Khan**, R. K. Rao, X. Wang, and A. Sheikh, "Dual-Hop Signal Space Cooperative Systems using Multiple DF Relays," *IET Communications*, provisionally accepted with minor revision.

[3] **M. A. Khan**, R. K. Rao, and X. Wang, "Two-Way Decode-and-Forward Cooperative Systems using Multiple Relays with Signal Space Diversity," *EURASIP Journal on Wireless Communications and Networking*, vol. 2016, no. 1, pp. 1–14, 2016.

[4] **M. A. Khan** and R. K. Rao, "Low Complexity PAPR Reduction Technique for OFDM Systems using Biased Subcarriers," *IEEE Canadian Journal of Electrical and Computer Engineering*, vol. 39, no. 1, pp. 19–25, winter 2016.

[5] **M. A. Khan**, R. K. Rao, and X. Wang, "Signal Space Diversity based Dual-Hop Network using a Decode-and-Forward Relay," *12th IEEE International Conference on Wireless and Mobile Computing, Networking and Communications (WiMob)*, submission: June 2016 (under review)

[6] **M. A. Khan**, R. K. Rao, and X. Wang, "Signal Space Diversity based Two-Way DF Cooperative Network using a Single Relay," *12th IEEE International Conference on Wireless and Mobile Computing, Networking and Communications (WiMob)*, submission: June 2016 (under review)

[7] **M. A. Khan** and R. K. Rao, "PAPR Reduction in OFDM Systems using Differentially Encoded Subcarriers," *27th IEEE Canadian Conference on Electrical and Computer Engineering*, Canada, pp. 1–5, May 2014.

[8] **M. A. Khan**, R. K. Rao, and X. Wang, "Non-Linear Trigonometric and Hyperbolic Chirps in Multiuser Spread Spectrum Communication Systems," *9th IEEE International Conference on Emerging Technologies*, pp. 1–6, Dec. 2013.

[9] **M. A. Khan**, R. K. Rao, and X. Wang, "Performance of quadratic and exponential multiuser chirp spread spectrum communication systems," *8th IEEE International Symposium on Performance Evaluation of Computer and Telecommunication Systems (SPECTS)*, Toronto, Canada, pp. 58–63, Jul. 2013.

[10] **M. A. Khan**, R. K. Rao, and X. Wang, "Performance of multiuser MIMO communication system using chirp modulation," *8th IEEE International Symposium on Performance Evaluation of Computer and Telecommunication Systems*, Toronto, Canada, pp. 115–119, Jul. 2013.

[11] **M. A. Khan**, R. K. Rao, and X. Wang, "Closed-Form Error Probability for M-ary Chirp Modulation in Frequency-Selective and -Nonselective Fading Channels," *26th IEEE Canadian Conference on Electrical and Computer Engineering*, Canada, pp. 1–4, May 2013.

[12] **M. A. Khan**, R. K. Rao, and X. Wang, "Performance Analysis of MRC-Chirp System over Independent and Correlated Fading Channels," *26th IEEE Canadian Conference on Electrical and Computer Engineering*, Canada, pp. 1–4, May 2013.

[13] P. Mi, X. Wang, and **M. A. Khan**, "Diverse QoS Support in Multimedia Communication with Multiple MAC Layer Queues using FSMC," *IEEE Global Telecommunications Conference (GlobeCom-2011)*, USA, pp. 1–5, Dec. 2011.

[14] E. Christopher, **M. A. Khan**, X. Wang, and J. Samarabandu, "Adaptive Modulation for OFDM System with varying speed receiver," *24th IEEE Canadian Conference on Electrical and Computer Engineering*, Canada, pp. 892–895, May 2011.